Floating Bodies in the Absence of Gravity

by

Todd Murray Kemp

A thesis
presented to the University of Waterloo
in fulfilment of the
thesis requirement for the degree of
Master of Mathematics
in
Applied Mathematics

Waterloo, Ontario, Canada, 2011

I hereby declare that I am the sole author of this thesis. This is a true copy of the thesis, including any required final revisions, as accepted by my examiners.

I understand that my thesis may be made electronically available to the public.

Abstract

The study of infinitely long cylinders of constant cross-section floating in an infinite fluid bath in zero-gravity environments has primarily been focused on bodies whose cross-sections are strictly convex and sufficiently smooth. In this thesis, our efforts are concentrated on the consideration of bodies that are only convex and piecewise smooth. These types of bodies are seldom considered in current literature. We have worked with a series expansion of the energy function in order to determine when configurations of a given body will be in equilibrium, stable or otherwise. We have proven that any convex body with a straight side cannot float in a stable equilibrium with the fluid interface intersecting the interior of the straight side in a single point. This fact is then used to prove necessary and sufficient conditions for stable equilibrium of polygons, bodies whose cross-sections are comprised of only straight sides. We illustrate these conditions with several examples.

In the latter portion of the thesis, we turn our attention to bodies in three dimensions. While past research has again been focused on strictly convex bodies, we began to consider bodies that do not meet these requirements by examining bodies of revolution. A condition for stability with respect to vertical variations of bodies of revolution is derived. We conclude with several examples of bodies of revolution, some of which interestingly relate back to an analogous two-dimensional shape.

Acknowledgements

I would like to thank the American Institute of Physics for the use of copyrighted material from their journal, *Physics of Fluids*. For his efforts in proofreading this thesis, I would additionally like to thank Robert Robinson. I would also like to thank my thesis committee members, Dr. Sue Ann Campbell and Dr. Marek Stastna. Finally, this thesis would not have been possible without my supervisor, Dr. David Siegel, whose guidance and encouragement over the last two years have been invaluable resources.

Table of Contents

List of Figures

List of Tables

Chapter 1

Introduction

From a very young age many people are fascinated by floating bodies; a rubber ducky played with in the bathtub was a source of endless entertainment. However, it is not until much later in life that many realize how ubiquitous floating bodies truly are. From ice cubes floating in a glass of water, to a buoy anchored in the ocean, to a container ship sailing around the world, floating bodies surround us and from that fact alone it is no surprise that the study of floating bodies (and in particular their *stability*) is a topic that continues to command the attention of researchers around the globe.

The problem itself is simply stated. Take an interface between two fluids and consider placing a given solid body[1] in the interface so that it is partially submerged in each of the two fluids. Will the body move completely into one of the two fluids, or will it settle at some equilibrium position in contact with the fluid interface? Despite this seemingly simple statement, beneath the surface it turns out to be a fundamentally complex problem which has been researched for quite some time now.

1.1 Previous Work on the Floating Body Problem

As mentioned above, the study of floating bodies is not a new subject. Researchers have considered problems in both two and three dimensions, with or without gravity, and with or without external constraints on the body. One of the most well known contributions to the study of floating bodies is credited to Thomas Young in 1805 (see reference [1]) who

[1]There are two main types of bodies that have been considered in past research. First, there are infinitely long cylinders in which every cross-section orthogonal to the cylinder is identical. This reduces the problem to one in two dimensions where we only need to consider one cross-section of the infinite cylinder. Second, there is the more physically intuitive type of body which is three-dimensional and finite in size.

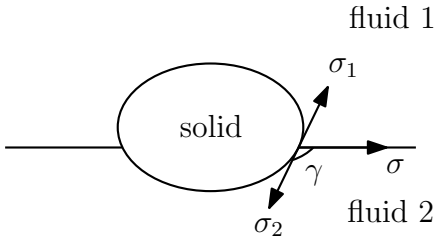

Figure 1.1: *The Young diagram. (Reprinted with permission from reference [14].)*

used his "Young diagram" as a means to explain the observed contact angle condition

$$\cos\gamma = \frac{\sigma_1 - \sigma_2}{\sigma}$$

where γ is the angle of contact between the fluid interface and the body as measured in the lower fluid. (See Figure 1.1.) σ_1 and σ_2 are the respective surface tensions between the solid body and the upper fluid for σ_1 and the lower fluid for σ_2, while σ is the surface tension at the interface between the two fluids. This contact angle condition (and accompanying justification using a force balance in a direction tangential to the body at both points of contact with the fluid interface) was accepted "as is" for many years until Finn indicated that there might be flaws in Young's justification. In reference [2], Finn presented what is now referred to as "The Floating Ball Paradox." In the construction of the paradox, Finn considered a spherical ball floating in equilibrium. He then showed that under the assumptions of Young, there is a net vertical force on the ball pulling it either upward or downward, so the ball could not be in equilibrium. Further, using an integration argument, Finn showed that although the surface tensions at the solid-liquid interfaces do result in forces tangent to the body, they will sum to zero no matter what depth the spherical ball is placed. Finn asserted that,

> *"Balance of forces applied on the contact line is consistent with equilibrium, but cannot be used to characterize equilibrium."*[2]

With this counterexample, Finn put into question the validity of the Young diagram and the consequent contact angle condition. However in that same reference Finn then gave an independent argument using a minimization of energy which verified that the contact angle condition was in fact true, despite any misgivings about the Young diagram itself.

Naturally, some researchers have been hesitant to condemn the Young diagram, pointing out potential flaws in Finn's reasoning found in reference [2] or offering explanations in attempt to make the issue seem less paradoxical. For example, in reference [3] Lunati

[2]This quote is taken from page 3 of reference [2].

rebutted the floating ball paradox by claiming that the tension force perpendicular to the solid (as introduced by Finn) is balanced by a net force that arises from different stresses acting on the solid body by the two different fluids. A year later in reference [4], Wente provided support for the idea that the net vertical force pulling on the body is counteracted by the rigidity of the solid ball. Around the same time, reference [5] was published by Finn containing a rebuttal to statements made by Lunati in reference [3]. Specifically, Finn presented another counterexample in which a sphere made of two hemispheres of different materials completely submerged in a fluid and constrained in some way so that it will move only horizontally along a circular path. Finn showed that under Lunati's reasoning, the sphere would be forced to move in perpetual motion. Clearly this is a touchy subject, and there are impassioned arguments for both sides.

Nonetheless, before the introduction of the floating ball paradox, both the force balance and energy minimization approaches to the floating body problem were able to peacefully coexist. Reference [6] by Raphaël et al. (published in 1992) took the energy approach showing that a two-dimensional, strictly convex body floating in a stable equilibrium at the fluid interface would satisfy the contact angle condition at both points of contact with the fluid interface. In fact, the approach used by Raphaël et al. to derive the contact angle condition is similar in nature to the approach that will be used in this thesis. Also in reference [6], the authors established that for every strictly convex body (in two dimensions) there will exist at least four configurations satisfying the contact angle condition (using The Four Vertex Theorem). Furthermore a result characterizing stable and unstable equilibria was developed. Although this result about stability is quite clever, it is of little practical use since it involves determining an area that is bound between the body and the tangents to the body at the points of contact with the fluid interface. The authors do, however, make use of the result to prove that for a strictly convex body, a stable equilibrium configuration will always exist provided $|\frac{\sigma_1-\sigma_2}{\sigma}| < 1$. The existence of a stable equilibrium for a strictly convex two-dimensional body when $|\frac{\sigma_1-\sigma_2}{\sigma}| < 1$ was re-iterated by Finn in reference [7] where he showed that there would exist a height and corresponding orientation of the body which would give an absolute minimum in energy over all possible heights and orientations of the body. (See Theorem 1.1 in that reference.) Finn also showed that in such a configuration, the contact angle condition was satisfied at both points of contact between the fluid interface and the two-dimensional body.

Although there is an ample amount of literature involving two-dimensional bodies, past work on the study of floating bodies has not been limited to the two-dimensional case. As mentioned earlier, there are two basic types of bodies that are considered: the infinitely long cylinder of constant cross-section, and the finite three-dimensional body. The problem of a floating three-dimensional body is perhaps more physically meaningful, but has been

found to be a much more difficult problem for a multitude of reasons. Perhaps the most significant of these reasons is that in the zero-gravity case, the flatness of the fluid interface is no longer guaranteed as it is in the two-dimensional scenario. Without strict knowledge of the shape of the fluid interface, the problem instantly becomes much more complex. As a way to simplify the problem, in reference [8] Finn introduced the concept of *neutral equilibrium* by assuming the fluid interface was planar. By making this assumption it is possible that Finn had ignored some potential equilibrium configurations in which the fluid interface is not flat; however, the difficulty in working with such fluid interfaces is great and the idea of neutral equilibrium was used as a starting point for working with three-dimensional bodies. Finn continued to work with bodies in three dimensions under the assumption of neutral equilibrium in a joint work with Vogel in reference [9]. In that paper Finn and Vogel extended Theorem 1.1 from an earlier work by Finn (see reference [7]) showing that it was also true that there existed a height and corresponding orientation of a three-dimensional body for which an absolute minimum energy occurred over all heights and orientations. Of course, this result had the restriction of the neutral equilibrium assumption.

The list of works discussed in this review of past literature is by no means exhaustive. In this section, we have examined only resources that relate directly to the topics contained in the thesis. However, there are many more references on the topic of floating bodies and in particular, on floating bodies in the presence of gravity. The reader can refer to references [10], [11], [12] and [13] for additional insight on this area of research.

1.2 Overview

From Section 1.1 it is clear that in the recent past there has been some apprehension concerning the classical "Young diagram" as a means to explain the contact angle condition. In this thesis, we will side with Finn and consider floating bodies from the point of view of energy minimization. We will consider an energy function similar to the one used in reference [6], and we will use it throughout to re-derive some already well known results and to prove some previously unknown results.

In Chapter 2, we will begin by presenting another derivation of the well known contact angle condition using an approach involving a parametric description of the body. In Chapter 3, we take our approach one step further and use the parametric representation of the body to examine the stability of the equilibria of an infinite cylinder whose cross-section is a simple smooth shape, the ellipse. We continue to use our parametric approach to consider new types of bodies that have been ignored in the past. Previous literature has been focused on strictly convex smooth bodies; the lack of literature on bodies that do not

satisfy the smoothness and convexity requirements could be due to a variety of reasons, but it is most likely caused by the fact that the most basic result in the theory of floating bodies, the contact angle condition, does not apply when the body is not smooth. Without the contact angle condition, it would seem that not much can be said about non-smooth convex bodies. However, in Chapter 4, we will begin to work with bodies of this type. We will use our parametric approach to prove that a convex body with a straight edge cannot float in a stable equilibrium with the fluid interface intersecting the interior of a straight edge in a single point. We then use this result in Chapter 5 to consider the floating configurations of bodies with a general polygonal cross-section, deriving a necessary condition for stable equilibrium of a body with a polygonal cross-section, and later deriving a condition which is necessary and sufficient for stable equilibrium. We will illustrate these findings in detail using several polygonal shapes as examples. Our discussion of two-dimensional bodies will conclude with the proof of several results concerning the existence of stable configurations for a general regular polygon, including a result stating that for every γ in $(0, \pi)$ there will always exist a stable global energy minimum. We will take this one step further and prove the existence of a stable global energy minimum for a body with a general polygonal cross-section.

In the latter portion of the thesis, we will begin to consider the more physically intuitive three-dimensional bodies. In particular, in Chapter 6 we consider vertical variations of bodies of revolution, recreating a result by Finn and Vogel and then extending it to types of bodies that are not considered in Finn and Vogel's work. We will illustrate our results using several examples, and these examples will allow to us to draw parallels between the physically unrealistic two-dimensional case and the more natural three-dimensional case.

Chapter 2

The Contact Angle Condition and Stability Definitions

Looking through past research on the topic of floating bodies, it is apparent that the force approach to these types of problems is less prevalent in the field than it was in the past. There is still some disagreement on whether the approach using a balance of forces is valid; in this thesis we will avoid the issue altogether and focus on the alternative energy approach to floating body problems. When using an energy approach, it is important to interpret σ_1, σ_2 and σ appropriately. In the force balance approach, each is interpreted as a tension force per unit length. However, each surface tension also has an interpretation as an energy distribution per unit area; it is this energy distribution interpretation of each surface tension that we will use in this thesis. We begin by deriving Young's renowned contact angle condition via minimization of the representative energy function.

2.1 The Contact Angle Condition

We begin by considering an infinitely long cylinder in which every cross-section orthogonal to the cylinder is identical. This basic assumption will reduce the problem to one in two dimensions where we consider only the shape of the cross-section orthogonal to the cylinder. The cross-section's boundary will be described by the parametric equation $\vec{r}(t) = (x(t), y(t))$. It is assumed that the parametrization is oriented counter-clockwise and the derivative $\vec{r'}(t)$ is never $\vec{0}$. Since we do not consider the effects of gravity, the interface between the two fluids will be a straight line. (See reference [2].) When the body is floating in the fluid interface, it is assumed that the interface is a continuation of the same

The content of Chapter 2 is taken from reference [14]. It is reprinted (with minor alterations) with permission.

line on both sides of the body. Similar to reference [6], we will keep the solid body fixed while varying the fluid interface. The straight line will intersect the body at two points (x_1, y_1) and (x_2, y_2), which for now are assumed to be distinct. We will define parameter values t_1^* and t_2^* to be such that $\vec{r}(t_1^*) = (x_1, y_1)$ and $\vec{r}(t_2^*) = (x_2, y_2)$. The values t_1^* and t_2^* define where the fluid interface touches the body, and hence will be used as our two defining parameters of a possible floating configuration, rather than the slope and intercept of the line as used in reference [6]. We also consider a nearby configuration defined by the parameter values t_1 and t_2 (see Figure 2.1) and proceed to find a series expansion of the energy of a given configuration.

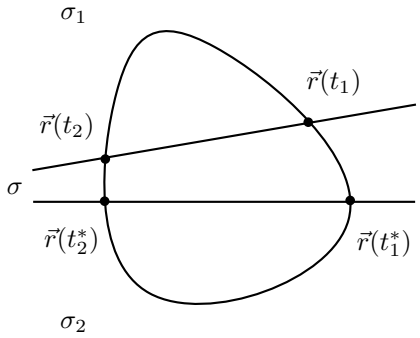

Figure 2.1: *Here we see a general convex body and two floating configurations; one defined by the parameter values* (t_1^*, t_2^*) *and another nearby configuration defined by the values* (t_1, t_2).

Since we do not consider the effects of gravity, the only energies present are surface energies. As such, the energy function E will be defined by

$$E = l_1\sigma_1 + l_2\sigma_2 - l_3\sigma$$

where l_1 and l_2 are the lengths along the body touching the upper and lower fluids respectively, and l_3 is the length *removed* from the fluid interface by the body. E is an energy per unit length along the infinite cylinder. From Figure 2.1 we will have that

$$\begin{aligned} & E(t_1, t_2) - E(t_1^*, t_2^*) \\ = \; & (\sigma_1 - \sigma_2)\left[\int_{t_2^*}^{t_2} \sqrt{x'(t)^2 + y'(t)^2}dt - \int_{t_1^*}^{t_1} \sqrt{x'(t)^2 + y'(t)^2}dt\right] \\ & +\sigma\left[\sqrt{(x(t_2^*) - x(t_1^*))^2 + (y(t_2^*) - y(t_1^*))^2}\right. \\ & \left.-\sqrt{(x(t_2) - x(t_1))^2 + (y(t_2) - y(t_1))^2}\right]. \end{aligned} \tag{2.1}$$

Expanding in series and keeping only linear terms gives

$$\begin{aligned} & E(t_1,t_2) - E(t_1^*,t_2^*) \\ = \; & (\sigma_1-\sigma_2)\left[\|\vec{r'}(t_2^*)\|(t_2-t_2^*) - \|\vec{r'}(t_1^*)\|(t_1-t_1^*)\right] \\ & +\sigma\left[\frac{\vec{r'}(t_1^*)\cdot[\vec{r}(t_2^*)-\vec{r}(t_1^*)]}{\|\vec{r}(t_2^*)-\vec{r}(t_1^*)\|}(t_1-t_1^*) - \frac{\vec{r'}(t_2^*)\cdot[\vec{r}(t_2^*)-\vec{r}(t_1^*)]}{\|\vec{r}(t_2^*)-\vec{r}(t_1^*)\|}(t_2-t_2^*)\right] \\ & +\mathcal{O}\left(\|(t_1,t_2)-(t_1^*,t_2^*)\|^2\right). \end{aligned}$$

Details of the series expansion, are included in Appendix A. Then, assuming that (t_1^*, t_2^*) corresponds to an equilibrium[1] configuration of the body, it must be that

$$\left.\frac{\partial E}{\partial t_1}\right|_{(t_1^*,t_2^*)} = 0 \qquad \text{and} \qquad \left.\frac{\partial E}{\partial t_2}\right|_{(t_1^*,t_2^*)} = 0$$

which leads to the two conditions

$$\frac{\vec{r'}(t_1^*)}{\|\vec{r'}(t_1^*)\|}\cdot\frac{\vec{r}(t_2^*)-\vec{r}(t_1^*)}{\|\vec{r}(t_2^*)-\vec{r}(t_1^*)\|} = \frac{\sigma_1-\sigma_2}{\sigma} \tag{2.2}$$

$$\frac{\vec{r'}(t_2^*)}{\|\vec{r'}(t_2^*)\|}\cdot\frac{\vec{r}(t_2^*)-\vec{r}(t_1^*)}{\|\vec{r}(t_2^*)-\vec{r}(t_1^*)\|} = \frac{\sigma_1-\sigma_2}{\sigma}. \tag{2.3}$$

If $\vec{r}$ is a sufficiently smooth curve, then the angles between $\vec{r'}(t_1^*)$, $\vec{r'}(t_2^*)$ and $\vec{r}(t_2^*)-\vec{r}(t_1^*)$ are γ and so conditions (2.2) and (2.3) both imply that

$$\cos\gamma = \frac{\sigma_1-\sigma_2}{\sigma} \tag{2.4}$$

as expected. Of course, we must have that $|\frac{\sigma_1-\sigma_2}{\sigma}| \leq 1$ in order for γ to be defined.

Remark 2.1. For the remainder of this thesis, we will assume that γ is not equal to 0 or π. For strictly convex bodies, when γ is 0 or π the contact angle condition implies that the body will be in contact with the fluid interface at only one point, and the reader can verify that configurations such as these will always be unstable per Definition 2.2 in Section 2.3; moving the body vertically downward in the $\gamma = 0$ case will leave the energy unchanged, and similarly moving the body vertically upward in the $\gamma = \pi$ case will also leave the energy unchanged. For bodies that are only convex, when γ is 0 or π, the fluid interface can be in contact with the body in only one point or it can touch along a straight edge. If it touches at only one point, it is again verifiable that the configuration is unstable. If the body touches along a straight side, it can be shown that the configuration will again be unstable. For details, see Appendix B. In consideration of all this, it is clear why these two values of γ can be ignored without consequence.

[1] A body is said to be in an equilibrium configuration when it lacks motion. That is, the external influences on the body are such that the configuration is unchanging in height and orientation.

Remark 2.2. It is rarely emphasized why one only considers configurations in which the body touches the fluid interface and not configurations where the body is completely immersed in one of the two fluids. In this section we have followed suit and simply assumed that floating configurations occurred with the fluid interface touching the body, but a formal reasoning for this assumption can be given. For a strictly convex body, Finn's Lemma 1.1 in reference [7] can be used to justify the exclusion of configurations not touching the fluid interface. In the case of a polygonal body, a similar result exists allowing us to consider only configurations touching the fluid interface. For details, see Appendix C.

2.2 Analysis of Second Order Terms

It is well known that the contact angle condition is only a necessary condition for equilibrium. That is, configurations that satisfy the contact angle condition may correspond to local maxima,[2] local minima, or saddle points of the energy function. In order to determine which configurations correspond to stable and unstable equilibria, it will be necessary to work with the second order terms in the series expansion of the energy function. Recalling equation (2.1), we expand in series again, only this time we keep both the linear and quadratic terms. Assuming that the body is in an equilibrium configuration, the contact angle condition will be satisfied and thus the linear terms will sum to zero, leaving only the terms of second order. Using the expansion in Appendix A, we obtain

$$
\begin{aligned}
& E(t_1,t_2) - E(t_1^*,t_2^*) \\
= \quad & \left[\sigma\left[\frac{(\vec{r'}(t_1^*)\cdot[\vec{r}(t_2^*)-\vec{r}(t_1^*)])^2}{2\|\vec{r}(t_2^*)-\vec{r}(t_1^*)\|^3} - \frac{\|\vec{r'}(t_1^*)\|^2 - \vec{r''}(t_1^*)\cdot[\vec{r}(t_2^*)-\vec{r}(t_1^*)]}{2\|\vec{r}(t_2^*)-\vec{r}(t_1^*)\|}\right]\right. \\
& \qquad \left. -(\sigma_1-\sigma_2)\frac{\vec{r'}(t_1^*)\cdot\vec{r''}(t_1^*)}{2\|\vec{r'}(t_1^*)\|}\right](t_1-t_1^*)^2 \\
& \quad +\sigma\left[\frac{\vec{r'}(t_1^*)\cdot\vec{r'}(t_2^*)}{\|\vec{r}(t_2^*)-\vec{r}(t_1^*)\|}\right. \\
& \qquad \left. -\frac{(\vec{r'}(t_1^*)\cdot[\vec{r}(t_2^*)-\vec{r}(t_1^*)])(\vec{r'}(t_2^*)\cdot[\vec{r}(t_2^*)-\vec{r}(t_1^*)])}{\|\vec{r}(t_2^*)-\vec{r}(t_1^*)\|^3}\right](t_1-t_1^*)(t_2-t_2^*) \\
& \quad +\left[\sigma\left[\frac{(\vec{r'}(t_2^*)\cdot[\vec{r}(t_2^*)-\vec{r}(t_1^*)])^2}{2\|\vec{r}(t_2^*)-\vec{r}(t_1^*)\|^3} - \frac{\|\vec{r'}(t_2^*)\|^2 + \vec{r''}(t_2^*)\cdot[\vec{r}(t_2^*)-\vec{r}(t_1^*)]}{2\|\vec{r}(t_2^*)-\vec{r}(t_1^*)\|}\right]\right. \\
& \qquad \left. +(\sigma_1-\sigma_2)\frac{\vec{r'}(t_2^*)\cdot\vec{r''}(t_2^*)}{2\|\vec{r'}(t_2^*)\|}\right](t_2-t_2^*)^2 + \mathcal{O}\left(\|(t_1,t_2)-(t_1^*,t_2^*)\|^3\right).
\end{aligned}
$$

[2] It is actually shown in reference [6] that for a strictly convex body in the zero gravity case a local maximum in energy will not occur; the energy function can only have local minima and saddle points.

From here, we can determine the second partial derivatives of the energy function $E(t_1, t_2)$ evaluated at the equilibrium configuration (t_1^*, t_2^*) and they are

$$\left.\frac{\partial^2 E}{\partial t_1^2}\right|_{(t_1^*,t_2^*)} = \sigma\left[\frac{(\vec{r'}(t_1^*)\cdot[\vec{r}(t_2^*)-\vec{r}(t_1^*])^2}{\|\vec{r}(t_2^*)-\vec{r}(t_1^*)\|^3} - \frac{\|\vec{r'}(t_1^*)\|^2 - \vec{r''}(t_1^*)\cdot[\vec{r}(t_2^*)-\vec{r}(t_1^*)]}{\|\vec{r}(t_2^*)-\vec{r}(t_1^*)\|}\right] - (\sigma_1-\sigma_2)\frac{\vec{r'}(t_1^*)\cdot\vec{r''}(t_1^*)}{\|\vec{r'}(t_1^*)\|}$$

$$\left.\frac{\partial^2 E}{\partial t_2^2}\right|_{(t_1^*,t_2^*)} = \sigma\left[\frac{(\vec{r'}(t_2^*)\cdot[\vec{r}(t_2^*)-\vec{r}(t_1^*])^2}{\|\vec{r}(t_2^*)-\vec{r}(t_1^*)\|^3} - \frac{\|\vec{r'}(t_2^*)\|^2 + \vec{r''}(t_2^*)\cdot[\vec{r}(t_2^*)-\vec{r}(t_1^*)]}{\|\vec{r}(t_2^*)-\vec{r}(t_1^*)\|}\right] + (\sigma_1-\sigma_2)\frac{\vec{r'}(t_2^*)\cdot\vec{r''}(t_2^*)}{\|\vec{r'}(t_2^*)\|}$$

$$\left.\frac{\partial^2 E}{\partial t_1 \partial t_2}\right|_{(t_1^*,t_2^*)} = \frac{\sigma^2\vec{r'}(t_1^*)\cdot\vec{r'}(t_2^*) - (\sigma_1-\sigma_2)^2\|\vec{r'}(t_1^*)\|\|\vec{r'}(t_2^*)\|}{\sigma\|\vec{r}(t_2^*)-\vec{r}(t_1^*)\|}.$$

These partial derivatives will be useful when determining the stability of the equilibria by analysing the approximating quadratic form at configurations that satisfy the contact angle condition. We will see an example of this in Chapter 3. However, we must first define what is meant by *stable* and *unstable* configurations.

2.3 Stability Definitions

Once we have found equilibrium configurations, it is desirable to classify them as stable or unstable, and in this thesis we will make use the following definitions.

Definition 2.1. *A configuration is said to be a* **stable configuration** *if all sufficiently small perturbations away from the configuration result in a* **greater energy**.

Definition 2.2. *A configuration is said to be an* **unstable configuration** *if there exists a sufficiently small perturbation away from the configuration which results in a* **lesser or equal energy**.

These two terms are most commonly applied to configurations which satisfy the contact angle condition and as such the configurations are referred to as *stable* or *unstable equilibria*. However, one will note that the above definitions make no mention of assumed equilibrium and consequently these definitions can be applied to configurations which do not necessarily satisfy Young's contact angle condition. This will be useful in our discussion of bodies with polygonal cross-sections beginning in Chapter 5. In that section, we will develop

a necessary condition for equilibrium of bodies with a polygonal cross-section, one that is different from Young's contact angle condition. Nonetheless, when a polygonal body satisfies the replacement necessary condition (Theorem 5.1), as well as one of the above definitions, the configuration will again be referred to as a *stable* or *unstable equilibrium* as appropriate.

In addition we will make use of a third term.

Definition 2.3. *A configuration is said to be a* **global energy minimum** *if it has an energy that is* **less than or equal to the energy of all other configurations**.

Remark 2.3. In this thesis we will always find that our global energy minima are stable, but one should take care to note that this will not always be the case. For example, a body with a circular cross-section in a configuration that satisfies the contact angle condition will be a global energy minimum, but it is unstable since we can rotate the circle about its center without changing the energy.

Chapter 3

A Smooth Example

In this chapter we will use an analysis of the second order terms in the series expansion of the energy function from Section 2.2 to discuss the stability of equilibrium configurations for a simple smooth shape, the ellipse.

3.1 The Ellipse

We will choose the parametrization

$$\vec{r}(t) = (g\cos t, h\sin t)$$

for t in $[0, 2\pi]$ and $g, h > 0$. We will then have that

$$\vec{r'}(t) = (-g\sin t, h\cos t)$$

and that

$$\vec{r''}(t) = (-g\cos t, -h\sin t) = -\vec{r}(t).$$

For the ellipse, we see that

$$\begin{aligned} \vec{r}(t)\cdot\vec{r'}(t) &= (g\cos t, h\sin t)\cdot(-g\sin t, h\cos t) \\ &= (h^2 - g^2)\sin t\cos t \end{aligned}$$

and that

$$\begin{aligned} \vec{r}(t)\cdot\vec{r''}(t) &= (g\cos t, h\sin t)\cdot(-g\cos t, -h\sin t) \\ &= -(g^2\cos^2 t + h^2\sin^2 t) \end{aligned}$$

Section 3.1 is reprinted with permission from reference [14].

and finally that

$$\begin{aligned}\vec{r'}(t)\cdot\vec{r''}(t) &= (-g\sin t, h\cos t)\cdot(-g\cos t, -h\sin t)\\ &= (g^2-h^2)\sin t\cos t\\ &= -\vec{r}(t)\cdot\vec{r'}(t).\end{aligned}$$

The necessary condition for equilibrium (as found earlier in Section 2.1) requires that the contact angle be the same on both sides of the body. This means that we can rule out any configuration which will not satisfy this requirement. Using Lemma D.1 in Appendix D we will be left with only configurations that have an even symmetry. That is, equilibrium configurations must be symmetric across a vertical line passing through the center of the ellipse. Such configurations are depicted in Figure 3.1.

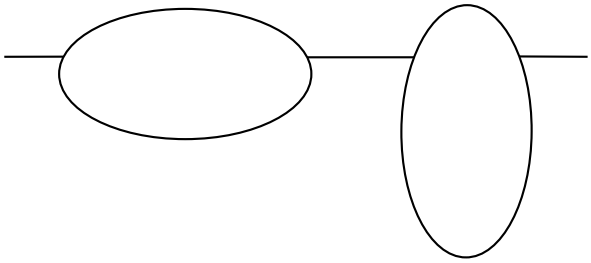

Figure 3.1: *We only consider configurations with an even symmetry as depicted here because the necessary condition for equilibrium tells us that the contact angle must be the same on both sides of the body. Lemma D.1 then tells us that the fluid interface must be vertical or horizontal leaving only configurations of this type.*

In these configurations we will always have that

$$\begin{cases}\cos t_1^* &= -\cos t_2^*\\ \sin t_1^* &= \sin t_2^*\end{cases}$$

or that

$$\begin{cases}\cos t_1^* &= \cos t_2^*\\ \sin t_1^* &= -\sin t_2^*.\end{cases}$$

Without loss of generality, we will assume that t_1^* is such that $\frac{-\pi}{2} \le t_1^* \le \frac{\pi}{2}$ and that t_2^* is such that $\frac{\pi}{2} \le t_2^* \le \frac{3\pi}{2}$ so that $\cos t_1^* = -\cos t_2^*$ and $\sin t_1^* = \sin t_2^*$. We will then have that

$$\|\vec{r}(t_2^*) - \vec{r}(t_1^*)\| = 2g\cos t_1^*$$

and the necessary condition for equilibrium (equation (2.4)) gives that

$$\begin{aligned}\frac{\sigma_1-\sigma_2}{\sigma} &= \frac{\vec{r'}(t_1^*)}{\|\vec{r'}(t_1^*)\|}\cdot\frac{\vec{r}(t_2^*)-\vec{r}(t_1^*)}{\|\vec{r}(t_2^*)-\vec{r}(t_1^*)\|}\\ &= \frac{(-g\sin t_1^*, h\cos t_1^*)}{\sqrt{g^2\sin^2 t_1^*+h^2\cos^2 t_1^*}}\cdot(-1,0)\\ &= \frac{g\sin t_1^*}{\sqrt{g^2\sin^2 t_1^*+h^2\cos^2 t_1^*}} \qquad (3.1)\end{aligned}$$

and we will make use of equation (3.1) later.

To determine the stability of equilibrium configurations for the ellipse we will need to consider the second partial derivatives of the energy function. Substituting $\vec{r}(t)$ into the expressions derived in Section 2.2 and simplifying will give that

$$\left.\frac{\partial^2 E}{\partial t_1^2}\right|_{(t_1^*,t_2^*)} = \frac{\sigma\cos t_1^* h^2}{2g(g^2\sin^2 t_1^*+h^2\cos^2 t_1^*)}\left[g^2+(g^2-h^2)\cos^2 t_1^*\right].$$

We will define the function f as a function of t_1^* to be

$$f(t_1^*) = g^2+(g^2-h^2)\cos^2(t_1^*)$$

and we note that

$$f'(t_1^*) = 2(h^2-g^2)\sin t_1^*\cos t_1^*$$

and so the critical points are $-\frac{\pi}{2}$, 0, and $\frac{\pi}{2}$. Evaluating at the critical points we see that

$$\begin{aligned}f(-\tfrac{\pi}{2}) &= g^2,\\ f(0) &= 2g^2-h^2, \text{ and}\\ f(\tfrac{\pi}{2}) &= g^2.\end{aligned}$$

From the continuity of the function f we can conclude that if $h<\sqrt{2}g$, then $f(t_1^*)>0$ for all $t_1^*\in\left[-\frac{\pi}{2},\frac{\pi}{2}\right]$. Consequently we will have that $\left.\frac{\partial^2 E}{\partial t_1^2}\right|_{(t_1^*,t_2^*)}>0$ for all t_1^*.

It can also be shown that the second partial derivative with respect to t_2^* is given by

$$\begin{aligned}\left.\frac{\partial^2 E}{\partial t_2^2}\right|_{(t_1^*,t_2^*)} &= \frac{\sigma g(h^2-g^2)\sin^2 t_1^*\cos t_1^*}{g^2\sin^2 t_1^*+h^2\cos^2 t_1^*}-\frac{\sigma}{2g}(h^2-2g^2)\cos t_1^*\\ &= \frac{\sigma g^2h^2\sin^2 t_1^*\cos t_1^*+2\sigma g^2h^2\cos^3 t_1^*-\sigma h^4\cos^2 t_1^*}{2g(g^2\sin^2 t_1^*+h^2\cos^2 t_1^*)}\\ &= \frac{\sigma h^2\cos t_1^*}{2g(g^2\sin^2 t_1^*+h^2\cos^2 t_1^*)}\left[g^2\sin^2 t_1^*+2g^2\cos^2 t_1^*-h^2\cos^2 t_1^*\right]\\ &= \frac{\sigma\cos t_1^* h^2}{2g(g^2\sin^2 t_1^*+h^2\cos^2 t_1^*)}\left[g^2+(g^2-h^2)\cos^2 t_1^*\right]\\ &= \left.\frac{\partial^2 E}{\partial t_1^2}\right|_{(t_1^*,t_2^*)} \qquad (3.2)\end{aligned}$$

and so these second partial derivatives are equal.

We now consider the case when $h < \sqrt{2}g$. We have already seen that in this case $\frac{\partial^2 E}{\partial t_1^2}\big|_{(t_1^*,t_2^*)} > 0$, but more work is required to determine the stability of such configurations. Since $\frac{\partial^2 E}{\partial t_1^2}\big|_{(t_1^*,t_2^*)} = \frac{\partial^2 E}{\partial t_2^2}\big|_{(t_1^*,t_2^*)}$, we consider

$$\begin{aligned}
&\left|\frac{\partial^2 E}{\partial t_1^2}\Big|_{(t_1^*,t_2^*)}\right| - \left|\frac{\partial^2 E}{\partial t_1 \partial t_2}\Big|_{(t_1^*,t_2^*)}\right| \\
= \;& \frac{\partial^2 E}{\partial t_1^2}\Big|_{(t_1^*,t_2^*)} - \sigma \left|\frac{\vec{r}'(t_1^*)\cdot\vec{r}'(t_2^*) - \left(\frac{\sigma_1-\sigma_2}{\sigma}\right)^2 \|\vec{r}(t_1^*)\|\cdot\|\vec{r}(t_2^*)\|}{\|\vec{r}(t_2^*)-\vec{r}(t_1^*)\|}\right| \\
= \;& \frac{\partial^2 E}{\partial t_1^2}\Big|_{(t_1^*,t_2^*)} - \frac{\sigma}{2g\cos t_1^*}\left|g^2\sin^2 t_1^* - h^2\cos^2 t_1^* - \frac{g^2\sin^2 t_1^*\left(g^2\sin^2 t_1^* + h^2\cos^2 t_1^*\right)}{g^2\sin^2 t_1^* + h^2\cos^2 t_1^*}\right| \\
= \;& \frac{\sigma\cos t_1^* h^2}{2g(g^2\sin^2 t_1^* + h^2\cos^2 t_1^*)}\left(g^2 + \left(g^2-h^2\right)\cos^2 t_1^*\right) - \frac{\sigma\left|-h^2\cos^2 t_1^*\right|}{2g\cos t_1^*} \\
= \;& \frac{\sigma\cos t_1^* h^2}{2g}\left[\frac{g^2 + (g^2-h^2)\cos^2 t_1^*}{g^2\sin^2 t_1^* + h^2\cos^2 t_1^*} - 1\right] \\
= \;& \frac{\sigma h^2\cos t_1^*\left[g^2 + (g^2-h^2)\cos^2 t_1^* - g^2\left(1-\cos^2 t_1^*\right) - h^2\cos^2 t_1^*\right]}{2g(g^2\sin^2 t_1^* + h^2\cos^2 t_1^*)} \\
= \;& \frac{\sigma\cos^3 t_1^* h^2}{g(g^2\sin^2 t_1^* + h^2\cos^2 t_1^*)}\left(g^2-h^2\right) \qquad (3.3)
\end{aligned}$$

where we have used equation (3.1) to express all occurrences of $\frac{\sigma_1-\sigma_2}{\sigma}$ in terms of t_1^*. From here we see that if we have $h < g$ then $\frac{\partial^2 E}{\partial t_1^2} > 0$ and $\left|\frac{\partial^2 E}{\partial t_1^2}\big|_{(t_1^*,t_2^*)}\right| - \left|\frac{\partial^2 E}{\partial t_1 \partial t_2}\big|_{(t_1^*,t_2^*)}\right| > 0$. Thus, we can conclude that (t_1^*, t_2^*) corresponds to a local minimum and so the corresponding configuration is stable. It can also be seen that when $g < h < \sqrt{2}g$ we have $\frac{\partial^2 E}{\partial t_1^2} > 0$ and $\left|\frac{\partial^2 E}{\partial t_1^2}\big|_{(t_1^*,t_2^*)}\right| - \left|\frac{\partial^2 E}{\partial t_1 \partial t_2}\big|_{(t_1^*,t_2^*)}\right| < 0$. Hence we can conclude that the configuration would be in this case unstable.

Now we must consider what happens when $h \geq \sqrt{2}g$. When this is true, $\frac{\partial^2 E}{\partial t_1^2}$ can be positive, negative or zero depending on the particular value of t_1^* that defines the configuration. We consider the separate possibilities here.

Case 1: $\frac{\partial^2 E}{\partial t_1^2}\big|_{(t_1^*,t_2^*)} > 0$

In this case we will still have that $\left|\frac{\partial^2 E}{\partial t_1^2}\big|_{(t_1^*,t_2^*)}\right| - \left|\frac{\partial^2 E}{\partial t_1 \partial t_2}\big|_{(t_1^*,t_2^*)}\right|$ is given by equation (3.3), but since $g < \sqrt{2}g \leq h$ here we have that the left hand side of equation (3.3) is negative and thus we have an unstable configuration.

Case 2: $\frac{\partial^2 E}{\partial t_1^2}\big|_{(t_1^*,t_2^*)} < 0$

In this case we will instead have that

$$\begin{aligned}
&\left|\frac{\partial^2 E}{\partial t_1^2}\big|_{(t_1^*,t_2^*)}\right| - \left|\frac{\partial^2 E}{\partial t_1 \partial t_2}\big|_{(t_1^*,t_2^*)}\right| \\
= \;& -\frac{\partial^2 E}{\partial t_1^2}\bigg|_{(t_1^*,t_2^*)} + \frac{\partial^2 E}{\partial t_1 \partial t_2}\bigg|_{(t_1^*,t_2^*)} \\
= \;& \frac{\sigma \cos t_1^* h^2}{2g\left(g^2 \sin^2 t_1^* + h^2 \cos^2 t_1^*\right)}\left[\left(h^2 - g^2\right)\cos^2 t_1^* - g^2\right] - \frac{\sigma h^2 \cos t_1^*}{2g} \\
= \;& -\frac{\sigma g h^2 \cos t_1^*}{g^2 \sin^2 t_1^* + h^2 \cos^2 t_1^*} \\
< \;& 0
\end{aligned}$$

and this implies that our configuration will be unstable in this case as well.

Case 3: $\frac{\partial^2 E}{\partial t_1^2}\big|_{(t_1^*,t_2^*)} = 0$

In this last case, we have that

$$\begin{aligned}
&\left|\frac{\partial^2 E}{\partial t_1^2}\big|_{(t_1^*,t_2^*)}\right| - \left|\frac{\partial^2 E}{\partial t_1 \partial t_2}\big|_{(t_1^*,t_2^*)}\right| \\
= \;& -\left|\frac{\partial^2 E}{\partial t_1 \partial t_2}\big|_{(t_1^*,t_2^*)}\right| \\
< \;& 0
\end{aligned}$$

and so the configuration will again be unstable.

Having considered all three cases, we see that no matter the sign of $\frac{\partial^2 E}{\partial t_1^2}\big|_{(t_1^*,t_2^*)}$, if we have that $h \geq \sqrt{2}g$ we always get an unstable configuration.

Summary

When $h < g$, equilibrium configurations of the assumed form are stable. When $g < h$, they are unstable. This important example is restated more simply in the following result.

Theorem 3.1. *If the major axis of the ellipse is resting parallel to the fluid interface, the equilibrium configuration will be stable. If the minor axis is resting parallel to the fluid interface, the equilibrium configuration will be unstable.*

Remark 3.1. The reader may notice that Theorem 3.1 cannot be applied to the special case where the ellipse is a circle. However, for the circle, it is intuitively clear that rotating the circle about its center does not change the energy. Thus, there will always exist a small perturbation away from any configuration resulting in the same energy. Hence any equilibrium configuration of the circle is unstable.

Remark 3.2. We note that our Theorem 3.1 is in keeping with a result found by Raphaël et al. in reference [6]. In Section 3 of that paper, the authors construct a region between the body and the tangents at the two points of contact with the fluid interface. It is shown that when the area of this region is maximal, the configuration is stable and when the area is minimal, the configuration is unstable. For the ellipse, the area in question will be maximal when the fluid interface is parallel to the major axis and minimal when the fluid interface is parallel to the minor axis, confirming our result.

Chapter 4

Bodies with Straight Sides

In the example discussed in Chapter 3 we only considered a shape that was *strictly* convex. However, in Chapter 2 we never made the assumption that our parametrization $\vec{r}(t)$ defined a body that was strictly convex. Thus the analysis in that chapter can be utilized to study bodies which are only convex. In this chapter, we will begin by proving a result for a general convex body with at least one straight side. We will then discuss the implications of this result.

4.1 Straight Side Instability

Consider a convex body with at least one straight side. Due to the fact that this type of body is seldom considered, one might expect that the presence of the straight side could cause a great deal of complications when searching for stable equilibrium configurations of the body, but exactly the opposite is true. It turns out that we can unexpectedly eliminate countless configurations using the following surprising theorem.

Theorem 4.1. *A convex body with a straight edge cannot float in a stable equilibrium with the fluid interface intersecting the interior of the straight edge in a single point.*

Proof. Consider a convex body with a linear edge in an equilibrium configuration such that the fluid interface intersects the interior of the line segment in a single point. Since the fluid interface and the edge of the body (which are two lines) intersect in only one point, they cannot be parallel and so the angle between them cannot be 0 or π. Without loss of generality, we will assume the body is linear surrounding $\vec{r}(t_2^*)$. This means that $\vec{r'}(t_2^*)$ is constant and $\vec{r''}(t_2^*) = 0$. Of course, it is possible that the parametrization $\vec{r}(t)$ is such that we do not have that $\vec{r'}(t_2^*)$ is constant and $\vec{r''}(t_2^*) = 0$, but it is always possible

Section 4.1 is reprinted with permission from reference [14].

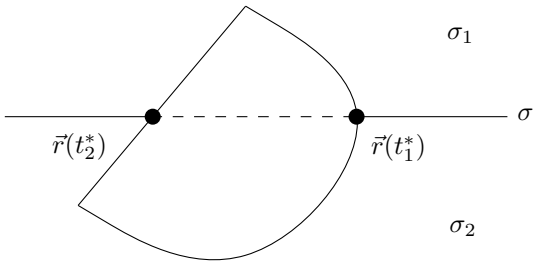

Figure 4.1: *The convex body with a linear side in consideration.*

to choose one such that we do have these two properties. We will use a parametrization that possesses these two desired properties. Using this, we keep the right point of contact fixed so that $t_1 = t_1^*$ and find the change in energy due to varying t_2^* only. Since the body is in equilibrium, the linear terms in the series expansion of the energy sum to zero. In addition, $t_1 = t_1^*$ eliminates all terms of $\mathcal{O}\left((t_1 - t_1^*)^2\right)$. We thus obtain

$$\begin{aligned} & E(t_1^*, t_2) - E(t_1^*, t_2^*) \\ = \; & \frac{\sigma}{2}\left[\frac{\left(\vec{r'}(t_2^*)\cdot[\vec{r}(t_2^*) - \vec{r}(t_1^*)]\right)^2}{\|\vec{r}(t_2^*) - \vec{r}(t_1^*)\|^3} - \frac{\|\vec{r'}(t_2^*)\|^2}{\|\vec{r}(t_2^*) - \vec{r}(t_1^*)\|}\right](t_2 - t_2^*)^2 \\ & + \mathcal{O}\left((t_2 - t_2^*)^3\right) \\ = \; & \frac{\sigma\left[\left(\vec{r'}(t_2^*)\cdot[\vec{r}(t_2^*) - \vec{r}(t_1^*)]\right)^2 - \|\vec{r'}(t_2^*)\|^2\cdot\|\vec{r}(t_2^*) - \vec{r}(t_1^*)\|^2\right]}{2\|\vec{r}(t_2^*) - \vec{r}(t_1^*)\|^3}(t_2 - t_2^*)^2 \\ & + \mathcal{O}\left((t_2 - t_2^*)^3\right). \end{aligned}$$

We recall the Cauchy-Schwarz Inequality:

$$|\,\vec{a}\cdot\vec{b}\,| \leq \|\vec{a}\|\cdot\|\vec{b}\| \qquad \Longleftrightarrow \qquad (\vec{a}\cdot\vec{b})^2 - \|\vec{a}\|^2\|\vec{b}\|^2 \leq 0$$

with equality holding only when $\vec{a}$ and $\vec{b}$ are parallel. If we let $\vec{a} = \vec{r'}(t_2^*)$ and $\vec{b} = \vec{r}(t_2^*) - \vec{r}(t_1^*)$ we see that

$$E(t_1^*, t_2) - E(t_1^*, t_2^*) = \frac{\sigma}{2\|\vec{b}\|^3}\left[(\vec{a}\cdot\vec{b})^2 - \|\vec{a}\|^2\|\vec{b}\|^2\right](t_2 - t_2^*)^2 + \mathcal{O}\left((t_2 - t_2^*)^3\right).$$

We note that $\vec{r'}(t_2^*)$ and $\vec{r}(t_2^*) - \vec{r}(t_1^*)$ cannot be parallel since they are vectors in the direction of the linear side of the body and the fluid interface respectively. The coefficient on $(t_2 - t_2^*)^2$ is thus negative and so there exists a small perturbation from this configuration giving a lesser energy and hence by definition this equilibrium is unstable. □

Remark 4.1. This is truly a remarkable result. When searching for stable equilibrium configurations of any body with a straight side, we can automatically ignore any configuration for which the fluid interface intersects the interior of the straight side in a single point since any equilibrium configuration for which the fluid interface intersects the interior of a straight side in a single point will be unstable. This will be particularly useful in our discussion of bodies with polygonal cross-sections in Chapter 5.

Chapter 5

Bodies with a Polygonal Cross-section

In this chapter we consider infinitely long cylinders whose cross-sections are convex polygons. This type of body is a subset of convex bodies with the unique property that the boundary is comprised of *only* straight lines. Of course, this also means that the boundary has corners where the various straight edges meet. These types of bodies are not strictly convex and have corners, and as a result much of the existing literature cannot be applied in general when attempting to find floating configurations of such bodies. In this chapter, we will begin to work with these types of bodies by developing a necessary and sufficient condition for stable equilibrium and then we look at several specific shapes in depth.

5.1 Necessary Condition for Stable Equilibrium of a Polygonal Body

Recalling Theorem 4.1, any configuration in which the fluid interface intersects the body on the interior of a straight edge cannot be a stable equilibrium. Also, it is easily verified using Definition 2.2 that if the fluid interface touches the body at only one point or not at all, then the configuration will be unstable. Since a polygonal body is comprised of only straight sides, stable equilibria can consequently only occur when the fluid interface intersects two corners of the polygon. With this reasoning we can give a necessary condition for stable equilibrium of polygonal bodies.

Theorem 5.1. *A necessary condition for a body with a polygonal cross-section to be in a stable equilibrium is that the fluid interface must intersect the body at two corners.*

Section 5.1 is reprinted with permission from reference [14].

Remark 5.1. Naturally, this necessary condition is different from the necessary condition for smooth convex bodies, the contact angle condition. Beyond the types of bodies that each may be applied to, there is another key difference between the two conditions. We note that the contact angle condition is a necessary condition for equilibrium, but it does not specify the stability of the equilibrium. However, Theorem 5.1 is a necessary condition for *stable* equilibrium. It is possible that other equilibrium configurations exist; they can be found using the contact angle condition. However, any equilibrium configuration found using the contact angle condition will intersect a straight edge and using Theorem 4.1 we know that these equilibrium configurations are unstable. Thus, we do not bother to search for them. This key difference between the two necessary conditions is crucial; one must never forget that for polygonal bodies the necessary condition given is necessary for stable equilibrium only.

5.2 Stability Condition for a Polygonal Body

Of course, Theorem 5.1 gives only a necessary condition for stable equilibrium of polygonal bodies. It *does not* give a sufficient condition for stable equilibrium. Nonetheless, a sufficient condition for stable equilibrium can be found and we will derive it here.

To begin, we consider an infinitely long cylinder with a polygonal cross-section floating with vertices $\vec{r}(t_1^*)$ and $\vec{r}(t_2^*)$ on the fluid interface on the right and left, respectively, as shown in Figure 5.1.

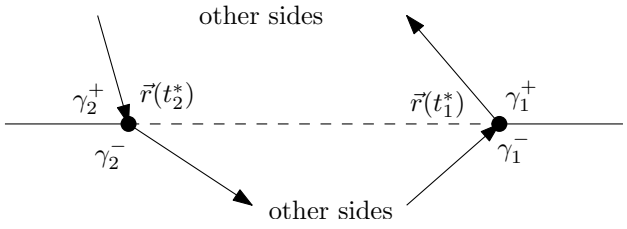

Figure 5.1: *Here the general set up of our floating configuration is depicted. Two corners of the polygonal cross-section are on the fluid interface and the sides that comprise these corners make four "floating angles" with the fluid interface which we label as shown.*

We consider a counter-clockwise parametrization of the body and we consider perturbations away from this configuration. Using our series expansion for the energy from Section 2.1 we can write an expression for $E(t_1, t_2) - E(t_1^*, t_2^*)$, but before doing so we note that since we are considering polygonal cross-sections, we are dealing with linear sides and so

Section 5.2 is reprinted with permission from reference [14].

the parametrization $\vec{r}(t)$ will have zero second derivatives. Thus we have that

$$\begin{aligned} & E(t_1,t_2) - E(t_1^*,t_2^*) \\ = \; & (\sigma_1-\sigma_2)\left[\|\vec{r'}(t_2^*)\|(t_2-t_2^*) - \|\vec{r'}(t_1^*)\|(t_1-t_1^*)\right] \\ & +\sigma\left[\|\vec{r'}(t_1^*)\|\cos\theta_1(t_1-t_1^*) - \|\vec{r'}(t_2^*)\|\cos\theta_2(t_2-t_2^*)\right] \\ & +\mathcal{O}\left(\|(t_1,t_2)-(t_1^*,t_2^*)\|^2\right) \\ = \; & \sigma\left[\|\vec{r'}(t_1^*)\|(t_1-t_1^*)(\cos\theta_1-\cos\gamma) + \|\vec{r'}(t_2^*)\|(t_2-t_2^*)(\cos\gamma-\cos\theta_2)\right] \\ & +\mathcal{O}\left(\|(t_1,t_2)-(t_1^*,t_2^*)\|^2\right) \end{aligned}$$

where θ_1 is the angle between $\vec{r'}(t_1^*)$ and $\vec{r}(t_2^*)-\vec{r}(t_1^*)$ and θ_2 is the angle between $\vec{r'}(t_2^*)$ and $\vec{r}(t_2^*)-\vec{r}(t_1^*)$. We must now consider 4 cases in order to consider *all* perturbations away from this configuration.

Case 1

In this case the fluid interface is perturbed upwards on both sides of the body. This implies that $\theta_1 = \pi - \gamma_1^+$ and $\theta_2 = \pi - \gamma_2^+$ and that $t_1 > t_1^*$ and $t_2 < t_2^* \Rightarrow |t_1 - t_1^*| = t_1 - t_1^*$ and $|t_2 - t_2^*| = -(t_2 - t_2^*)$. This gives us that

$$\begin{aligned} & E(t_1,t_2) - E(t_1^*,t_2^*) \\ = \; & \sigma\left[\|\vec{r'}(t_1^*)\|\,|t_1-t_1^*|\,(\cos\theta_1-\cos\gamma) + \|\vec{r'}(t_2^*)\|\,|t_2-t_2^*|\,(\cos\theta_2-\cos\gamma)\right] \\ & +\mathcal{O}\left(\|(t_1,t_2)-(t_1^*,t_2^*)\|^2\right). \end{aligned}$$

If we have that

$$\begin{array}{ccccc} & \cos\theta_1 > \cos\gamma & \text{and} & \cos\theta_2 > \cos\gamma \\ \iff & \theta_1 < \gamma & \text{and} & \theta_2 < \gamma \\ \iff & \pi - \gamma_1^+ < \gamma & \text{and} & \pi - \gamma_2^+ < \gamma \end{array}$$

then $E(t_1,t_2) > E(t_1^*,t_2^*)$ for (t_1,t_2) sufficiently close to (t_1^*,t_2^*) and we have stability with respect to perturbations in this case. If $\gamma < \pi - \gamma_1^+$, fixing t_2 to be t_2^* and allowing t_1 to vary gives the existence of a perturbation to a configuration giving a lower energy and hence the configuration is unstable. Similarly, if $\gamma < \pi - \gamma_2^+$, fixing t_1 to be t_1^* and allowing t_2 to vary gives that the configuration is unstable. If $\gamma = \pi - \gamma_1^+$ or $\gamma = \pi - \gamma_2^+$, further analysis is required and will be dealt with later.

Case 2

In this case the fluid interface is perturbed downwards on both sides of the body. This implies that $\theta_1 = \gamma_1^-$ and $\theta_2 = \gamma_2^-$ and that $t_1 < t_1^*$ and $t_2 > t_2^* \Rightarrow |t_1 - t_1^*| = -(t_1 - t_1^*)$ and

$|t_2 - t_2^*| = t_2 - t_2^*$. This gives us that

$$\begin{aligned} & E(t_1, t_2) - E(t_1^*, t_2^*) \\ = \; & \sigma \left[\|\vec{r'}(t_1^*)\| \, |t_1 - t_1^*| \, (\cos\gamma - \cos\theta_1) + \|\vec{r'}(t_2^*)\| \, |t_2 - t_2^*| \, (\cos\gamma - \cos\theta_2) \right] \\ & + \mathcal{O}\left(\|(t_1, t_2) - (t_1^*, t_2^*)\|^2 \right). \end{aligned}$$

If we have that

$$\begin{array}{ccccc} & \cos\gamma > \cos\theta_1 & \text{and} & \cos\gamma > \cos\theta_2 \\ \iff & \gamma < \theta_1 & \text{and} & \gamma < \theta_2 \\ \iff & \gamma < \gamma_1^- & \text{and} & \gamma < \gamma_2^- \end{array}$$

then $E(t_1, t_2) > E(t_1^*, t_2^*)$ for (t_1, t_2) sufficiently close to (t_1^*, t_2^*) and we have stability with respect to perturbations in this case. If $\gamma > \gamma_1^-$, fixing t_2 to be t_2^* and allowing t_1 to vary gives the existence of a perturbation to a configuration giving a lower energy and hence the configuration is unstable. Similarly, if $\gamma > \gamma_2^-$, fixing t_1 to be t_1^* and allowing t_2 to vary gives that the configuration is unstable. If $\gamma = \gamma_1^-$ or $\gamma = \gamma_2^-$, further analysis is required and will be dealt with later.

Cases 3 and 4

In case 3 the fluid interface is perturbed upwards on the left and downwards on the right. In case 4 the fluid interface is perturbed downwards on the left and upwards on the right. We do not consider these two cases in detail; we do however note that if the four conditions on γ found in cases 1 and 2 are satisfied, the required conditions for stability with respect to perturbations in cases 3 and 4 will also be satisfied. Thus, we conclude that if the configuration is stable with respect to the perturbations in cases 1 and 2, it will also be stable with respect to those in cases 3 and 4.

Thus in order to have stability with respect to the types of perturbations in all four cases we must have that each of the following four conditions are satisfied

$$\begin{cases} \pi - \gamma_1^+ < \gamma \\ \pi - \gamma_2^+ < \gamma \\ \gamma < \gamma_1^+ \\ \gamma < \gamma_2^- \end{cases}$$

which is equivalent to the requirement that

$$\pi - \min(\gamma_1^+, \gamma_2^+) < \gamma < \min(\gamma_1^-, \gamma_2^-)$$

and so if the above condition is met, then the configuration in question will be stable. We can also say that if $\gamma > \min(\gamma_1^-, \gamma_2^-)$ or $\gamma < \pi - \min(\gamma_1^+, \gamma_2^+)$ then there exists a perturbation to a configuration giving a lesser energy and thus the configuration is unstable.

We now consider the endpoints of the interval of γ for which the configuration is stable. To deal with these two values it will be necessary to work with higher order terms since the linear terms will be zero for these values of γ. Recalling that the second derivatives of $\vec{r}(t)$ will be zero gives us that

$$\begin{aligned}
& E(t_1,t_2) - E(t_1^*,t_2^*) \\
= \;& \sigma\left[\|\vec{r'}(t_1^*)\|(t_1-t_1^*)(\cos\theta_1-\cos\gamma) + \|\vec{r'}(t_2^*)\|(t_2-t_2^*)(\cos\gamma-\cos\theta_2)\right] \\
& -\sigma\left[\frac{\|\vec{r'}(t_1^*)\|^2}{2\|\vec{r}(t_2^*)-\vec{r}(t_1^*)\|} - \frac{(\vec{r'}(t_1^*)\cdot[\vec{r}(t_2^*)-\vec{r}(t_1^*)])^2}{2\|\vec{r}(t_2^*)-\vec{r}(t_1^*)\|^3}\right](t_1-t_1^*)^2 \\
& -\sigma\left[\frac{\|\vec{r'}(t_2^*)\|^2}{2\|\vec{r}(t_2^*)-\vec{r}(t_1^*)\|} - \frac{(\vec{r'}(t_2^*)\cdot[\vec{r}(t_2^*)-\vec{r}(t_1^*)])^2}{2\|\vec{r}(t_2^*)-\vec{r}(t_1^*)\|^3}\right](t_2-t_2^*)^2 \\
& -\beta(t_1-t_1^*)(t_2-t_2^*) + \mathcal{O}\left(\|(t_1,t_2)-(t_1^*,t_2^*)\|^3\right)
\end{aligned}$$

where the coefficient of the mixed term will simply be called β as it will not be required here. We can simplify further by writing

$$\begin{aligned}
& E(t_1,t_2) - E(t_1^*,t_2^*) \\
= \;& \sigma\|\vec{r'}(t_1^*)\|(\cos\theta_1-\cos\gamma)(t_1-t_1^*) + \sigma\|\vec{r'}(t_2^*)\|(\cos\gamma-\cos\theta_2)(t_2-t_2^*) \\
& -\frac{\sigma\|\vec{r'}(t_1^*)\|^2}{2\|\vec{r}(t_2^*)-\vec{r}(t_1^*)\|}\left[1-\cos^2\theta_1\right](t_1-t_1^*)^2 \\
& -\frac{\sigma\|\vec{r'}(t_2^*)\|^2}{2\|\vec{r}(t_2^*)-\vec{r}(t_1^*)\|}\left[1-\cos^2\theta_2\right](t_2-t_2^*)^2 \\
& +\beta(t_1-t_1^*)(t_2-t_2^*) + \mathcal{O}\left(\|(t_1,t_2)-(t_1^*,t_2^*)\|^3\right).
\end{aligned}$$

We will prove that when $\gamma = \pi - \min(\gamma_1^+, \gamma_2^+)$ or $\gamma = \min(\gamma_1^-, \gamma_2^-)$ the configuration will be unstable by showing the existence of a small perturbation to a nearby configuration giving lesser energy.

First consider when $\gamma = \pi - \min(\gamma_1^+, \gamma_2^+)$. Clearly, either $\gamma = \pi - \gamma_1^+$ or $\gamma = \pi - \gamma_2^+$. We consider either possibility below.

- When $\gamma = \pi - \gamma_1^+$, consider case 1 and set $t_2 = t_2^*$. We then have that $\theta_1 = \pi - \gamma_1^+ = \gamma$ and so

$$\begin{aligned}
& E(t_1,t_2^*) - E(t_1^*,t_2^*) \\
= \;& -\frac{\sigma}{2}\cdot\frac{\|\vec{r'}(t_1^*)\|^2}{\|\vec{r}(t_2^*)-\vec{r}(t_1^*)\|}[1-\cos^2\gamma](t_1-t_1^*)^2 + \mathcal{O}\left((t_1-t_1^*)^3\right) \\
< \;& 0
\end{aligned}$$

for t_1 sufficiently close to t_1^* since $\gamma \neq 0, \pi$. Hence, there exists a small perturbation away from the configuration giving lesser energy and thus when $\gamma = \pi - \gamma_1^+$ the configuration is unstable.

- When $\gamma = \pi - \gamma_2^+$, consider case 1 and set $t_1 = t_1^*$. We then have that $\theta_2 = \pi - \gamma_2^+ = \gamma$ and so

$$\begin{aligned} & E(t_1^*, t_2) - E(t_1^*, t_2^*) \\ = & -\frac{\sigma}{2} \cdot \frac{\|\vec{r'}(t_2^*)\|^2}{\|\vec{r}(t_2^*) - \vec{r}(t_1^*)\|}[1 - \cos^2\gamma](t_2 - t_2^*)^2 + \mathcal{O}\left((t_2 - t_2^*)^3\right) \\ < & \ 0 \end{aligned}$$

for t_2 sufficiently close to t_2^* since $\gamma \neq 0, \pi$. Hence, there exists a small perturbation away from the configuration giving lesser energy and thus when $\gamma = \pi - \gamma_2^+$ the configuration is unstable.

Now consider when $\gamma = \min(\gamma_1^-, \gamma_2^-)$. Clearly, either $\gamma = \gamma_1^-$ or $\gamma = \gamma_2^-$. We consider either possibility below.

- When $\gamma = \gamma_1^-$, consider case 2 and set $t_2 = t_2^*$. We then have that $\theta_1 = \gamma_1^- = \gamma$ and so

$$\begin{aligned} & E(t_1, t_2^*) - E(t_1^*, t_2^*) \\ = & -\frac{\sigma}{2} \cdot \frac{\|\vec{r'}(t_1^*)\|^2}{\|\vec{r}(t_2^*) - \vec{r}(t_1^*)\|}[1 - \cos^2\gamma](t_1 - t_1^*)^2 + \mathcal{O}\left((t_1 - t_1^*)^3\right) \\ < & \ 0 \end{aligned}$$

for t_1 sufficiently close to t_1^* since $\gamma \neq 0, \pi$. Hence, there exists a small perturbation away from the configuration giving lesser energy and thus when $\gamma = \gamma_1^-$ the configuration is unstable.

- When $\gamma = \gamma_2^-$, consider case 2 and set $t_1 = t_1^*$. We then have that $\theta_2 = \gamma_2^- = \gamma$ and so

$$\begin{aligned} & E(t_1^*, t_2) - E(t_1^*, t_2^*) \\ = & -\frac{\sigma}{2} \cdot \frac{\|\vec{r'}(t_2^*)\|^2}{\|\vec{r}(t_2^*) - \vec{r}(t_1^*)\|}[1 - \cos^2\gamma](t_2 - t_2^*)^2 + \mathcal{O}\left((t_2 - t_2^*)^3\right) \\ < & \ 0 \end{aligned}$$

for t_2 sufficiently close to t_2^* since $\gamma \neq 0, \pi$. Hence, there exists a small perturbation away from the configuration giving lesser energy and thus when $\gamma = \gamma_2^-$ the configuration is unstable.

Using the above derivation as justification, we can now state the following result.

Theorem 5.2. *Consider an infinitely long cylinder with a polygonal cross-section with two vertices on the fluid interface and whose floating angles $\gamma_1^+, \gamma_2^+, \gamma_1^-$ and γ_2^- are as shown in Figure 5.1. Let the three materials in consideration be such that we have contact angle γ. Then the configuration will be stable if we have that*

$$\pi - \min(\gamma_1^+, \gamma_2^+) < \gamma < \min(\gamma_1^-, \gamma_2^-)$$

and unstable otherwise.

Remark 5.2. This necessary and sufficient condition for stable equilibrium of polygonal bodies is noteworthy. It is unexpected that we can conclude the stability of any configuration of a polygonal body with two corners on the fluid interface as long as we are able to determine the four relevant angles. Nonetheless, Theorem 5.2 proves that it really is that straightforward and we will demonstrate the theorem's simplicity with several examples.

5.3 Examples

We will now use the stability condition from Theorem 5.2 to look at the stability of configurations satisfying the necessary condition for stable equilibrium for several different polygonal shapes. Additionally, we will determine the global energy minimum for each of these shapes.

5.3.1 The Triangle

Our first example will be that of a floating infinite cylinder with a constant cross-section in the shape of a triangle. We will denote the triangle's three interior angles by α_1, α_2, and α_3. Clearly each angle is an element of the interval $(0, \pi)$ and we will assume that

$$\alpha_1 \leq \alpha_2 \leq \alpha_3.$$

Due to Theorem 5.1 the only possible floating configurations are ones in which the fluid interface intersects two corners of the triangle. There are six configurations of this type for a general triangle and they are depicted in Figure 5.2. We wish to determine the stability of all configurations for this triangle which we will do using our condition for stability of polygonal cross-sections, Theorem 5.2.

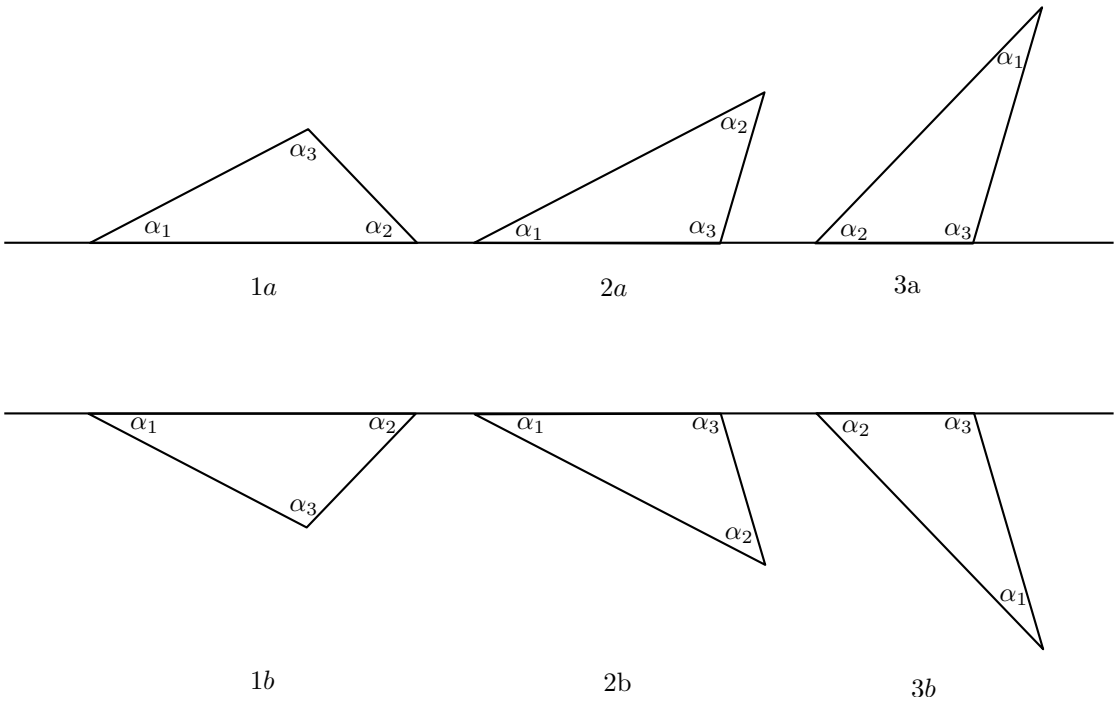

Figure 5.2: *The six possible floating configurations for general triangular cross-section.*

- Configuration 1a has floating angles $\gamma_1^+ = \pi - \alpha_2$, $\gamma_2^+ = \pi - \alpha_1$, $\gamma_1^- = \pi$ and $\gamma_2^- = \pi$ and thus the configuration will be stable if we have that

$$\begin{aligned} & \pi - \min\{\pi - \alpha_2, \pi - \alpha_1\} < \gamma < \min\{\pi, \pi\} \\ \iff \quad & \pi - \pi - \min\{-\alpha_2, -\alpha_1\} < \gamma < \pi \\ \iff \quad & \max\{\alpha_2, \alpha_1\} < \gamma < \pi \\ \iff \quad & \alpha_2 < \gamma < \pi. \end{aligned}$$

- Configuration 1b has floating angles $\gamma_1^+ = \pi$, $\gamma_2^+ = \pi$, $\gamma_1^- = \pi - \alpha_2$ and $\gamma_2^- = \pi - \alpha_1$ and thus the configuration will be stable if we have that

$$\begin{aligned} & \pi - \min\{\pi, \pi\} < \gamma < \min\{\pi - \alpha_2, \pi - \alpha_1\} \\ \iff \quad & 0 < \gamma < \pi + \min\{-\alpha_2, -\alpha_1\} \\ \iff \quad & 0 < \gamma < \pi - \max\{\alpha_1, \alpha_2\} \\ \iff \quad & 0 < \gamma < \pi - \alpha_2. \end{aligned}$$

- Configuration 2a has floating angles $\gamma_1^+ = \pi - \alpha_3$, $\gamma_2^+ = \pi - \alpha_1$, $\gamma_1^- = \pi$ and $\gamma_2^- = \pi$

and thus the configuration will be stable if we have that

$$\begin{aligned} & \pi - \min\{\pi - \alpha_1, \pi - \alpha_3\} < \gamma < \min\{\pi, \pi\} \\ \iff \quad & \pi - \pi - \min\{-\alpha_1, -\alpha_3\} < \gamma < \pi \\ \iff \quad & \max\{\alpha_1, \alpha_3\} < \gamma < \pi \\ \iff \quad & \alpha_3 < \gamma < \pi. \end{aligned}$$

- Configuration 2b has floating angles $\gamma_1^+ = \pi$, $\gamma_2^+ = \pi$, $\gamma_1^- = \pi - \alpha_3$ and $\gamma_2^- = \pi - \alpha_1$ and thus the configuration will be stable if we have that

$$\begin{aligned} & \pi - \min\{\pi, \pi\} < \gamma < \min\{\pi - \alpha_1, \pi - \alpha_3\} \\ \iff \quad & 0 < \gamma < \pi + \min\{-\alpha_1, -\alpha_3\} \\ \iff \quad & 0 < \gamma < \pi - \max\{\alpha_1, \alpha_3\} \\ \iff \quad & 0 < \gamma < \pi - \alpha_3. \end{aligned}$$

- Configuration 3a has floating angles $\gamma_1^+ = \pi - \alpha_3$, $\gamma_2^+ = \pi - \alpha_2$, $\gamma_1^- = \pi$ and $\gamma_2^- = \pi$ and thus the configuration will be stable if we have that

$$\begin{aligned} & \pi - \min\{\pi - \alpha_2, \pi - \alpha_3\} < \gamma < \min\{\pi, \pi\} \\ \iff \quad & \pi - \pi - \min\{-\alpha_2, -\alpha_3\} < \gamma < \pi \\ \iff \quad & \max\{\alpha_2, \alpha_3\} < \gamma < \pi \\ \iff \quad & \alpha_3 < \gamma < \pi. \end{aligned}$$

- Configuration 3b has floating angles $\gamma_1^+ = \pi$, $\gamma_2^+ = \pi$, $\gamma_1^- = \pi - \alpha_3$ and $\gamma_2^- = \pi - \alpha_2$ and thus the configuration will be stable if we have that

$$\begin{aligned} & \pi - \min\{\pi, \pi\} < \gamma < \min\{\pi - \alpha_2, \pi - \alpha_3\} \\ \iff \quad & 0 < \gamma < \pi + \min\{-\alpha_2, -\alpha_3\} \\ \iff \quad & 0 < \gamma < \pi - \max\{\alpha_2, \alpha_3\} \\ \iff \quad & 0 < \gamma < \pi - \alpha_3. \end{aligned}$$

The conditions on the angles as found in the above six cases can then be used to prove the following theorem.

Theorem 5.3. *Consider any triangle floating in one of the six possible configurations with the three materials in consideration giving contact angle γ. Then:*

- *If the body is above the fluid interface (in the σ_1 medium) the configuration will be stable provided γ is greater than the bigger of the two angles of the triangle's corners on the fluid interface but less than π.*

- *If the body is below the fluid interface (in the σ_2 medium) the configuration will be stable provided γ is greater than 0 but less than the supplement of the larger of the two angles of the triangle's corners on the fluid interface.*
- *If neither of the above two statements is true, then the configuration is unstable.*

We can now extend this result for stability of a general triangular cross-section to one that also includes information about the global energy minimum by directly comparing the energies associated with the six possible floating configurations to one another. We consider the same general triangle with interior angles obeying the same relationship:

$$0 < \alpha_1 \leq \alpha_2 \leq \alpha_3 < \pi.$$

We will also label the side lengths as in Figure 5.3.

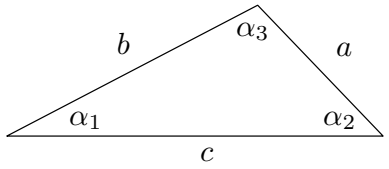

Figure 5.3: *The labelling of the angles and side lengths in our general triangle.*

By the property of triangles, we will then have that

$$0 < a \leq b \leq c.$$

We now have that the energies of the six configurations are given by

$$\begin{aligned}
E_{1a} &= (a+b)\sigma_1 + c\sigma_2 - c\sigma \\
E_{1b} &= c\sigma_1 + (a+b)\sigma_2 - c\sigma \\
E_{2a} &= (a+c)\sigma_1 + b\sigma_2 - b\sigma \\
E_{2b} &= b\sigma_1 + (a+c)\sigma_2 - b\sigma \\
E_{3a} &= (b+c)\sigma_1 + a\sigma_2 - a\sigma \\
E_{3b} &= a\sigma_1 + (b+c)\sigma_2 - a\sigma
\end{aligned}$$

and now we can compare these energies. The relationship between the energies of the six configurations will depend on the relationship between the lengths of the sides of the triangle. There are three cases; the relationships between the six energies in each of the three cases for each possible value of γ are summarized in Tables 5.1, 5.2, and 5.3, which are located at the end of this subsection. For details behind the creation of the three tables, see Section E.1 in Appendix E. In all three cases it is clear from a close examination of these tables that

- when $\gamma \in \left(0, \frac{\pi}{2}\right)$, configuration 1b gives the global energy minimum,
- when $\gamma = \frac{\pi}{2}$, configurations 1a and 1b give the same energy which is also the global energy minimum, and
- when $\gamma \in \left(\frac{\pi}{2}, \pi\right)$, configuration 1a gives the global energy minimum.

So, we can extend Theorem 5.3 to give a result concerning the global energy minimum and stability of configurations of the triangular cross-section as well.

Theorem 5.4. *Consider any triangle floating in one of the six possible floating configurations with the three materials giving contact angle γ. Then:*

1. *If the body is floating in the σ_1 medium with the longest side incident with the fluid interface and $\gamma \in \left[\frac{\pi}{2}, \pi\right)$, the configuration will be a stable global energy minimum.*
2. *If the body is floating in the σ_1 medium without the longest side incident with the fluid interface and γ is greater than the larger of the two angles of the triangle's corners on the fluid interface but less than π, the configuration will be stable, but not a global energy minimum.*
3. *If the body is floating in the σ_2 medium with the longest side incident with the fluid interface and $\gamma \in \left(0, \frac{\pi}{2}\right]$, the configuration will be a stable global energy minimum.*
4. *If the body is floating in the σ_2 medium without the longest side incident with the fluid interface and γ is greater than 0 but less than the supplement of the larger of the two angles of the triangle's corners on the interface, the configuration will be stable, but not a global energy minimum.*
5. *If none of the above hold, the configuration is unstable.*

Proof.

1. Since the longest side is incident with the fluid interface, it must mean that the two corners of the triangle that are on the fluid interface are the corners with interior angles α_1 and α_2, the larger of which is α_2. Applying Theorem 5.3 tells us that the configuration will be stable when $\gamma \in (\alpha_2, \pi)$. Since $\alpha_2 < \frac{\pi}{2}$ and $\gamma \in \left[\frac{\pi}{2}, \pi\right)$ we have that the configuration is stable.[1] In addition, using Tables 5.1, 5.2, and 5.3, $\gamma \in \left[\frac{\pi}{2}, \pi\right)$ also implies that the configuration is a global energy minimum.

[1] We must have that $\alpha_2 < \frac{\pi}{2}$. If not, then α_3 is also greater than or equal to $\frac{\pi}{2}$. Then $\alpha_2 + \alpha_3 \geq \pi$ meaning $\alpha_1 \leq 0$ which is clearly a contradiction.

2. The configuration is stable by Theorem 5.3. It will not be a global energy minimum since a global energy minimum requires that the longest side be incident with the fluid interface.

3. Since the longest side is incident with the fluid interface, it must mean that the two corners of the triangle that are on the fluid interface are the corners with interior angles α_1 and α_2, the larger of which is α_2. Applying Theorem 5.3 tells us that the configuration will be stable when $\gamma \in (0, \pi - \alpha_2)$. Since $\alpha_2 < \frac{\pi}{2}$ and $\gamma \in \left(0, \frac{\pi}{2}\right]$ we have that the configuration is stable. In addition, using Tables 5.1, 5.2, and 5.3, $\gamma \in \left(0, \frac{\pi}{2}\right]$ also implies that the configuration is a global energy minimum.

4. Same as proof item 2.

5. Theorem 5.3 applies, giving the desired result. □

Table 5.1: *Relationships between the energies of the six possible floating configurations of the triangle for each value of* $\gamma \in (0, \pi)$ *in the* $b < \frac{a^2+c^2}{a+c}$ *case.*

Values for γ	**Energy Relationships**
$\left(0, \arccos\left(\frac{c-a}{b}\right)\right)$	$E_{1b} < E_{2b} < E_{3b} < E_{1a} < E_{2a} < E_{3a}$
$\arccos\left(\frac{c-a}{b}\right)$	$E_{1b} < E_{2b} < E_{3b} = E_{1a} < E_{2a} < E_{3a}$
$\left(\arccos\left(\frac{c-a}{b}\right), \arccos\left(\frac{c-b}{a}\right)\right)$	$E_{1b} < E_{2b} < E_{1a} < E_{3b} < E_{2a} < E_{3a}$
$\arccos\left(\frac{c-b}{a}\right)$	$E_{1b} < E_{2b} = E_{1a} < E_{3b} < E_{2a} < E_{3a}$
$\left(\arccos\left(\frac{c-b}{a}\right), \arccos\left(\frac{b-a}{c}\right)\right)$	$E_{1b} < E_{1a} < E_{2b} < E_{3b} < E_{2a} < E_{3a}$
$\arccos\left(\frac{b-a}{c}\right)$	$E_{1b} < E_{1a} < E_{2b} < E_{3b} = E_{2a} < E_{3a}$
$\left(\arccos\left(\frac{b-a}{c}\right), \frac{\pi}{2}\right)$	$E_{1b} < E_{1a} < E_{2b} < E_{2a} < E_{3b} < E_{3a}$
$\frac{\pi}{2}$	$E_{1b} = E_{1a} < E_{2b} = E_{2a} < E_{3b} = E_{3a}$
$\left(\frac{\pi}{2}, \pi - \arccos\left(\frac{b-a}{c}\right)\right)$	$E_{1a} < E_{1b} < E_{2a} < E_{2b} < E_{3a} < E_{3b}$
$\pi - \arccos\left(\frac{b-a}{c}\right)$	$E_{1a} < E_{1b} < E_{2a} < E_{2b} = E_{3a} < E_{3b}$
$\left(\pi - \arccos\left(\frac{b-a}{c}\right), \pi - \arccos\left(\frac{c-b}{a}\right)\right)$	$E_{1a} < E_{1b} < E_{2a} < E_{3a} < E_{2b} < E_{3b}$
$\pi - \arccos\left(\frac{c-b}{a}\right)$	$E_{1a} < E_{1b} = E_{2a} < E_{3a} < E_{2b} < E_{3b}$
$\left(\pi - \arccos\left(\frac{c-b}{a}\right), \pi - \arccos\left(\frac{c-a}{b}\right)\right)$	$E_{1a} < E_{2a} < E_{1b} < E_{3a} < E_{2b} < E_{3b}$
$\pi - \arccos\left(\frac{c-a}{b}\right)$	$E_{1a} < E_{2a} < E_{1b} = E_{3a} < E_{2b} < E_{3b}$
$\left(\pi - \arccos\left(\frac{c-a}{b}\right), \pi\right)$	$E_{1a} < E_{2a} < E_{3a} < E_{1b} < E_{2b} < E_{3b}$

Table 5.2: *Relationships between the energies of the six possible floating configurations of the triangle for each value of* $\gamma \in (0, \pi)$ *in the* $b = \frac{a^2+c^2}{a+c}$ *case.*

Values for γ	**Energy Relationships**
$\left(0, \arccos\left(\frac{c-a}{b}\right)\right)$	$E_{1b} < E_{2b} < E_{3b} < E_{1a} < E_{2a} < E_{3a}$
$\arccos\left(\frac{c-a}{b}\right)$	$E_{1b} < E_{2b} < E_{3b} = E_{1a} < E_{2a} < E_{3a}$
$\left(\arccos\left(\frac{c-a}{b}\right), \arccos\left(\frac{c-b}{a}\right)\right)$	$E_{1b} < E_{2b} < E_{1a} < E_{3b} < E_{2a} < E_{3a}$
$\arccos\left(\frac{c-b}{a}\right)$	$E_{1b} < E_{2b} = E_{1a} < E_{3b} = E_{2a} < E_{3a}$
$\left(\arccos\left(\frac{c-b}{a}\right), \frac{\pi}{2}\right)$	$E_{1b} < E_{1a} < E_{2b} < E_{2a} < E_{3b} < E_{3a}$
$\frac{\pi}{2}$	$E_{1b} = E_{1a} < E_{2b} = E_{2a} < E_{3b} = E_{3a}$
$\left(\frac{\pi}{2}, \pi - \arccos\left(\frac{c-b}{a}\right)\right)$	$E_{1a} < E_{1b} < E_{2a} < E_{2b} < E_{3a} < E_{3b}$
$\pi - \arccos\left(\frac{c-b}{a}\right)$	$E_{1a} < E_{1b} = E_{2a} < E_{2b} = E_{3a} < E_{3b}$
$\left(\pi - \arccos\left(\frac{c-b}{a}\right), \pi - \arccos\left(\frac{c-a}{b}\right)\right)$	$E_{1a} < E_{2a} < E_{1b} < E_{3a} < E_{2b} < E_{3b}$
$\pi - \arccos\left(\frac{c-a}{b}\right)$	$E_{1a} < E_{2a} < E_{1b} = E_{3a} < E_{2b} < E_{3b}$
$\left(\pi - \arccos\left(\frac{c-a}{b}\right), \pi\right)$	$E_{1a} < E_{2a} < E_{3a} < E_{1b} < E_{2b} < E_{3b}$

Table 5.3: *Relationships between the energies of the six possible floating configurations of the triangle for each value of* $\gamma \in (0, \pi)$ *in the* $b > \frac{a^2+c^2}{a+c}$ *case.*

Values for γ	**Energy Relationships**
$\left(0, \arccos\left(\frac{c-a}{b}\right)\right)$	$E_{1b} < E_{2b} < E_{3b} < E_{1a} < E_{2a} < E_{3a}$
$\arccos\left(\frac{c-a}{b}\right)$	$E_{1b} < E_{2b} < E_{3b} = E_{1a} < E_{2a} < E_{3a}$
$\left(\arccos\left(\frac{c-a}{b}\right), \arccos\left(\frac{b-a}{c}\right)\right)$	$E_{1b} < E_{2b} < E_{1a} < E_{3b} < E_{2a} < E_{3a}$
$\arccos\left(\frac{b-a}{c}\right)$	$E_{1b} < E_{2b} < E_{1a} < E_{3b} = E_{2a} < E_{3a}$
$\left(\arccos\left(\frac{b-a}{c}\right), \arccos\left(\frac{c-b}{a}\right)\right)$	$E_{1b} < E_{2b} < E_{1a} < E_{2a} < E_{3b} < E_{3a}$
$\arccos\left(\frac{c-b}{a}\right)$	$E_{1b} < E_{2b} = E_{1a} < E_{2a} < E_{3b} < E_{3a}$
$\left(\arccos\left(\frac{c-b}{a}\right), \frac{\pi}{2}\right)$	$E_{1b} < E_{1a} < E_{2b} < E_{2a} < E_{3b} < E_{3a}$
$\frac{\pi}{2}$	$E_{1b} = E_{1a} < E_{2b} = E_{2a} < E_{3b} = E_{3a}$
$\left(\frac{\pi}{2}, \pi - \arccos\left(\frac{c-b}{a}\right)\right)$	$E_{1a} < E_{1b} < E_{2a} < E_{2b} < E_{3a} < E_{3b}$
$\pi - \arccos\left(\frac{c-b}{a}\right)$	$E_{1a} < E_{1b} = E_{2a} < E_{2b} < E_{3a} < E_{3b}$
$\left(\pi - \arccos\left(\frac{c-b}{a}\right), \pi - \arccos\left(\frac{b-a}{c}\right)\right)$	$E_{1a} < E_{2a} < E_{1b} < E_{2b} < E_{3a} < E_{3b}$
$\pi - \arccos\left(\frac{b-a}{c}\right)$	$E_{1a} < E_{2a} < E_{1b} < E_{2b} = E_{3a} < E_{3b}$
$\left(\pi - \arccos\left(\frac{b-a}{c}\right), \pi - \arccos\left(\frac{c-a}{b}\right)\right)$	$E_{1a} < E_{2a} < E_{1b} < E_{3a} < E_{2b} < E_{3b}$
$\pi - \arccos\left(\frac{c-a}{b}\right)$	$E_{1a} < E_{2a} < E_{1b} = E_{3a} < E_{2b} < E_{3b}$
$\left(\pi - \arccos\left(\frac{c-a}{b}\right), \pi\right)$	$E_{1a} < E_{2a} < E_{3a} < E_{1b} < E_{2b} < E_{3b}$

5.3.2 The Square

For our second example we consider an infinitely long cylinder with a square cross-section of unit side length. Using Theorem 5.1 we know that the only possible floating configurations are ones in which the fluid interface intersects two corners of the square. There are three such configurations as shown in Figure 5.4. Using Theorem 5.2 we can classify the stability of these three configurations.

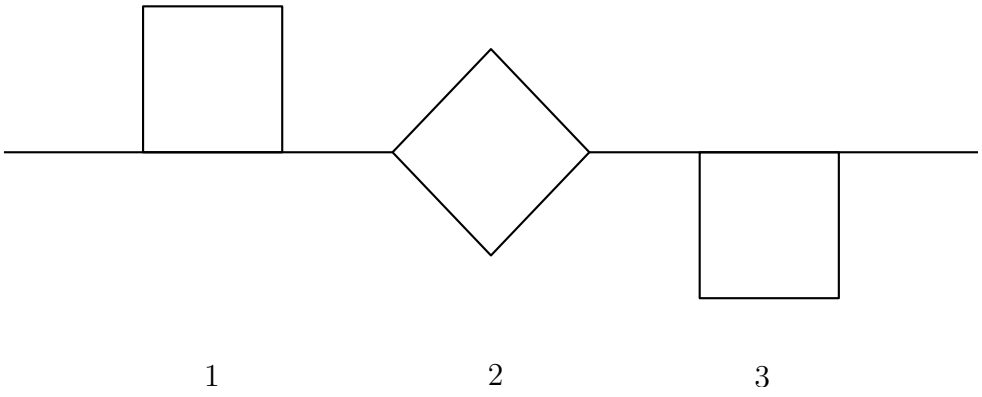

Figure 5.4: *The three possible floating configurations for a square cross-section.*

- Configuration 1 has floating angles $\gamma_1^+ = \gamma_2^+ = \frac{\pi}{2}$ and $\gamma_1^- = \gamma_2^- = \pi$ so it will be stable when we have that $\pi - \frac{\pi}{2} < \gamma < \pi \Leftrightarrow \frac{\pi}{2} < \gamma < \pi$.
- Configuration 2 has floating angles $\gamma_1^+ = \gamma_2^+ = \gamma_1^- = \gamma_2^- = \frac{3\pi}{4}$ so it will be stable when we have that $\pi - \frac{3\pi}{4} < \gamma < \frac{3\pi}{4} \Leftrightarrow \frac{\pi}{4} < \gamma < \frac{3\pi}{4}$.
- Configuration 3 has floating angles $\gamma_1^+ = \gamma_2^+ = \pi$ and $\gamma_1^- = \gamma_2^- = \frac{\pi}{2}$ so it will be stable when we have that $\pi - \pi < \gamma < \frac{\pi}{2} \Leftrightarrow 0 < \gamma < \frac{\pi}{2}$.

Otherwise, when γ is not within the specified range of values, the configuration will be unstable.

Now, to determine which configuration is a global energy minimum, we need to directly compare the energy associated with each of the three configurations. The energies of the three configurations are given by

$$\begin{aligned} E_1 &= 3\sigma_1 + \sigma_2 - \sigma \\ E_2 &= 2\sigma_1 + 2\sigma_2 - \sqrt{2}\sigma \\ E_3 &= \sigma_1 + 3\sigma_2 - \sigma. \end{aligned}$$

Subsection 5.3.2 is reprinted with permission from reference [14].

The relationships between the energies change depending on the value of γ. The relationships are summarized in Table 5.4; for the underlying details of the creation of Table 5.4 see Section E.2 in Appendix E. Using Table 5.4 we are able to determine which configuration is the global energy minimum for each value of γ and since we already know the stability of each of the three configurations for each value of γ we can summarize the stability behaviour of the square cross-section in Table 5.5.

Table 5.4: *Relationships between the energies of the three possible configurations of the square for each value of* $\gamma \in (0, \pi)$.

Values for γ	**Energy Relationships**
$(0, \arccos(\sqrt{2}-1))$	$E_3 < E_2 < E_1$
$\arccos(\sqrt{2}-1)$	$E_3 = E_2 < E_1$
$(\arccos(\sqrt{2}-1), \frac{\pi}{2})$	$E_2 < E_3 < E_1$
$\frac{\pi}{2}$	$E_2 < E_3 = E_1$
$(\frac{\pi}{2}, \arccos(1-\sqrt{2}))$	$E_2 < E_1 < E_3$
$\arccos(1-\sqrt{2})$	$E_2 = E_1 < E_3$
$(\arccos(1-\sqrt{2}), \pi)$	$E_1 < E_2 < E_3$

Table 5.5: *The stability of each of the three possible floating configurations for the square (as depicted in Figure 5.4)and for each value of* $\gamma \in (0, \pi)$ *is shown here. Note that here we have* $v = \arccos(\sqrt{2}-1)$.

	$\left(0, \frac{\pi}{4}\right]$	$\left(\frac{\pi}{4}, v\right)$	v	$\left(v, \frac{\pi}{2}\right)$	$\frac{\pi}{2}$
Configuration 1	Unstable				
Configuration 2	Unstable	Stable	Stable Global Energy Minimum		
Configuration 3	Stable Global Energy Minimum			Stable	Unstable

	$\left(\frac{\pi}{2}, \pi - v\right)$	$\pi - v$	$\left(\pi - v, \frac{3\pi}{4}\right)$	$\left[\frac{3\pi}{4}, \pi\right)$
Configuration 1	Stable	Stable Global Energy Minimum		
Configuration 2	Stable Global Energy Minimum		Stable	Unstable
Configuration 3	Unstable			

5.3.3 The Rectangle

Our next example will be that of a more general quadrilateral, the rectangle. We consider an infinitely long cylinder with rectangular cross-section having side lengths 1 and b where $b > 1$. Similar to the square cross-section, the only configurations for which floating is possible are ones in which the fluid interface intersects two corners of the rectangle. There are six configurations of this type for a rectangular cross-section. However, the fifth and would-be sixth configurations are symmetric about a vertical line, so we will consider only the first five configurations, shown in Figure 5.5.

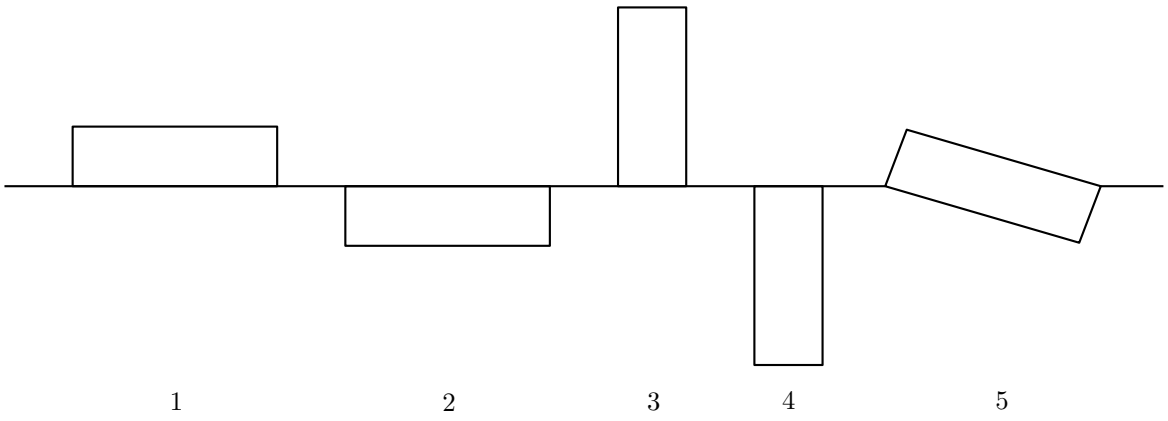

Figure 5.5: *The five possible floating configurations for a rectangular cross-section.*

Again, using our stability criterion for equilibrium configurations of polygonal cross-sections (Theorem 5.2) we can classify the stability of these five configurations.

- Configurations 1 and 3 have floating angles $\gamma_1^+ = \gamma_2^+ = \frac{\pi}{2}$ and $\gamma_1^- = \gamma_2^- = \pi$ and hence are stable when we have that $\frac{\pi}{2} < \gamma < \pi$.
- Configurations 2 and 4 have floating angles $\gamma_1^+ = \gamma_2^+ = \pi$ and $\gamma_1^- = \gamma_2^- = \frac{\pi}{2}$ and hence are stable when we have that $0 < \gamma < \frac{\pi}{2}$.
- Configuration 5 has $\gamma_1^+ = \gamma_2^- = \pi - \arctan(\frac{1}{b})$ and $\gamma_1^- = \gamma_2^+ = \pi - \arctan b$ and hence is stable when $\arctan(b) < \gamma < \pi - \arctan(b)$ since we have that

$$\begin{aligned} & \min\left\{\pi - \arctan\left(\frac{1}{b}\right), \pi - \arctan b\right\} \\ = \;& \pi - \max\left\{\arctan\left(\frac{1}{b}\right), \arctan b\right\} \\ = \;& \pi - \arctan\left(\max\left\{\frac{1}{b}, b\right\}\right) \\ = \;& \pi - \arctan b. \end{aligned}$$

Now, to determine which configuration is the global energy minimum, we need to directly compare the energy associated with each of the five configurations. The energies of the five configurations are given by

$$\begin{aligned} E_1 &= (b+2)\sigma_1 + b\sigma_2 - b\sigma \\ E_2 &= b\sigma_1 + (b+2)\sigma_2 - b\sigma \\ E_3 &= (2b+1)\sigma_1 + \sigma_2 - \sigma \\ E_4 &= \sigma_1 + (2b+1)\sigma_2 - \sigma \\ E_5 &= (b+1)(\sigma_1 + \sigma_2) - \sqrt{1+b^2}\sigma. \end{aligned}$$

Again, the relationships between the various energies depends on γ, and we will also find that the relationships between the energies depends on b. There are three cases: $1 < b < \sqrt{3}$, $b = \sqrt{3}$, and $b > \sqrt{3}$; the energy relationships in each of these three cases for each value of γ are summarized in Tables 5.6, 5.7, and 5.8 and are shown at the end of this subsection. For a detailed account of the creation of these tables, see Section E.3 in Appendix E.

From Tables 5.6, 5.7 and 5.8 it can be seen that the configuration giving least energy changes from one configuration to another at the following values of γ:

$$\arccos\left(\sqrt{1+b^2} - b\right), \qquad \text{and} \qquad \arccos\left(b - \sqrt{1+b^2}\right).$$

Other values of γ do not result in a change in the configuration giving least energy. Using this, we can see which configuration gives the global energy minimum for each γ in each of the three cases. This, together with the stability requirements outlined earlier, allows us to summarize the floating behaviour for each possible configuration and each $\gamma \in (0, \pi)$ for the rectangular cross-section as shown in Table 5.9 on page 41.

Table 5.6: *Relationships between the energies of the five possible floating configurations for the rectangle for each value of* $\gamma \in (0, \pi)$ *in the* $1 < b < \sqrt{3}$ *case.*

Values for γ	**Energy Relationships**
$\left(0, \arccos\left(\frac{\sqrt{1+b^2}-1}{b}\right)\right)$	$E_2 < E_4 < E_5 < E_1 < E_3$
$\arccos\left(\frac{\sqrt{1+b^2}-1}{b}\right)$	$E_2 < E_4 = E_5 < E_1 < E_3$
$\left(\arccos\left(\frac{\sqrt{1+b^2}-1}{b}\right), \arccos\left(\sqrt{1+b^2}-b\right)\right)$	$E_2 < E_5 < E_4 < E_1 < E_3$
$\arccos\left(\sqrt{1+b^2}-b\right)$	$E_2 = E_5 < E_4 < E_1 < E_3$
$\left(\arccos\left(\sqrt{1+b^2}-b\right), \arccos\left(\frac{b-1}{b+1}\right)\right)$	$E_5 < E_2 < E_4 < E_1 < E_3$
$\arccos\left(\frac{b-1}{b+1}\right)$	$E_5 < E_2 < E_4 = E_1 < E_3$
$\left(\arccos\left(\frac{b-1}{b+1}\right), \frac{\pi}{2}\right)$	$E_5 < E_2 < E_1 < E_4 < E_3$
$\frac{\pi}{2}$	$E_5 < E_2 = E_1 < E_4 = E_3$
$\left(\frac{\pi}{2}, \arccos\left(\frac{1-b}{b+1}\right)\right)$	$E_5 < E_1 < E_2 < E_3 < E_4$
$\arccos\left(\frac{1-b}{b+1}\right)$	$E_5 < E_1 < E_2 = E_3 < E_4$
$\left(\arccos\left(\frac{1-b}{b+1}\right), \arccos\left(b-\sqrt{1+b^2}\right)\right)$	$E_5 < E_1 < E_3 < E_2 < E_4$
$\arccos\left(b-\sqrt{1+b^2}\right)$	$E_5 = E_1 < E_3 < E_2 < E_4$
$\left(\arccos\left(b-\sqrt{1+b^2}\right), \arccos\left(\frac{1-\sqrt{1+b^2}}{b}\right)\right)$	$E_1 < E_5 < E_3 < E_2 < E_4$
$\arccos\left(\frac{1-\sqrt{1+b^2}}{b}\right)$	$E_1 < E_5 = E_3 < E_2 < E_4$
$\left(\arccos\left(\frac{1-\sqrt{1+b^2}}{b}\right), \pi\right)$	$E_1 < E_3 < E_5 < E_2 < E_4$

Table 5.7: *Relationships between the energies of the five possible floating configurations for the rectangle for each value of* $\gamma \in (0, \pi)$ *in the* $b = \sqrt{3}$ *case.*

Values for γ	**Energy Relationships**
$\left(0, \arccos\left(\frac{\sqrt{1+b^2}-1}{b}\right)\right)$	$E_2 < E_4 < E_5 < E_1 < E_3$
$\arccos\left(\frac{\sqrt{1+b^2}-1}{b}\right)$	$E_2 < E_4 = E_5 < E_1 < E_3$
$\left(\arccos\left(\frac{\sqrt{1+b^2}-1}{b}\right), \arccos\left(\sqrt{1+b^2}-b\right)\right)$	$E_2 < E_5 < E_4 < E_1 < E_3$
$\arccos\left(\sqrt{1+b^2}-b\right)$	$E_2 = E_5 < E_4 < E_1 < E_3$
$\left(\arccos\left(\sqrt{1+b^2}-b\right), \frac{\pi}{2}\right)$	$E_5 < E_2 < E_1 < E_4 < E_3$
$\frac{\pi}{2}$	$E_5 < E_2 = E_1 < E_4 = E_3$
$\left(\frac{\pi}{2}, \arccos\left(b-\sqrt{1+b^2}\right)\right)$	$E_5 < E_1 < E_2 < E_3 < E_4$
$\arccos\left(b-\sqrt{1+b^2}\right)$	$E_5 = E_1 < E_3 < E_2 < E_4$
$\left(\arccos\left(b-\sqrt{1+b^2}\right), \arccos\left(\frac{1-\sqrt{1+b^2}}{b}\right)\right)$	$E_1 < E_5 < E_3 < E_2 < E_4$
$\arccos\left(\frac{1-\sqrt{1+b^2}}{b}\right)$	$E_1 < E_5 = E_3 < E_2 < E_4$
$\left(\arccos\left(\frac{1-\sqrt{1+b^2}}{b}\right), \pi\right)$	$E_1 < E_3 < E_5 < E_2 < E_4$

Table 5.8: *Relationships between the energies of the five possible floating configurations for the rectangle for each value of $\gamma \in (0, \pi)$ in the $b > \sqrt{3}$ case.*

Values for γ	**Energy Relationships**
$\left(0, \arccos\left(\frac{\sqrt{1+b^2}-1}{b}\right)\right)$	$E_2 < E_4 < E_5 < E_1 < E_3$
$\arccos\left(\frac{\sqrt{1+b^2}-1}{b}\right)$	$E_2 < E_4 = E_5 < E_1 < E_3$
$\left(\arccos\left(\frac{\sqrt{1+b^2}-1}{b}\right), \arccos\left(\frac{b-1}{b+1}\right)\right)$	$E_2 < E_5 < E_4 < E_1 < E_3$
$\arccos\left(\frac{b-1}{b+1}\right)$	$E_2 < E_5 < E_4 = E_1 < E_3$
$\left(\arccos\left(\frac{b-1}{b+1}\right), \arccos\left(\sqrt{1+b^2}-b\right)\right)$	$E_2 < E_5 < E_1 < E_4 < E_3$
$\arccos\left(\sqrt{1+b^2}-b\right)$	$E_2 = E_5 < E_1 < E_4 < E_3$
$\left(\arccos\left(\sqrt{1+b^2}-b\right), \frac{\pi}{2}\right)$	$E_5 < E_2 < E_1 < E_4 < E_3$
$\frac{\pi}{2}$	$E_5 < E_2 = E_1 < E_4 = E_3$
$\left(\frac{\pi}{2}, \arccos\left(b-\sqrt{1+b^2}\right)\right)$	$E_5 < E_1 < E_2 < E_3 < E_4$
$\arccos\left(b-\sqrt{1+b^2}\right)$	$E_5 = E_1 < E_2 < E_3 < E_4$
$\left(\arccos\left(b-\sqrt{1+b^2}\right), \arccos\left(\frac{1-b}{b+1}\right)\right)$	$E_1 < E_5 < E_2 < E_3 < E_4$
$\arccos\left(\frac{1-b}{b+1}\right)$	$E_1 < E_5 < E_2 = E_3 < E_4$
$\left(\arccos\left(\frac{1-b}{b+1}\right), \arccos\left(\frac{1-\sqrt{1+b^2}}{b}\right)\right)$	$E_1 < E_5 < E_3 < E_2 < E_4$
$\arccos\left(\frac{1-\sqrt{1+b^2}}{b}\right)$	$E_1 < E_5 = E_3 < E_2 < E_4$
$\left(\arccos\left(\frac{1-\sqrt{1+b^2}}{b}\right), \pi\right)$	$E_1 < E_3 < E_5 < E_2 < E_4$

Table 5.9: *The stability of each of the five possible floating configurations for the rectangle (as depicted in Figure 5.5) and each value of* $\gamma \in (0, \pi)$ *is shown here. Note that* $v = \sqrt{1 + b^2} - b$.

	$(0, \arctan b]$	$(\arctan b, \arccos v)$	$\arccos v$	$\left(\arccos v, \frac{\pi}{2}\right)$	$\frac{\pi}{2}$
Configuration 1	Unstable				
Configuration 2	Stable Global Energy Minimum			Stable	Unstable
Configuration 3	Unstable				
Configuration 4	Stable				Unstable
Configuration 5	Unstable	Stable	Stable Global Energy Minimum		

	$\left(\frac{\pi}{2}, \pi - \arccos v\right)$	$\pi - \arccos v$	$(\pi - \arccos v, \pi - \arctan b)$	$[\pi - \arctan b, \pi)$
Configuration 1	Stable	Stable Global Energy Minimum		
Configuration 2	Unstable			
Configuration 3	Stable			
Configuration 4	Unstable			
Configuration 5	Stable Global Energy Minimum		Stable	Unstable

5.3.4 The Regular Pentagon

We will now consider an infinitely long cylinder with pentagonal cross-section. For simplicity, the pentagon will be assumed to be regular, with each side length being 1. Using Theorem 5.1, the only configurations for which floating is possible are ones in which the fluid interface intersects two corners of the pentagon. There are four distinct configurations of this type for a pentagonal cross-section and they are depicted in Figure 5.6.

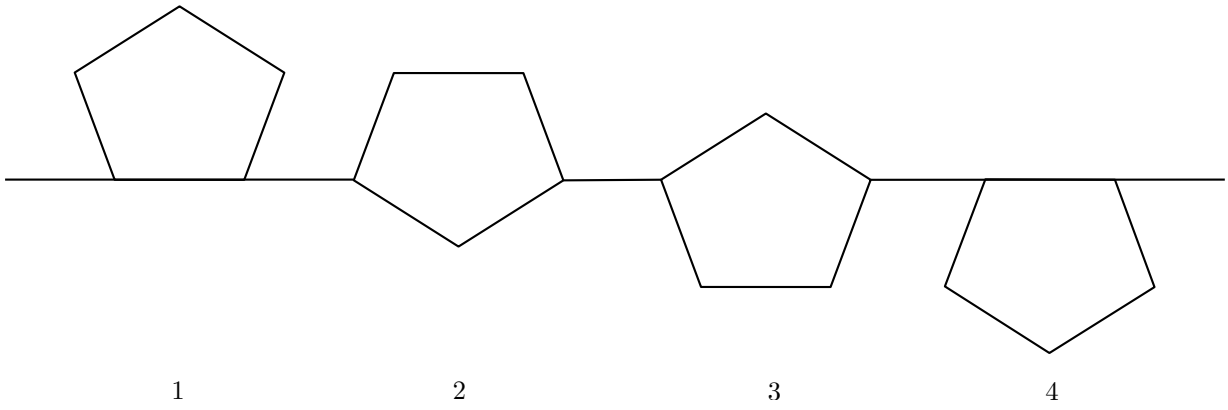

Figure 5.6: *The four possible floating configurations for the pentagonal cross-section.*

Again, using Theorem 5.2 we can classify the stability of these four configurations.

- Configuration 1 has floating angles $\gamma_1^+ = \gamma_2^+ = \frac{2\pi}{5}$ and $\gamma_1^- = \gamma_2^- = \pi$ and hence will be stable when we have that $\frac{3\pi}{5} < \gamma < \pi$.
- Configuration 2 has floating angles $\gamma_1^+ = \gamma_2^+ = \frac{3\pi}{5}$ and $\gamma_1^- = \gamma_2^- = \frac{4\pi}{5}$ and hence will be stable when we have that $\frac{2\pi}{5} < \gamma < \frac{4\pi}{5}$.
- Configuration 3 has floating angles $\gamma_1^+ = \gamma_2^+ = \frac{4\pi}{5}$ and $\gamma_1^- = \gamma_2^- = \frac{3\pi}{5}$ and hence will be stable when we have that $\frac{\pi}{5} < \gamma < \frac{3\pi}{5}$.
- Configuration 4 has floating angles $\gamma_1^+ = \gamma_2^+ = \pi$ and $\gamma_1^- = \gamma_2^- = \frac{2\pi}{5}$ and hence will be stable when we have that $\frac{3\pi}{5} < \gamma < \pi$.

Otherwise, when γ is outside of these specified ranges, the configurations are unstable.

Now, to determine which configuration gives the global energy minimum we need to directly compare the energy associated with each of the four configurations. Using Figure

5.7 we have that the energies of the configurations are given by

$$\begin{aligned} E_1 &= 4\sigma_1 + \sigma_2 - \sigma \\ E_2 &= 3\sigma_1 + 2\sigma_2 - \varphi\sigma \\ E_3 &= 2\sigma_1 + 3\sigma_2 - \varphi\sigma \\ E_4 &= \sigma_1 + 4\sigma_2 - \sigma \end{aligned}$$

where φ is the golden ratio[2] $\varphi = \frac{\sqrt{5}+1}{2}$. We directly compare the energies in Section E.4 of Appendix E. A comparison of the energies reveals that the relationships between the energies of the various configurations change depending on the value of γ. The relationships are given in Table 5.10 and we can then summarize the stability of each of the four configurations for each possible value of γ in Table 5.11.

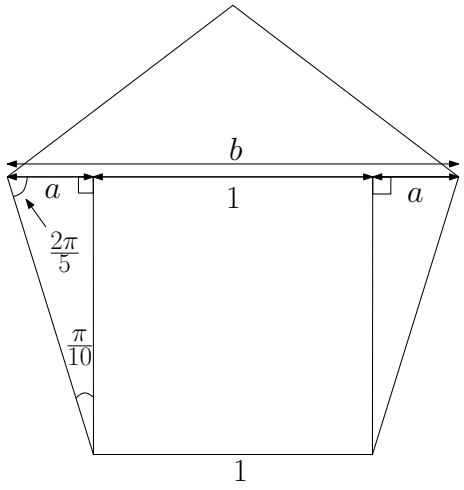

Figure 5.7: *The unknown length b is found using the angles of the indicated triangle. Using the Sine Law, length* $a = \sin\left(\frac{\pi}{10}\right) = \frac{\sqrt{5}-1}{4}$ *and then since length b is twice length a plus one, we have* $b = 2\left(\frac{\sqrt{5}-1}{4}\right) + 1 = \frac{\sqrt{5}+1}{2} = \varphi$*, the golden ratio.*

[2]Recall that $\varphi - 1 = \frac{1}{\varphi}$.

Table 5.10: *Relationships between the energies of the four possible floating configurations for the pentagon for each value of* $\gamma \in (0, \pi)$.

Values for γ	**Energy Relationships**
$\left(0, \arccos\left(\frac{1}{\varphi}\right)\right)$	$E_4 < E_3 < E_2 < E_1$
$\arccos\left(\frac{1}{\varphi}\right)$	$E_4 = E_3 < E_2 < E_1$
$\left(\arccos\left(\frac{1}{\varphi}\right), \frac{2\pi}{5}\right)$	$E_3 < E_4 < E_2 < E_1$
$\frac{2\pi}{5}$	$E_3 < E_4 = E_2 < E_1$
$\left(\frac{2\pi}{5}, \frac{\pi}{2}\right)$	$E_3 < E_2 < E_4 < E_1$
$\frac{\pi}{2}$	$E_3 = E_2 < E_4 = E_1$
$\left(\frac{\pi}{2}, \frac{3\pi}{5}\right)$	$E_2 < E_3 < E_1 < E_4$
$\frac{3\pi}{5}$	$E_2 < E_3 = E_1 < E_4$
$\left(\frac{3\pi}{5}, \pi - \arccos\left(\frac{1}{\varphi}\right)\right)$	$E_2 < E_1 < E_3 < E_4$
$\pi - \arccos\left(\frac{1}{\varphi}\right)$	$E_2 = E_1 < E_3 < E_4$
$\left(\pi - \arccos\left(\frac{1}{\varphi}\right), \pi\right)$	$E_1 < E_2 < E_3 < E_4$

Table 5.11: *The stability of each of the four possible floating configurations for the pentagon (as depicted in Figure 5.6) and each value of* $\gamma \in (0, \pi)$ *is shown here. Note that* $v = \arccos\left(\frac{1}{\varphi}\right)$ *where* φ *is the golden ratio* $\varphi = \frac{\sqrt{5}+1}{2}$.

	$\left(0, \frac{\pi}{5}\right]$	$\left(\frac{\pi}{5}, v\right)$	v	$\left(v, \frac{2\pi}{5}\right)$	$\frac{2\pi}{5}$	$\left(\frac{2\pi}{5}, \frac{\pi}{2}\right)$	$\frac{\pi}{2}$
Configuration 1	Unstable						
Configuration 2	Unstable					Stable	Stable Global Energy Minimum
Configuration 3	Unstable	Stable	Stable Global Energy Minimum				
Configuration 4	Stable Global Energy Minimum			Stable	Unstable		

	$\left(\frac{\pi}{2}, \frac{3\pi}{5}\right)$	$\frac{3\pi}{5}$	$\left(\frac{3\pi}{5}, \pi - v\right)$	$\pi - v$	$\left(\pi - v, \frac{4\pi}{5}\right)$	$\left[\frac{4\pi}{5}, \pi\right)$
Configuration 1	Unstable		Stable	Stable Global Energy Minimum		
Configuration 2	Stable Global Energy Minimum				Stable	Unstable
Configuration 3	Stable	Unstable				
Configuration 4	Unstable					

5.3.5 The Regular Hexagon

For our final polygonal example, we consider a regular hexagonal cross-section whose sides are assumed to be unit length. Again, the only possible floating configurations are ones in which the fluid interface intersects two corners of the hexagon by Theorem 5.1. There are five such configurations which are depicted in Figure 5.8.

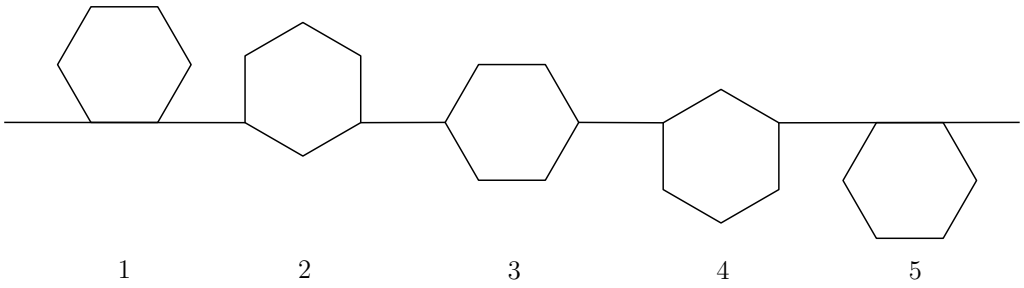

Figure 5.8: *The five possible floating configurations for the hexagonal cross-section.*

Using Theorem 5.2 we can classify the stability of these five configurations.

- Configuration 1 has floating angles $\gamma_1^+ = \gamma_2^+ = \frac{\pi}{3}$ and $\gamma_1^- = \gamma_2^- = \pi$ and so it will be stable when we have that $\frac{2\pi}{3} < \gamma < \pi$.
- Configuration 2 has floating angles $\gamma_1^+ = \gamma_2^+ = \frac{\pi}{2}$ and $\gamma_1^- = \gamma_2^- = \frac{5\pi}{6}$ and so it will be stable when we have that $\frac{\pi}{2} < \gamma < \frac{5\pi}{6}$.
- Configuration 3 has floating angles $\gamma_1^+ = \gamma_2^+ = \gamma_1^- = \gamma_2^- = \frac{2\pi}{3}$ and so it will be stable when we have that $\frac{\pi}{3} < \gamma < \frac{2\pi}{3}$.
- Configuration 4 has floating angles $\gamma_1^+ = \gamma_2^+ = \frac{5\pi}{6}$ and $\gamma_1^- = \gamma_2^- = \frac{\pi}{2}$ and so it will be stable when we have that $\frac{\pi}{6} < \gamma < \frac{\pi}{2}$.
- Configuration 5 has floating angles $\gamma_1^+ = \gamma_2^+ = \pi$ and $\gamma_1^- = \gamma_2^- = \frac{\pi}{3}$ and so it will be stable when we have that $0 < \gamma < \frac{\pi}{3}$.

Otherwise, when γ is not within the specified range of values, the configuration will be unstable.

Now, to determine which configuration gives the global energy minimum, we need to directly compare the energies associated with each of the five configurations. Using Figure 5.9 to determine the unknown lengths, we find that the energies of the five configurations

are given by

$$\begin{aligned} E_1 &= 5\sigma_1 + \sigma_2 - \sigma \\ E_2 &= 4\sigma_1 + 2\sigma_2 - \sqrt{3}\sigma \\ E_3 &= 3\sigma_1 + 3\sigma_2 - 2\sigma \\ E_4 &= 2\sigma_1 + 4\sigma_2 - \sqrt{3}\sigma \\ E_5 &= \sigma + 5\sigma_2 - \sigma. \end{aligned}$$

The relationships between each of the energies for each possible value of γ are given in Table 5.12. The details behind the creation of this table can be found in Section E.5 of Appendix E.

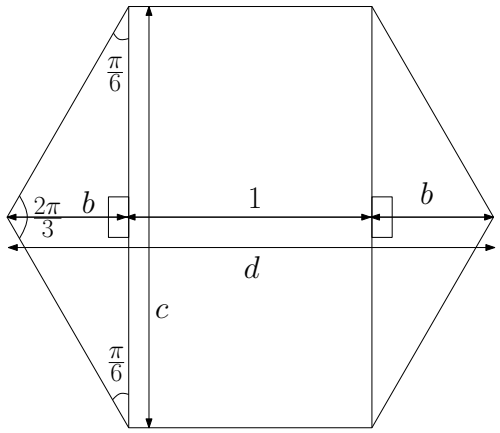

Figure 5.9: *The unknown length d is found using the angles of the indicated triangle. Using the Sine Law, length $c = \frac{\sin\left(\frac{2\pi}{3}\right)}{\sin\left(\frac{\pi}{6}\right)} = \frac{\frac{\sqrt{3}}{2}}{\frac{1}{2}} = \sqrt{3}$. Then using the Pythagorean Theorem, we find that $b = \frac{1}{2}$. Finally, since length d is twice length b plus one, we have $d = 2$.*

From Table 5.12, it is clear that the global energy minimum changes from one configuration to another at the following values of γ:

$$\begin{gathered} \arccos\left(\sqrt{3} - 1\right), \\ \arccos\left(2 - \sqrt{3}\right), \\ \frac{\pi}{2}, \\ \pi - \arccos\left(2 - \sqrt{3}\right), \text{ and} \\ \pi - \arccos\left(\sqrt{3} - 1\right). \end{gathered}$$

We also know the stability of certain configurations change when γ is one of 0, $\frac{\pi}{6}$, $\frac{\pi}{3}$, $\frac{\pi}{2}$, $\frac{2\pi}{3}$, $\frac{5\pi}{6}$ or π. From this, we can then summarize the stability of each of the five configurations for each possible value of γ in Table 5.13.

Table 5.12: *Relationships between the energies of the five possible floating configurations for the hexagon for each value of* $\gamma \in (0, \pi)$.

Values for γ	**Energy Relationships**
$\left(0, \arccos\left(\sqrt{3}-1\right)\right)$	$E_5 < E_4 < E_3 < E_2 < E_1$
$\arccos\left(\sqrt{3}-1\right)$	$E_4 = E_5 < E_3 < E_2 < E_1$
$\left(\arccos\left(\sqrt{3}-1\right), \frac{\pi}{3}\right)$	$E_4 < E_5 < E_3 < E_2 < E_1$
$\frac{\pi}{3}$	$E_4 < E_5 = E_3 < E_2 < E_1$
$\left(\frac{\pi}{3}, \arccos\left(2-\sqrt{3}\right)\right)$	$E_4 < E_3 < E_5 < E_2 < E_1$
$\arccos\left(2-\sqrt{3}\right)$	$E_4 = E_3 < E_5 < E_2 < E_1$
$\left(\arccos\left(2-\sqrt{3}\right), \arccos\left(\frac{\sqrt{3}-1}{3}\right)\right)$	$E_3 < E_4 < E_5 < E_2 < E_1$
$\arccos\left(\frac{\sqrt{3}-1}{3}\right)$	$E_3 < E_4 < E_5 = E_2 < E_1$
$\left(\arccos\left(\frac{\sqrt{3}-1}{3}\right), \frac{\pi}{2}\right)$	$E_3 < E_4 < E_2 < E_5 < E_1$
$\frac{\pi}{2}$	$E_3 < E_4 = E_2 < E_5 = E_1$
$\left(\frac{\pi}{2}, \pi - \arccos\left(\frac{\sqrt{3}-1}{3}\right)\right)$	$E_3 < E_2 < E_4 < E_1 < E_5$
$\pi - \arccos\left(\frac{\sqrt{3}-1}{3}\right)$	$E_3 < E_2 < E_4 = E_1 < E_5$
$\left(\pi - \arccos\left(\frac{\sqrt{3}-1}{3}\right), \pi - \arccos\left(2-\sqrt{3}\right)\right)$	$E_3 < E_2 < E_1 < E_4 < E_5$
$\pi - \arccos\left(2-\sqrt{3}\right)$	$E_3 = E_2 < E_1 < E_4 < E_5$
$\left(\pi - \arccos\left(2-\sqrt{3}\right), \frac{2\pi}{3}\right)$	$E_2 < E_3 < E_1 < E_4 < E_5$
$\frac{2\pi}{3}$	$E_2 < E_3 = E_1 < E_4 < E_5$
$\left(\frac{2\pi}{3}, \pi - \arccos\left(\sqrt{3}-1\right)\right)$	$E_2 < E_1 < E_3 < E_4 < E_5$
$\pi - \arccos\left(\sqrt{3}-1\right)$	$E_2 = E_1 < E_3 < E_4 < E_5$
$\left(\pi - \arccos\left(\sqrt{3}-1\right), \pi\right)$	$E_1 < E_2 < E_3 < E_4 < E_5$

Table 5.13: *The stability of each of the five possible floating configurations for the hexagon (as depicted in Figure 5.8) and each value of* $\gamma \in (0, \pi)$ *is shown here. Note that* $v = \arccos\left(\sqrt{3} - 1\right)$ *and* $w = \arccos\left(2 - \sqrt{3}\right)$.

	$\left(0, \frac{\pi}{6}\right]$	$\left(\frac{\pi}{6}, v\right)$	v	$\left(v, \frac{\pi}{3}\right)$	$\frac{\pi}{3}$	$\left(\frac{\pi}{3}, w\right)$	w	$\left(w, \frac{\pi}{2}\right)$	$\frac{\pi}{2}$
Configuration 1	Unstable								
Configuration 2	Unstable								
Configuration 3	Unstable					Stable	Stable Global Energy Minimum		
Configuration 4	Unstable	Stable	Stable Global Energy Minimum					Stable	Unstable
Configuration 5	Stable Global Energy Minimum			Stable	Unstable				

	$\left(\frac{\pi}{2}, \pi - w\right)$	w	$\left(\pi - w, \frac{2\pi}{3}\right)$	$\frac{2\pi}{3}$	$\left(\frac{2\pi}{3}, \pi - v\right)$	$\pi - v$	$\left(\pi - v, \frac{5\pi}{6}\right)$	$\left[\frac{5\pi}{6}, \pi\right)$
Configuration 1	Unstable				Stable	Stable Global Energy Minimum		
Configuration 2	Stable	Stable Global Energy Minimum					Stable	Unstable
Configuration 3	Stable Global Energy Minimum		Stable	Unstable				
Configuration 4	Unstable							
Configuration 5	Unstable							

5.4 Results Involving Regular Polygons

With a careful observation of the regular polygon examples in Section 5.3, one can begin to envisage several results concerning the number of stable and unstable configurations for a given regular polygon, as well as the relationship between stable configurations. We state several of these results in the following theorem and verify them in the accompanying proof.

Theorem 5.5. *For an n-sided regular polygon ($n \geq 3$) we will have that:*

1. *For each $\gamma \in (0, \pi)$ there exists a stable global energy minimum.*
2. *For each $\gamma \in (0, \pi)$ there are at most two stable configurations.*
3. *For each $\gamma \in (0, \pi)$ there are at least $n - 3$ unstable configurations with two vertices on the fluid interface.*
4. *If $\gamma \in \bigcup_{i=1}^{n-2} \left(\frac{i\pi}{n}, \frac{(i+1)\pi}{n}\right)$ there are two stable configurations. Otherwise, there is only one stable configuration.*
5. *When there are two stable configurations, the stable configurations will be adjacent. (We say that two configurations are adjacent if the absolute value of the difference between the number of vertices in fluid 1 is equal to 1.)*

Proof. Lemma F.1 in Appendix F tells us that when there are m vertices above the fluid interface, the floating angles are

$$\gamma_1^+ = \gamma_2^+ = \pi\left(1 - \frac{m}{n}\right)$$
$$\gamma_1^- = \gamma_2^- = \frac{\pi}{n}(m+2)$$

and so using the stability condition for polygonal bodies we have that the configuration is stable when

$$\pi - \pi\left(1 - \frac{m}{n}\right) < \gamma < (m+2)\left(\frac{\pi}{n}\right)$$

or equivalently

$$\left(\frac{\pi}{n}\right) m < \gamma < \left(\frac{\pi}{n}\right)(m+2).$$

Since m ranges from 0 to $n-2$, the family of intervals

$$I_m \;=\; \left(\frac{\pi m}{n}, \frac{\pi(m+2)}{n}\right) \text{ for } m = 0, 1 \ldots (n-2)$$

Section 5.4 is reprinted with permission from reference [14].

forms a cover of $(0, \pi)$. This means that for every $\gamma \in (0, \pi)$, γ is also contained in I_m for at least one value of m which proves the existence of at least one stable configuration. One of these stable configurations will have an energy that is less than or equal to the others and so we also have the existence of a stable global energy minimum. This proves statement 1.

We also note that

$$I_p \cap I_q = \emptyset$$

when $|p - q| > 1$, but the intersection is non-empty when $|p - q| = 1$. This tells us that intervals I_p and I_q only intersect when p and q are at most one apart. Consequently only two intervals can intersect each other; that is, given $\gamma \in (0, \pi)$, γ may be an element of at most two intervals of the form of the I_m. This proves statement 2. It also proves statement 5 as two stable configurations must occur for a γ such that γ is an element of the intersection of two intervals of the above form which can only occur when $|p - q| = 1$ implying that the configurations are adjacent. Since there are $n-1$ configurations with two vertices on the fluid interface in total, and at most 2 stable configurations by statement 2, there must be at least $n - 3$ unstable configurations, proving statement 3. Finally, if

$$\gamma \in \bigcup_{i=1}^{n-2} \left(\frac{i\pi}{n}, \frac{(i+1)\pi}{n} \right)$$

then $\frac{m\pi}{n} < \gamma < \frac{(m+1)\pi}{n}$ for some $m, 1 \leq m \leq (n-2)$, which implies that $\gamma \in I_{m-1} \cap I_m$ but no other interval I_p. This implies that there are two stable configurations. Otherwise, if

$$\gamma \notin \bigcup_{i=1}^{n-2} \left(\frac{i\pi}{n}, \frac{(i+1)\pi}{n} \right)$$

then

$$\gamma \in \left(0, \frac{\pi}{n}\right] \bigcup \left\{ \frac{2\pi}{n}, \frac{3\pi}{n}, \ldots, \frac{(n-2)\pi}{n} \right\} \bigcup \left[\frac{(n-1)\pi}{n}, \pi \right).$$

Then, if $\gamma \in \left(0, \frac{\pi}{n}\right]$ then $\gamma \in I_0$ but no other I_m. If $\gamma \in \left(\frac{(n-1)\pi}{n}, \pi \right)$ then $\gamma \in I_{n-2}$ but no other I_m. If $\gamma = \frac{m\pi}{n}$ for $2 \leq m \leq n-2$ then $\gamma \in I_{m-1}$ but no other I_m. So, we can conclude that γ can be an element of one interval I_m at a time, and consequently we conclude that there can be only one stable configuration. This proves statement 4. □

5.5 Existence of a Stable Global Energy Minimum for a General Polygon

In the Section 5.4 we found that for every value of $\gamma \in (0, \pi)$ and every regular polygonal cross-section, a global energy minimum would exist and it would be stable. We now extend

that result (with an independent proof) to one that guarantees the existence of a stable global energy minimum for all polygonal cross-sections, regular or otherwise.

Theorem 5.6. *A global energy minimum exists for every convex polygonal cross-section and every value of $\gamma \in (0, \pi)$. Furthermore, the global energy minimum will be stable.*

Proof. Using Theorem 4.1 we know that any configuration in which the fluid interface intersects the interior of a straight edge will be unstable, and hence by definition cannot be the global energy minimum. Thus, if a global energy minimum were to exist, it must be a configuration that has two corners on the fluid interface. Since there are finitely many configurations of this kind, one must be the global energy minimum. Hence, a global energy minimum exists for every convex polygonal cross-section.

It remains to be shown that the global energy minimum is stable. We assume for the sake of contradiction that the global energy minimum is *not* stable. Then, according to Theorem 5.2 it must be that either

$$\gamma \geq \min(\gamma_1^-, \gamma_2^-) \qquad \text{or} \qquad \gamma \leq \pi - \min(\gamma_1^+, \gamma_2^+) \tag{5.1}$$

where $\gamma_1^-, \gamma_2^-, \gamma_1^+$ and γ_2^+ are the floating angles (as defined in Section 5.2) associated with the global energy minimum. It must then be that

$$\gamma \geq \gamma_1^-, \qquad \gamma \geq \gamma_2^-, \qquad \gamma \leq \pi - \gamma_1^+, \qquad \text{or} \qquad \gamma \leq \pi - \gamma_2^+.$$

We will show the existence of a small perturbation away from the global energy minimum configuration that decreases energy for each of these four possibilities.

- If $\gamma \geq \gamma_1^-$ we perturb the fluid interface downward on the right hand side of the body, decreasing t_1^*. This creates a new floating angle Ψ_1^- that is less than γ_1^- due to convexity. Then

$$\begin{aligned}
& & \Psi_1^- &< \gamma_1^- \\
\iff & & \Psi_1^- &< \gamma \\
\iff & & \cos\gamma &< \cos\Psi_1^- \\
\iff & & \frac{\sigma_1 - \sigma_2}{\sigma} &< \frac{\vec{r'}(t_1^*)}{\|\vec{r'}(t_1^*)\|} \cdot \frac{\vec{r}(t_2^*) - \vec{r}(t_1^*)}{\|\vec{r}(t_2^*) - \vec{r}(t_1^*)\|} \\
\iff & -(\sigma_1 - \sigma_2)\|\vec{r'}(t_1^*)\| + \sigma & \left(\frac{\vec{r'}(t_1^*) \cdot (\vec{r}(t_2^*) - \vec{r}(t_1^*))}{\|\vec{r}(t_2^*) - \vec{r}(t_1^*)\|} \right) &> 0 \\
\iff & & \left. \frac{\partial E}{\partial t_1} \right|_{(t_1^*, t_2^*)} &> 0
\end{aligned}$$

  and since t_1^* decreases, this perturbation decreases energy.

- If $\gamma \geq \gamma_2^-$ we perturb the fluid interface downward on the left hand side of the body, increasing t_2^*. This creates a new floating angle Ψ_2^- that is less than γ_2^- due to convexity. Then

$$\begin{aligned}
& & \Psi_2^- &< \gamma_2^- \\
\iff & & \Psi_2^- &< \gamma \\
\iff & & \cos\gamma &< \cos\Psi_2^- \\
\iff & & \frac{\sigma_1 - \sigma_2}{\sigma} &< \frac{\vec{r'}(t_2^*)}{\|\vec{r'}(t_2^*)\|} \cdot \frac{\vec{r}(t_2^*) - \vec{r}(t_1^*)}{\|\vec{r}(t_2^*) - \vec{r}(t_1^*)\|} \\
\iff & (\sigma_1 - \sigma_2)\|\vec{r'}(t_2^*)\| - \sigma & \left(\frac{\vec{r'}(t_2^*) \cdot (\vec{r}(t_2^*) - \vec{r}(t_1^*))}{\|\vec{r}(t_2^*) - \vec{r}(t_1^*)\|} \right) &< 0 \\
\iff & & \left. \frac{\partial E}{\partial t_2} \right|_{(t_1^*, t_2^*)} &< 0
\end{aligned}$$

  and since t_2^* increases, this perturbation decreases energy.

- If $\gamma \leq \pi - \gamma_1^+$ we perturb the fluid interface upward on the right hand side of the body, increasing t_1^*. This creates a new floating angle Ψ_1^+ that is less than γ_1^+ due to convexity. Then

$$\begin{aligned}
& & \Psi_1^+ &< \gamma_1^+ \\
\iff & & \pi - \Psi_1^+ &> \pi - \gamma_1^+ \\
\iff & & \pi - \Psi_1^+ &> \gamma \\
\iff & & \left. \frac{\partial E}{\partial t_1} \right|_{(t_1^*, t_2^*)} &< 0
\end{aligned}$$

  and since t_1^* increases, this perturbation decreases energy.

- If $\gamma \leq \pi - \gamma_2^+$ we perturb the fluid interface upward on the left hand side of the body, decreasing t_2^*. This creates a new floating angle Ψ_2^+ that is less than γ_2^+ due to convexity. Then

$$\begin{aligned}
& & \Psi_2^+ &< \gamma_2^+ \\
\iff & & \pi - \Psi_2^+ &> \pi - \gamma_2^+ \\
\iff & & \pi - \Psi_2^+ &> \gamma \\
\iff & & \left. \frac{\partial E}{\partial t_2} \right|_{(t_1^*, t_2^*)} &> 0
\end{aligned}$$

  and since t_2^* decreases, this perturbation decreases energy.

In all four cases, there exists a small perturbation to a configuration giving lesser energy. By Definition 2.3 the configuration cannot be a global energy minimum, but this is a contradiction. Hence the global energy minimum is stable. □

Remark 5.3. So far in this thesis, we have only considered bodies that are convex. One might ask why this is the case, as the energy function introduced in Section 2.1 would seemingly be applicable to any body of general shape, including those that are not convex. However, we recall that in Section 2.1 we began with the assumption that the fluid interface would intersect the body in two distinct points. This assumption was true for any strictly convex body (and any contact angle different from 0 and π), and we were able to relax this assumption to consider bodies that were only convex. However, a body that is not convex will admit configurations in which the fluid interface would intersect the body in more than two points, and consequently the energy function used in Section 2.1 would no longer be appropriate.

Chapter 6

Bodies in Three Dimensions

Until this point, we have discussed only infinitely long cylinders of constant cross-section, thus reducing our considerations to two dimensions. However, the more physically intuitive problem of a floating finite three-dimensional body is one of practical importance that many researchers consider today. In this chapter we will recreate a result by Finn and Vogel from reference [9] restricting our efforts to a specific type of three-dimensional body, but we will then extend the logic to derive a similar result concerning a type of body that Finn and Vogel do not consider.

6.1 Vertical Variations of a Body of Revolution

Consider a body of revolution generated by rotating the curve $r(z) \geq 0$ from $z = h_1$ to $z = h_2$ around the z-axis. (See Figure 6.1.) We note that we allow $r(z)$ to be zero only at the endpoints of the interval $[h_1, h_2]$ and nowhere in the interior. When $r(h_1) \neq 0$ or $r(h_2) \neq 0$ the body formed by rotation will not be closed; in such a case we will close the body by affixing an appropriately sized circle to each open end of the body.

We will consider vertical variations of the body in terms of a single parameter h. The exterior fluid surface is represented by the plane[1] $z = h$, for some $h \in [h_1, h_2]$. The energy function will be described by

$$E = \mathcal{S}_1\sigma_1 + \mathcal{S}_2\sigma_2 - \mathcal{A}\sigma \tag{6.1}$$

where $\mathcal{S}_1$ is the area of the body in contact with the upper fluid 1, $\mathcal{S}_2$ is the area of the body in contact with the lower fluid 2, and $\mathcal{A}$ is the area that is deleted from the fluid

[1] We have *not* made the simplifying assumption of neutral equilibrium as discussed earlier in Section 1.1. Instead, we have used Theorem 2.6 from reference [9] which tells us that since the fluid interface is rotationally symmetric, it will be flat and hence is representable by a plane.

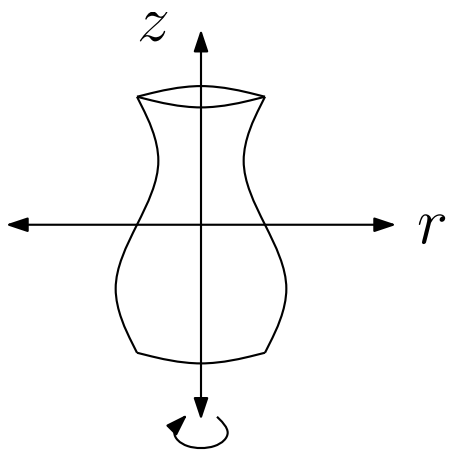

Figure 6.1: *A body of revolution generated by revolving the curve $r(z)$ around the z-axis. The solid pictured does not have the property that $r(h_1) = r(h_2) = 0$ and so it is considered to have a circular disc on either end closing the surface.*

interface by the body. Then

$$\begin{aligned}\mathcal{S}_1 &= \int_h^{h_2} 2\pi r(z)\sqrt{1+\left(\frac{dr}{dz}\right)^2}\,dz + \pi(r(h_2))^2,\\ \mathcal{S}_2 &= \int_{h_1}^{h} 2\pi r(z)\sqrt{1+\left(\frac{dr}{dz}\right)^2}\,dz + \pi(r(h_1))^2,\end{aligned}$$

and

$$\mathcal{A} = \pi(r(h))^2.$$

So using equation (6.1) we have

$$\begin{aligned}E(h) &= \sigma_1\left[\int_h^{h_2} 2\pi r(z)\sqrt{1+\left(\frac{dr}{dz}\right)^2}\,dz + \pi(r(h_2))^2\right]\\ &\quad +\sigma_2\left[\int_{h_1}^{h} 2\pi r(z)\sqrt{1+\left(\frac{dr}{dz}\right)^2}\,dz + \pi(r(h_1))^2\right] - \pi\sigma(r(h))^2.\end{aligned}$$

The derivative of the energy function will then be

$$\begin{aligned}E'(h) &= 2\pi\sigma_1\left[-r(h)\sqrt{1+(r'(h))^2}\right] + 2\pi\sigma_2\left[r(h)\sqrt{1+(r'(h))^2}\right] - 2\pi\sigma r(h)r'(h)\\ &= 2\pi r(h)\left[(\sigma_2-\sigma_1)\sqrt{1+(r'(h))^2} - \sigma r'(h)\right]. \qquad (6.2)\end{aligned}$$

Since $r(h) \neq 0$ for $h \in (h_1, h_2)$ we see that

$$\begin{aligned} E'(h) = 0 \qquad &\iff \qquad (\sigma_2 - \sigma_1)\sqrt{1 + (r'(h))^2} = \sigma r'(h) \\ &\iff \qquad \frac{\sigma_1 - \sigma_2}{\sigma} = \frac{-r'(h)}{\sqrt{1 + (r'(h))^2}}. \end{aligned} \tag{6.3}$$

Next we see that

$$\begin{aligned} E''(h) &= 2\pi r'(h)\left[(\sigma_2 - \sigma_1)\sqrt{1 + (r'(h))^2} - \sigma r'(h)\right] \\ &\quad +2\pi r(h)\left[\frac{(\sigma_2 - \sigma_1)r'(h)r''(h)}{\sqrt{1 + (r'(h))^2}} - \sigma r''(h)\right]. \end{aligned}$$

Assuming the body is in equilibrium, it must be that equation (6.3) is satisfied. Making this assumption will allow us to simplify $E''(h)$.

$$\begin{aligned} E''(h) &= 2\pi r'(h)\left[\sigma r'(h) - \sigma r'(h)\right] + 2\pi r(h)\left[\frac{\sigma r'(h)}{\sqrt{1 + (r'(h))^2}} \cdot \frac{r'(h)r''(h)}{\sqrt{1 + (r'(h))^2}} - \sigma r''(h)\right] \\ &= 2\pi r(h)r''(h)\left[\frac{\sigma(r'(h))^2}{1 + (r'(h))^2} - 1\right] \\ &= 2\pi\sigma r(h)r''(h)\left[\frac{(r'(h))^2 - 1 - (r'(h))^2}{1 + (r'(h))^2}\right] \\ &= -\frac{2\pi\sigma r(h)r''(h)}{1 + (r'(h))^2}. \end{aligned} \tag{6.4}$$

So, when a body is in an equilibrium configuration, the second derivative of the energy will have a sign opposite to that of $r''(h)$.

Now, we consider the function

$$f(h) = \frac{-r'(h)}{\sqrt{1 + (r'(h))^2}}.$$

We note that

$$\begin{aligned} f'(h) &= \frac{-r''(h)\sqrt{1 + (r'(h))^2} + r'(h)(\frac{1}{2})(1 + (r'(h))^2)^{-\frac{1}{2}}(2)r'(h)r''(h)}{1 + (r'(h))^2} \\ &= r''(h)\left[\frac{-(1 + (r'(h))^2) + (r'(h))^2}{(1 + (r'(h))^2)^{\frac{3}{2}}}\right] \\ &= -\frac{r''(h)}{(1 + (r'(h))^2)^{\frac{3}{2}}}. \end{aligned}$$

We will now consider a smooth body which is strictly convex. Strict convexity implies that $r''(h) < 0$ for all $h \in (h_1, h_2)$ and so $f'(h) > 0$. Thus, f is increasing. In addition,

since the body is smooth, f will be continuous and it must be that $r'(h) \longrightarrow \infty$ as $h \longrightarrow h_1$ and $r'(h) \longrightarrow -\infty$ as $h \longrightarrow h_2$, with $r(h_1) = r(h_2) = 0$. So, we see that

$$\begin{aligned} &\lim_{h\to h_1} f(h) && \text{and} && \lim_{h\to h_2} f(h) \\ &= \lim_{h\to h_1} \frac{-r'(h)}{\sqrt{1+(r'(h))^2}} && && = \lim_{h\to h_2} \frac{-r'(h)}{\sqrt{1+(r'(h))^2}} \\ &= \lim_{x\to\infty} \frac{-x}{\sqrt{1+x^2}} && && = \lim_{x\to-\infty} \frac{-x}{\sqrt{1+x^2}} \\ &= -1 && && = +1. \end{aligned}$$

So for $h \in (h_1, h_2)$, $f(h)$ increases monotonically from -1 to 1, provided the body is strictly convex and sufficiently smooth. So, when $|\frac{\sigma_1-\sigma_2}{\sigma}| < 1$, there will exist a unique value h_c such that

$$f(h_c) = \frac{\sigma_1 - \sigma_2}{\sigma}$$

i.e. there exists a unique height h_c at which $E'(h_c) = 0$. Furthermore, since the body is strictly convex, we have that $r''(h) < 0$ for all $h \in (h_1, h_2)$ and so $E''(h_c) > 0$ and thus the equilibrium configuration is stable. Hence the unique height h_c gives the global energy minimum over the range of vertical positions.

Remark 6.1. So far, this is all in keeping with Finn and Vogel's Lemma 2.1 in reference [9] in which it is proved that when $|\frac{\sigma_1-\sigma_2}{\sigma}| < 1$ there is a unique height h at which $E'(h) = 0$ and this height gives the absolute minimum over the range of vertical positions. Finn and Vogel's lemma is more general than what we have done here thus far; they consider a general strictly convex body in three dimensions where we have restricted ourselves to considering only bodies that are rotationally symmetric. However, we will use this same approach to make some conclusions about bodies that are not necessarily strictly convex, something that Finn and Vogel have not considered in reference [9].

Now, we relax the requirement that the body be strictly convex. The body is still rotationally symmetric, as well as sufficiently smooth, but we will allow the curve $r(z)$ to have any curvature: positive, negative or zero. Due to the smoothness of the body, we still have that $r(h_1) = r(h_2) = 0$ and that $r'(h) \to \infty$, $r'(h) \to -\infty$ as h approaches h_1 and h_2 respectively. Under these new assumptions, the range of $f(h) = \frac{-r'(h)}{\sqrt{1+(r'(h))^2}}$ is still $(-1, 1)$ but we can no longer conclude that f is monotone. We can say for certain that when $|\frac{\sigma_1-\sigma_2}{\sigma}| < 1$, equilibrium configurations exist but we can no longer be certain *how many* of them exist. In addition, we can also characterize the stability of any equilibrium configuration defined by the height h_c for any configuration in which $r''(h_c) \neq 0$. We recall that $E''(h)$ has sign opposite to that of $r''(h)$ and so for an equilibrium configuration where the body is locally strictly convex, $r''(h_c) < 0$ and thus $E''(h_c) > 0$ and so the equilibrium

will be stable. On the other hand, if the body is locally strictly concave, $r''(h_c) > 0$ and thus $E''(h_c) < 0$ and so the equilibrium will be unstable. We highlight this new result in the following theorem.

Theorem 6.1. *Consider a smooth rotationally symmetric body created by rotating the curve $r(z)$ around the z-axis. When $|\frac{\sigma_1-\sigma_2}{\sigma}| < 1$ there will exist at least one height h_c in the range of heights for which the body is in contact with the fluid interface that will be in equilibrium with respect to vertical translations. Furthermore, if $r''(h_c) < 0$ the configuration will be stable with respect to vertical translations. If $r''(h_c) > 0$ the configuration will be unstable with respect to vertical translations.*

Remark 6.2. Consider a body where $r(h_1)$ and $r(h_2)$ are not necessarily zero and we do not have slopes as required for smoothness at h_1 and h_2. $f(h)$ will not necessarily approach -1 as $h \to h_1$ nor will it approach 1 as $h \to h_2$. So, we cannot guarantee equilibrium configurations exist for every value of $\frac{\sigma_1-\sigma_2}{\sigma} \in (-1, 1)$. However, if one does exist, it will still obey the stability criteria as outlined in Theorem 6.1. We will see an example of a body of this type in Subsection 6.2.1.

Remark 6.3. Defining γ to be the angle of contact between the fluid interface and the body as measured in the lower fluid, and referring to Figure 6.2 we note that

$$\begin{aligned}
\frac{-r'(h)}{\sqrt{1+(r'(h))^2}} &= \frac{-r'(h)}{\|(-r'(h),-1)\|} \\
&= \frac{(-r'(h),-1)\cdot(1,0)}{\|(-r'(h),-1)\|\ \|(1,0)\|} \\
&= \frac{-(r'(h),1)\cdot(1,0)}{\|(r'(h),1)\|\ \|(1,0)\|} \\
&= -\cos(\pi-\gamma) \\
&= \cos\gamma
\end{aligned}$$

and so equation (6.3) is equivalent to the contact angle condition (as expected) for a sufficiently smooth body.

Remark 6.4. In Remark 5.3 we discussed how our assumption that the fluid interface would meet the body in only two points implicitly restricted our consideration of two-dimensional bodies to those that were convex. However, in the discussion of three-dimensional bodies in this chapter we did in fact consider bodies that were not convex. Nonetheless, since we were considering only vertical variations of three-dimensional bodies of revolution the bodies that were not convex did not create any complications. This is due to the fact that the intersection between the fluid interface and the boundary of the body will always be a single circle.

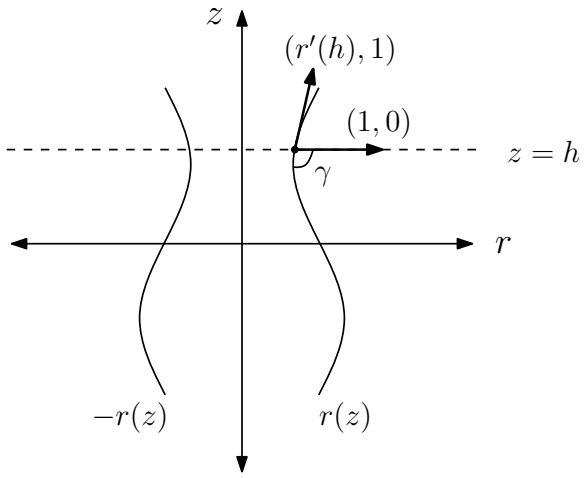

Figure 6.2: *The contact angle between the fluid interface and a three-dimensional body of revolution as measured in the lower fluid.*

6.2 Examples

We will now consider three examples of bodies of revolution to illustrate our findings from the previous section.

6.2.1 A Vase-like Body

Consider the vase-like body created by rotating the curve

$$r(z) = \cos(z) + 2, \ z \in \left[-\tfrac{\pi}{2}, \tfrac{3\pi}{2}\right]$$

about the z-axis and affixing a circle of radius 2 to either end. We have that $r'(z) = -\sin z$

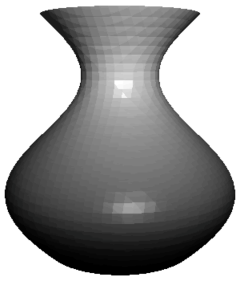

Figure 6.3: *Our vase-like body of revolution considered in this example.*

and so $f(h) = \frac{\sin h}{\sqrt{1+\sin^2 h}}$. We then note that

$$f'(h) = \frac{\cos h}{(1+\sin^2 h)^{\frac{3}{2}}},$$

giving a critical point at $\frac{\pi}{2}$. Evaluating f at the critical points and the endpoints of the interval in consideration shows that for $h \in \left(-\frac{\pi}{2}, \frac{3\pi}{2}\right)$, $f(h) \in \left[\frac{-\sqrt{2}}{2}, \frac{\sqrt{2}}{2}\right)$. So there will only exist equilibrium configurations when we have that

$$\frac{-\sqrt{2}}{2} \leq \frac{\sigma_1 - \sigma_2}{\sigma} < \frac{\sqrt{2}}{2}.$$

Let us take a specific value in this region, say $\frac{\sigma_1-\sigma_2}{\sigma} = 0$, to illustrate the results found in this chapter. $\frac{\sigma_1-\sigma_2}{\sigma} = 0$ implies that $\gamma = \frac{\pi}{2}$ and it is clear from Figure 6.3 (and it can be shown analytically) that two equilibria exist, one where the fluid interface meets the vase at its widest point and another where the interface meets the vase at its thinnest point. The configuration where the interface meets the vase at its widest point will be stable since the body is strictly convex there, and the configuration where the interface meets the base at its thinnest point will be unstable since the body is strictly concave there.

6.2.2 An Ellipsoid

In this subsection we will consider vertical variations of an ellipsoid of the form

$$\frac{r^2}{a^2} + \frac{z^2}{b^2} = 1.$$

This is clearly a body of revolution since we can rewrite it as

$$r(z) = a\sqrt{1 - \frac{z^2}{b^2}}.$$

Differentiating once, we obtain

$$\begin{aligned} r'(z) &= a\left(\frac{1}{2}\right)\left(1 - \frac{z^2}{b^2}\right)^{-\frac{1}{2}}(-2z)\left(\frac{1}{b^2}\right) \\ &= \frac{-az}{b\sqrt{b^2 - z^2}} \end{aligned}$$

and differentiating again gives

$$\begin{aligned} r''(z) &= \frac{-ab\sqrt{b^2 - z^2} + azb(\frac{1}{2})(b^2 - z^2)^{-\frac{1}{2}}(-2z)}{b^2(b^2 - z^2)} \\ &= \frac{-ab(b^2 - z^2) - abz^2}{b^2(b^2 - z^2)^{\frac{3}{2}}} \\ &= \frac{-ab}{(b^2 - z^2)^{\frac{3}{2}}} \\ &< 0. \end{aligned}$$

Since $r''(z) < 0$, using equation (6.4) gives that $E''(h) > 0$ for any configuration satisfying the condition for equilibrium with respect to vertical variations, and thus the ellipsoid is stable with respect to vertical variations, independent of the eccentricity.

We will now compare this result to an analogous two-dimensional problem; the problem of an infinitely long cylinder with elliptical cross-section. This problem was considered earlier in Section 3.1 where we found that for an equilibrium configuration of the ellipse to be stable with respect to all variations, the major axis of the ellipse must be parallel to the fluid interface. Here, we will restrict ourselves to considering only vertical variations in order to compare with the ellipsoid.

To consider only vertical variations, we define $t_2 = \pi - t_1$ and restrict t_1 so that $t_1 \in \left(-\frac{\pi}{2}, \frac{\pi}{2}\right)$. Then, a new energy function $\tilde{E}$ is defined by

$$\tilde{E} = E(t_1, \pi - t_1)$$

and thus we see that

$$\begin{aligned} \tilde{E}'(t_1^*) &= \left[\frac{\partial E}{\partial t_1} + \frac{\partial E}{\partial t_2} \cdot \frac{d}{dt_1}(\pi - t_1)\right]\Bigg|_{(t_1^*, \pi - t_1^*)} \\ &= \left[\frac{\partial E}{\partial t_1} - \frac{\partial E}{\partial t_2}\right]\Bigg|_{(t_1^*, \pi - t_1^*)} \end{aligned}$$

and then that

$$\begin{aligned} \tilde{E}''(t_1^*) &= \left[\frac{\partial^2 E}{\partial t_1^2} + \frac{\partial^2 E}{\partial t_1 \partial t_2} \cdot \frac{d}{dt_1}(\pi - t_1) - \left(\frac{\partial^2 E}{\partial t_2 \partial t_1} + \frac{\partial^2 E}{\partial t_2^2} \cdot \frac{d}{dt_1}(\pi - t_1)\right)\right]\Bigg|_{(t_1^*, \pi - t_1^*)} \\ &= \left[\frac{\partial^2 E}{\partial t_1^2} - 2\frac{\partial^2 E}{\partial t_1 \partial t_2} + \frac{\partial^2 E}{\partial t_2^2}\right]\Bigg|_{(t_1^*, \pi - t_1^*)}. \end{aligned}$$

We recall that in Section 3.1 (under the same assumption that $t_2^* = \pi - t_1^*$) we found in equation (3.2) that the second partial derivatives with respect to t_1 and t_2 would be equal. So, we now have that

$$\tilde{E}''(t_1^*) = 2\left[\frac{\partial^2 E}{\partial t_1^2} - \frac{\partial^2 E}{\partial t_1 \partial t_2}\right]\Bigg|_{(t_1^*, \pi - t_1^*)}.$$

Recalling our parametrization of the ellipse to be $\vec{r}(t) = (g\cos t, h \sin t)$ and using the

derivatives of the energy function from Section 2.2 we see that

$$\begin{aligned}
& \left[\frac{\partial^2 E}{\partial t_1^2} - \frac{\partial^2 E}{\partial t_1 \partial t_2}\right]\Bigg|_{(t_1^*, \pi - t_1^*)} \\
= \; & \frac{\sigma \cos t_1^* h^2}{2g(g^2 \sin^2 t_1^* + h^2 \cos^2 t_1^*)} \left[g^2 + (g^2 - h^2)\cos^2 t_1^*\right] - \frac{\sigma}{2g \cos t_1^*} \left[-h^2 \cos^2 t_1^*\right] \\
= \; & \frac{\sigma h^2 \cos t_1^*}{2g} \left[\frac{g^2 + (g^2 - h^2)\cos^2 t_1^*}{g^2 \sin^2 t_1^* + h^2 \cos^2 t_1^*} + 1\right] \\
= \; & \frac{\sigma g h^2 \cos t_1^*}{g^2 \sin^2 t_1^* + h^2 \cos^2 t_1^*} \\
> \; & 0.
\end{aligned}$$

Thus, any equilibrium configuration of the infinite elliptical cylinder will be stable with respect to vertical variations, regardless of the eccentricity of the elliptical cross-section.

Remark 6.5. Since any equilibrium configuration of an infinite elliptical cylinder is stable with respect to vertical variations, it means that when placed in an unstable equilibrium the ellipse will move to a new configuration via rotation, not translation. Finn makes note of this in reference [7].

Remark 6.6. In both the two-dimensional elliptical cylinder and three-dimensional ellipsoid problems, we found that any equilibrium configuration would be stable with respect to vertical variations regardless of the orientation of the (generating) ellipse. However, for stability with respect to all perturbations in the two-dimensional problem, there was a restriction on the orientation of the ellipse. The relationship between the two-dimensional and three-dimensional problems suggests that a similar requirement might exist for stability with respect to all variations in the three-dimensional case, but we will not investigate that here.

6.2.3 A Body Comprised of Conical Frustums

Before we get to a body comprised of multiple conical frustums, we consider a single conical frustum which is a body generated by rotating a line segment $r(z)$ around the z-axis and affixing two appropriately sized circles to either end. Vertical equilibrium configurations can only occur on the smooth portion of the body, provided $\frac{\sigma_1 - \sigma_2}{\sigma}$ is the very specific value required to make the necessary contact angle with the frustum. However, even if equilibria of this type exist, they will be unstable since the energy is constant while the smooth portion of the frustum is in contact with the fluid interface.[2] So, vertically stable

[2]Every configuration in which the frustum touches the fluid interface gives the same contact angle, so $E'(h) = 0 \; \forall h \in (h_1, h_2)$ implying that the energy is constant on that interval.

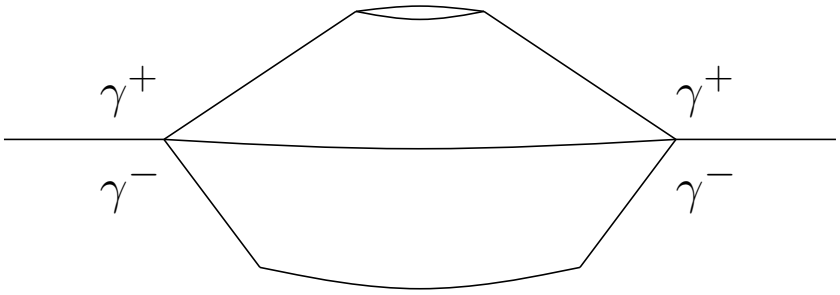

Figure 6.4: *A body comprised of only conical frustums. The floating angles γ^+ and γ^- are also depicted here.*

equilibrium of a conical frustum must occur with either the base or top of the frustum incident to the fluid interface.

Now, if we consider a body of revolution that is comprised of a "stack" of conical frustums (see Figure 6.4) we note that vertically stable equilibrium can occur only at the top or bottom of the body or where two frustums meet. Of course, this does not necessarily imply that any configuration where the fluid interface coincides with the top of bottom of one of the frustums is a vertically stable equilibrium. However, a condition guaranteeing vertically stable equilibrium for such a configuration can be found and we will derive it now.

Consider a body comprised of two conical frustums as shown in Figure 6.4. Let γ^+ and γ^- be the angles that the body makes with the fluid interface as measured in the upper and lower fluids respectively. Then recalling equation (6.2) we see that

$$\begin{aligned} E'(h) &= 2\pi r(h)\left[(\sigma_2-\sigma_1)\sqrt{1+r'((h))^2}-\sigma r'(h)\right] \\ &= 2\pi\sigma r(h)\sqrt{1+(r'(h))^2}\left[\frac{\sigma_2-\sigma_1}{\sigma}-\frac{r'(h)}{\sqrt{1+(r'(h))^2}}\right] \\ &= 2\pi\sigma r(h)\sqrt{1+(r'(h))^2}\left[-\cos\gamma+\cos\Psi\right] \end{aligned}$$

where Ψ is the angle (as measured in the lower fluid) between the body and the fluid interface. We then see that

$$\begin{aligned} & & \Psi &< \gamma \\ &\iff & \cos\Psi &> \cos\gamma \\ &\iff & E'(h) &> 0 \end{aligned}$$

and that

$$\begin{aligned} & \Psi > \gamma \\ \iff \quad & \cos\Psi < \cos\gamma \\ \iff \quad & E'(h) < 0. \end{aligned}$$

Then, starting at the configuration shown in Figure 6.4, if we raise the fluid interface slightly, h increases and $\Psi = \pi - \gamma^+$. For stability with respect to this perturbation we must have that

$$\pi - \gamma^+ < \gamma. \tag{6.5}$$

Next, again starting at the configuration shown in Figure 6.4, if we lower the fluid interface slightly, h decreases and $\Psi = \gamma^-$. For stability with respect to this perturbation we must have that

$$\gamma^- > \gamma. \tag{6.6}$$

Overall, for stability with respect to vertical variations we require both equations (6.5) and (6.6) to be satisfied which is equivalent to the requirement that

$$\pi - \gamma^+ < \gamma < \gamma^-. \tag{6.7}$$

Outside this interval, the configuration will be unstable.

Remark 6.7. It is interesting to note the similarities between the condition on the floating angles for vertically stable equilibrium of a body comprised of conical frustums and the condition on the floating angles for stable equilibrium of an infinitely long cylinder with a polygonal cross-section (Theorem 5.2). The stability condition for the two-dimensional polygonal cross-section reduces to condition (6.7) when the two upper floating angles are equal and two lower angles are equal. This surprising likeness may have been expected based on the similarities between the two problems: the presence of straight lines in the body and the corners created when straight portions of the body meet. Nonetheless, it is still quite remarkable that we obtain almost identical conditions on the floating angles in both two- and three-dimensional problems.

Remark 6.8. In Section 6.1 we were able to determine the stability of any equilibrium configuration (with respect to vertical variations only) of a body of revolution provided that r'' was not zero at the equilibrium height. The analysis of a single conical frustum now allows us to make the conclusion that any body of revolution that is linear in some neighbourhood of the equilibrium height will be unstable. This follows directly from the fact that the energy $E(h)$ is constant while the fluid interface intersects the linear portion of the body. We are still unable to determine the vertical stability of an equilibrium where $r''(h_c) = 0$ at only a point without looking at higher order derivatives of $E(h)$.

Chapter 7

Summary and Conclusions

In this thesis, we have looked at a variety of results involving both two- and three-dimensional bodies which we summarize here.

1. **Two-dimensional bodies**

   (a) We used a parametric representation of the cross-section of an infinitely long cylinder to re-derive Young's contact angle condition using a minimization of an appropriate energy function. (See Section 2.1.)

   (b) We continued to use the parametric representation of the cross-section of the body to look at the second order terms of a series expansion of the energy function (in Section 2.2) and used these terms to illustrate the stability of equilibrium configurations of an infinite cylinder with an elliptical cross-section (in Section 3.1).

   (c) We proved that any equilibrium configuration in which the fluid interface intersected the interior of a straight side of the body in a single point would be unstable, allowing us to immediately ignore any such configuration when searching for stable equilibria of a body. (See Section 4.1.)

   (d) The theorem concerning the instability of configurations where the fluid interface intersected the interior of a straight side was applied directly to polygonal bodies in which *all* sides are straight, giving that a necessary condition for stable equilibrium of a cylinder with polygonal cross-section is that the fluid interface must intersect two corners of the polygon. (See Theorem 5.1.) Furthermore, we derived a necessary and sufficient condition for stable equilibrium of polygonal bodies (Theorem 5.2) and illustrated these results with several examples.

   (e) We completed our discussion of polygonal bodies with some general results about the existence and number of stable equilibrium configurations for polygonal

bodies (Theorem 5.5) and a result proving the existence of a stable global energy minimum for any convex polygonal cross-section. (See Section 5.5.)

2. **Three-dimensional bodies**

   (a) We considered vertical perturbations of bodies of revolution, proving the existence of at least one equilibrium height for any sufficiently smooth body of revolution. (See Theorem 6.1.) In that same theorem we also classified the stability of any equilibrium height of a body of revolution based on the local curvature of the body.

   (b) We looked at several examples of bodies of revolution, including an ellipsoid (in Subsection 6.2.2) and a body composed of conical frustums (in Subsection 6.2.3).

Also, in our discussion of three-dimensional bodies we made note in two of our examples (the body composed of conical frustums and the ellipsoid) that similarities existed between the three-dimensional bodies and their two-dimensional counterpart. This suggests that even though problems involving infinitely long cylinders of constant cross-section are essentially unrealistic, they could potentially provide valuable insight into the behaviour of an analogous body in three dimensions. Due to the fact that three-dimensional bodies are often difficult to work with, an analysis of a related two-dimensional body could be a good place to begin when considering a three-dimensional shape.

Permissions

Dear Mr. Kemp:

Thank you for requesting permission to reproduce material from American Institute of Physics publications.

Permission is granted - subject to the conditions outlined below - for the following:

accepted article in Physics of Fluids, "Floating Bodies in Two Dimensions without Gravity" (manuscript number 10-0784),

To be used in the following manner:

Included as part of your thesis for submission to the University of Waterloo. It is understood that you will grant a non-exclusive license to Library and Archives Canada to reproduce, publish, archive, preserve, conserve, communicate to the public by telecommunication or on the Internet, loan, distribute and sell your thesis worldwide, for commercial or non-commercial purposes, in microform, paper, electronic and/or any other formats; and to authorize, sub-license, sub-contract or procure any of the acts previously mentioned.

1. The American Institute of Physics grants you the right to reproduce the material indicated above on a one-time, non-exclusive basis, solely for the purpose described. Permission must be requested separately for any future or additional use.

2. This permission pertains only to print use and its electronic equivalent, including CD-ROM or DVD.

3. The following copyright notice must appear with the material (please fill in the information indicated by capital letters): "Reprinted with permission from [FULL CITATION]. Copyright [PUBLICATION YEAR], American Institute of Physics." Full citation format is as follows: Author names, journal title, Vol. #, Page #, (Year of publication). For an article, the copyright notice must be printed on the first page of the article or book chapter. For figures, photographs, covers, or tables, the notice may appear with the material, in a footnote, or in the reference list.

4. This permission does not apply to any materials credited to sources other than the copyright holder.

Please let us know if you have any questions.

Sincerely,

Susann Brailey

Office of the Publisher, Journals and Technical Publications
Rights & Permissions
American Institute of Physics
Suite 1NO1
2 Huntington Quadrangle
Melville, NY 11747-4502
516-576-2268 TEL
516-576-2450 FAX
rights@aip.org

Bibliography

[1] T. Young. "An Essay on the Cohesion of Fluids." *Philos. Trans. R. Soc. London* **95**, 65-87. (1805)

[2] R. Finn. "The contact angle in capillarity." *Phys. Fluids* **18**(4), 047102 (2006). DOI: 10.1063/1.2185655

[3] I. Lunati. "Young's law and the effects of interfacial energy on the pressure at the solid-fluid interface." *Phys. Fluids* **19**(11), 118105 (2007). DOI: 10.1063/1.2800040

[4] H. Wente. "The Floating Ball Paradox." *J. Math. Fluid Mech.* **10**(4), 569-582 (2008). DOI: 10.1007/s00021-007-0251-0

[5] R. Finn. "Comments related to my paper 'The contact angle in capillarity'." *Phys. Fluids* **20**(10), 107104 (2008). DOI: 10.1063/1.2970895

[6] E. Raphaël, J.-M. di Meglio, M. Berger, and E. Calabi. "Convex particles at interfaces." *J. Phys. I France* **2**, 571-579 (1992).

[7] R. Finn. "Criteria for Floating I." *J. Math. Fluid Mech.* **13**(1), 103-115 (2009). DOI: 10.1007/s00021-009-0009-y

[8] R. Finn. "Floating Bodies Subject to Capillary Attractions." *J. Math. Fluid Mech.* **11**(3), 443-458 (2008). DOI: 10.1007/s00021-008-0268-z

[9] R. Finn and T.I. Vogel. "Floating criteria in three dimensions." *Analysis* **29**, 387-402 (2009). DOI: 10.1524/anly.2009.0931

[10] R. Finn and M. Sloss, "Floating Bodies in Neutral Equilibrium." *J. Math. Fluid Mech.* **11**(3), 459-463 (2008). DOI: 10.1007/s00021-008-0269-y

[11] C. Rorres. "Completing Book II of Archimedes's *On Floating Bodies*." *The Mathematical Intelligencer* **26**(3), 32-42 (2004). DOI: 10.1007/BF02986750

[12] R. Bhatnagar and R. Finn. "Equilibrium configurations of an infinite cylinder in an unbounded fluid." *Phys. Fluids* **18**(4), 047103 (2006). DOI: 10.1063/1.2185661

[13] J. McCuan. "A Variational Formula for Floating Bodies." *Pacific Journal of Mathematics* **231**(1), 167-191 (2007).

[14] T.M. Kemp and D. Siegel. "Floating Bodies in Two Dimensions without Gravity." Accepted for publication in *Physics of Fluids*, 2011. Portions reprinted with permission from T.M. Kemp and D. Siegel, *Physics of Fluids*, article in press. Copyright 2011, American Institute of Physics.

Appendix A

Series Expansion of the Energy Function

In Section 2.1 we found that our energy function E was given by equation (2.1). Then, in Sections 2.1 and 2.2 we used a series expansion of this energy function. In this appendix we will derive in detail the series expansion used in those two sections. To expand in series, we will work with individual terms of the energy function separately.

We begin with $\sqrt{x'(t)^2 + y'(t)^2}$. Using Taylor series expansions for functions $x(t)$ and $y(t)$ we have that

$$\begin{aligned}
& \sqrt{x'(t)^2 + y'(t)^2} \\
= \; & \sqrt{\left[x'(t_1^*) + x''(t_1^*)(t - t_1^*) + \mathcal{O}\left((t - t_1^*)^2\right)\right]^2 + \left[y'(t_1^*) + y''(t_1^*)(t - t_1^*) + \mathcal{O}\left((t - t_1^*)^2\right)\right]^2} \\
= \; & \sqrt{x'(t_1^*)^2 + 2x'(t_1^*)x''(t_1^*)(t - t_1^*) + y'(t_1^*)^2 + 2y'(t_1^*)y''(t_1^*)(t - t_1^*) + \mathcal{O}\left((t - t_1^*)^2\right)} \\
= \; & \sqrt{x'(t_1^*)^2 + y'(t_1^*)^2 + 2\left[x'(t_1^*)x''(t_1^*) + y'(t_1^*)y''(t_1^*)\right](t - t_1^*) + \mathcal{O}\left((t - t_1^*)^2\right)} \\
= \; & \sqrt{\|\vec{r'}(t_1^*)\|^2 + 2\left[\vec{r'}(t_1^*) \cdot \vec{r''}(t_1^*)\right](t - t_1^*) + \mathcal{O}\left((t - t_1^*)^2\right)} \\
= \; & \|\vec{r'}(t_1^*)\| \sqrt{1 + \frac{2\left[\vec{r'}(t_1^*) \cdot \vec{r''}(t_1^*)\right]}{\|\vec{r'}(t_1^*)\|^2}(t - t_1^*) + \mathcal{O}\left((t - t_1^*)^2\right)}.
\end{aligned}$$

Then using the known series $\sqrt{1+u} = 1 + \frac{u}{2} + \mathcal{O}(u^2)$ we obtain

$$\begin{aligned}
& \sqrt{x'(t)^2 + y'(t)^2} \\
= \; & \|\vec{r'}(t_1^*)\| \left[1 + \frac{\vec{r'}(t_1^*) \cdot \vec{r''}(t_1^*)}{\|\vec{r'}(t_1^*)\|^2}(t - t_1^*) + \mathcal{O}\left((t - t_1^*)^2\right)\right].
\end{aligned}$$

We now integrate to obtain

$$\begin{aligned}
&\int_{t_1^*}^{t_1} \sqrt{x'(t)^2 + y'(t)^2}dt \\
= &\int_{t_1^*}^{t_1} \|\vec{r'}(t_1^*)\| \left[1 + \frac{\vec{r'}(t_1^*) \cdot \vec{r''}(t_1^*)}{\|\vec{r'}(t_1^*)\|^2}(t - t_1^*) + \mathcal{O}\left((t - t_1^*)^2\right)\right] dt \\
= &\|\vec{r'}(t_1^*)\|(t_1 - t_1^*) + \frac{\vec{r'}(t_1^*) \cdot \vec{r''}(t_1^*)}{2\|\vec{r'}(t_1^*)\|}(t_1 - t_1^*)^2 + \mathcal{O}\left((t_1 - t_1^*)^3\right).
\end{aligned}$$

In a similar fashion we can obtain that

$$\begin{aligned}
&\int_{t_2^*}^{t_2} \sqrt{x'(t)^2 + y'(t)^2}dt \\
= &\|\vec{r'}(t_2^*)\|(t_2 - t_2^*) + \frac{\vec{r'}(t_2^*) \cdot \vec{r''}(t_2^*)}{2\|\vec{r'}(t_2^*)\|}(t_2 - t_2^*)^2 + \mathcal{O}\left((t_2 - t_2^*)^3\right).
\end{aligned}$$

Next, we define the function $g(t_1, t_2)$ to be given by

$$g(t_1, t_2) = \sqrt{[x(t_2) - x(t_1)]^2 + [y(t_2) - y(t_1)]^2}$$

and we need a series expression for $g(t_1^*, t_2^*) - g(t_1, t_2)$. We note that

$$\begin{aligned}
&g(t_1^*, t_2^*) - g(t_1, t_2) \\
= &-[g(t_1, t_2) - g(t_1^*, t_2^*)] \\
= &-\frac{\partial g}{\partial t_1}\Big|_{(t_1^*, t_2^*)}(t_1 - t_1^*) - \frac{\partial g}{\partial t_2}\Big|_{(t_1^*, t_2^*)}(t_2 - t_2^*) - \frac{1}{2}\frac{\partial^2 g}{\partial t_1^2}\Big|_{(t_1^*, t_2^*)}(t_1 - t_1^*)^2 \\
&-\frac{\partial^2 g}{\partial t_1 \partial t_2}\Big|_{(t_1^*, t_2^*)}(t_1 - t_1^*)(t_2 - t_2^*) - \frac{1}{2}\frac{\partial^2 g}{\partial t_2^2}\Big|_{(t_1^*, t_2^*)}(t_2 - t_2^*)^2 + \mathcal{O}\left(\|(t_1, t_2) - (t_1^*, t_2^*)\|^3\right)
\end{aligned}$$

using a Taylor series expansion in two variables. To determine the series expansion we need to calculate the necessary derivatives of g.

$$\begin{aligned}
\frac{\partial g}{\partial t_1}\Big|_{(t_1^*, t_2^*)} &= \frac{-x'(t_1^*)[x(t_2) - x(t_1)] - y'(t_1)[y(t_2) - y(t_1)]}{\sqrt{(x(t_2) - x(t_1))^2 + (y(t_2) - y(t_1))^2}} \\
&= \frac{-\vec{r'}(t_1^*) \cdot [\vec{r}(t_2^*) - \vec{r}(t_1^*)]}{\|\vec{r}(t_2^*) - \vec{r}(t_1^*)\|}
\end{aligned}$$

$$\begin{aligned}
\frac{\partial g}{\partial t_2}\Big|_{(t_1^*, t_2^*)} &= \frac{x'(t_2^*)[x(t_2) - x(t_1)] + y'(t_2)[y(t_2) - y(t_1)]}{\sqrt{(x(t_2) - x(t_1))^2 + (y(t_2) - y(t_1))^2}} \\
&= \frac{\vec{r'}(t_2^*) \cdot [\vec{r}(t_2^*) - \vec{r}(t_1^*)]}{\|\vec{r}(t_2^*) - \vec{r}(t_1^*)\|}
\end{aligned}$$

$$\begin{aligned}
\frac{\partial^2 g}{\partial t_1^2}\Big|_{(t_1^*,t_2^*)} &= \frac{-x''(t_1^*)[x(t_2^*)-x(t_1^*)]+x'(t_1^*)^2-y''(t_1^*)[y(t_2^*)-y(t_1^*)]+y'(t_1^*)^2}{\sqrt{[x(t_2^*)-x(t_1^*)]^2+[y(t_2^*)-y(t_1^*)]^2}} \\
&\quad -\frac{[x'(t_1^*)[x(t_2^*)-x(t_1^*)]+y'(t_1^*)[y(t_2^*)-y(t_1^*)]]^2}{[[x(t_2^*)-x(t_1^*)]^2+[y(t_2^*)-y(t_1^*)]^2]^{\frac{3}{2}}} \\
&= \frac{-\vec{r''}(t_1^*)\cdot[\vec{r}(t_2^*)-\vec{r}(t_1^*)]+\|\vec{r'}(t_1^*)\|^2}{\|\vec{r}(t_2^*)-\vec{r}(t_1^*)\|} - \frac{(\vec{r'}(t_1^*)\cdot[\vec{r}(t_2^*)-\vec{r}(t_1^*)])^2}{\|\vec{r}(t_2^*)-\vec{r}(t_1^*)\|^3}
\end{aligned}$$

$$\begin{aligned}
\frac{\partial^2 g}{\partial t_2^2}\Big|_{(t_1^*,t_2^*)} &= \frac{x''(t_2^*)[x(t_2^*)-x(t_1^*)]+x'(t_2^*)^2+y''(t_1^*)[y(t_2^*)-y(t_1^*)]+y'(t_2^*)^2}{\sqrt{[x(t_2^*)-x(t_1^*)]^2+[y(t_2^*)-y(t_1^*)]^2}} \\
&\quad -\frac{[x'(t_2^*)[x(t_2^*)-x(t_1^*)]+y'(t_2^*)[y(t_2^*)-y(t_1^*)]]^2}{[[x(t_2^*)-x(t_1^*)]^2+[y(t_2^*)-y(t_1^*)]^2]^{\frac{3}{2}}} \\
&= \frac{\vec{r''}(t_2^*)\cdot[\vec{r}(t_2^*)-\vec{r}(t_1^*)]+\|\vec{r'}(t_2^*)\|^2}{\|\vec{r}(t_2^*)-\vec{r}(t_1^*)\|} - \frac{(\vec{r'}(t_2^*)\cdot[\vec{r}(t_2^*)-\vec{r}(t_1^*)])^2}{\|\vec{r}(t_2^*)-\vec{r}(t_1^*)\|^3}
\end{aligned}$$

$$\begin{aligned}
\frac{\partial^2 g}{\partial t_1 \partial t_2}\Big|_{(t_1^*,t_2^*)} &= \frac{-x'(t_1^*)x'(t_2^*)-y'(t_1^*)y'(t_2^*)}{\sqrt{[x(t_2^*)-x(t_1^*)]^2+[y(t_2^*)-y(t_1^*)]^2}} \\
&\quad +\frac{[x'(t_1^*)(x(t_2^*)-x(t_1^*))+y'(t_1^*)(y(t_2^*)-y(t_1^*))]\cdot[x'(t_2^*)(x(t_2^*)-x(t_1^*))]}{[[x(t_2^*)-x(t_1^*)]^2+[y(t_2^*)-y(t_1^*)]]^{\frac{3}{2}}} \\
&\quad +\frac{[x'(t_1^*)(x(t_2^*)-x(t_1^*))+y'(t_1^*)(y(t_2^*)-y(t_1^*))]\cdot[y'(t_2^*)y(t_2^*)-y(t_1^*))]}{[[x(t_2^*)-x(t_1^*)]^2+[y(t_2^*)-y(t_1^*)]]^{\frac{3}{2}}} \\
&= \frac{-\vec{r'}(t_1^*)\cdot\vec{r'}(t_2^*)}{\|\vec{r}(t_2^*)-\vec{r}(t_1^*)\|} + \frac{(\vec{r'}(t_1^*)\cdot[\vec{r}(t_2^*)-\vec{r}(t_1^*)])(\vec{r'}(t_2^*)\cdot[\vec{r}(t_2^*)-\vec{r}(t_1^*)])}{\|\vec{r}(t_2^*)-\vec{r}(t_1^*)\|^3}
\end{aligned}$$

Using equation (2.1) and putting all of the pieces together gives us our series expansion for the energy function to be given by

$$\begin{aligned}
& E(t_1,t_2) - E(t_1^*,t_2^*) \\
= \quad & \left[\sigma \frac{\vec{r'}(t_1^*)\cdot[\vec{r}(t_2^*)-\vec{r}(t_1^*)]}{\|\vec{r}(t_2^*)-\vec{r}(t_1^*)\|} - (\sigma_1-\sigma_2)\|\vec{r'}(t_1^*)\|\right](t_1-t_1^*) \\
& + \left[(\sigma_1-\sigma_2)\|\vec{r'}(t_2^*)\| - \sigma\frac{\vec{r'}(t_2^*)\cdot[\vec{r}(t_2^*)-\vec{r}(t_1^*)]}{\|\vec{r}(t_2^*)-\vec{r}(t_1^*)\|}\right](t_2-t_2^*) \\
& + \left[\sigma\left[\frac{(\vec{r'}(t_1^*)\cdot[\vec{r}(t_2^*)-\vec{r}(t_1^*)])^2}{2\|\vec{r}(t_2^*)-\vec{r}(t_1^*)\|^3} - \frac{\|\vec{r'}(t_1^*)\|^2 - \vec{r''}(t_1^*)\cdot[\vec{r}(t_2^*)-\vec{r}(t_1^*)]}{2\|\vec{r}(t_2^*)-\vec{r}(t_1^*)\|}\right]\right. \\
& \quad \left. -(\sigma_1-\sigma_2)\frac{\vec{r'}(t_1^*)\cdot\vec{r''}(t_1^*)}{2\|\vec{r'}(t_1^*)\|}\right](t_1-t_1^*)^2 \\
& + \sigma\left[\frac{\vec{r'}(t_1^*)\cdot\vec{r'}(t_2^*)}{\|\vec{r}(t_2^*)-\vec{r}(t_1^*)\|}\right. \\
& \quad \left. -\frac{(\vec{r'}(t_1^*)\cdot[\vec{r}(t_2^*)-\vec{r}(t_1^*)])(\vec{r'}(t_2^*)\cdot[\vec{r}(t_2^*)-\vec{r}(t_1^*)])}{\|\vec{r}(t_2^*)-\vec{r}(t_1^*)\|^3}\right](t_1-t_1^*)(t_2-t_2^*) \\
& + \left[\sigma\left[\frac{(\vec{r'}(t_2^*)\cdot[\vec{r}(t_2^*)-\vec{r}(t_1^*)])^2}{2\|\vec{r}(t_2^*)-\vec{r}(t_1^*)\|^3} - \frac{\|\vec{r'}(t_2^*)\|^2 - \vec{r''}(t_2^*)\cdot[\vec{r}(t_2^*)-\vec{r}(t_1^*)]}{2\|\vec{r}(t_2^*)-\vec{r}(t_1^*)\|}\right]\right. \\
& \quad \left. +(\sigma_1-\sigma_2)\frac{\vec{r'}(t_2^*)\cdot\vec{r''}(t_2^*)}{2\|\vec{r'}(t_2^*)\|}\right](t_2-t_2^*)^2 + \mathcal{O}\left(\|(t_1-t_1^*,t_2-t_2^*)\|^3\right).
\end{aligned}$$

This is the series expansion of the energy function that we use in Sections 2.1 and 2.2.

Appendix B

Reasons for Excluding $\gamma = 0, \pi$

In Remark 2.1 from Section 2.1 we noted that the cases where γ was equal to 0 or π could be ignored without consequence. For strictly convex bodies, the reason was clear, but for bodies which are only convex, the reasoning is not as obvious. When γ is 0 or π, the body is contained beneath or above the fluid interface, respectively, with either a single point or a straight side touching the fluid interface. If the body touches only at a single point, we use the same reasoning as a body that is strictly convex to conclude that the body is unstable. If the body touches along a straight side and is beneath the fluid interface (see Figure B.1) we note that since $\gamma = 0$ then $\cos(0) = \frac{\sigma_1 - \sigma_2}{\sigma} \Rightarrow \sigma_1 - \sigma_2 = \sigma$ and thus

$$\begin{aligned} E &= l_1\sigma_1 + l_2\sigma_2 - l_1\sigma \\ &= l_1(\sigma_1 - \sigma) + l_2\sigma_2 \\ &= (l_1 + l_2)\sigma_2 \end{aligned}$$

where l_1 and l_2 sum to the perimeter of the body. Thus the energy of the body touching the fluid interface along the straight edge is the same as the energy it would possess if it were entirely underneath the fluid interface. Pulling the body slightly downward gives the existence of a small perturbation to a configuration with the same energy and thus the configuration is unstable. If the body touches the fluid interface along a straight side and is above the fluid interface, we note that since $\gamma = \pi$, $\cos\pi = \frac{\sigma_1 - \sigma_2}{\sigma} \Rightarrow \sigma_1 - \sigma_2 = -\sigma \Rightarrow \sigma_1 = \sigma_2 - \sigma$ and thus

$$\begin{aligned} E &= l_1\sigma_1 + l_2\sigma_2 - l_2\sigma \\ &= l_1\sigma_1 + l_2(\sigma_2 - \sigma) \\ &= (l_1 + l_2)\sigma_1. \end{aligned}$$

Appendix B is reprinted with permission from reference [14]. The material presented here has had some minor additions from what appears in that reference.

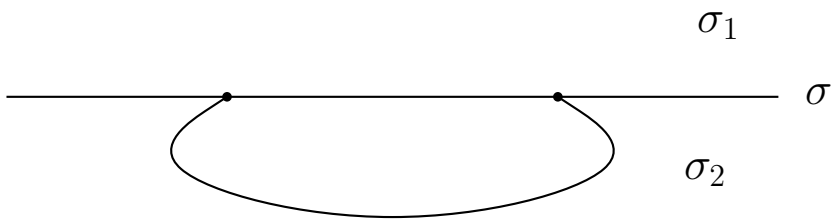

Figure B.1: *A body beneath the fluid interface, yet touching the fluid interface along a straight side.*

Thus the energy of the body touching the fluid interface along the straight edge is the same as the energy it would possess if it were entirely above the fluid interface. Pulling the body slightly upward gives the existence of a small perturbation to a configuration with the same energy and thus the configuration is unstable.

Appendix C

Reason for Considering Only Contact Configurations

In Remark 2.2 it was noted that Finn's Lemma 1.1 in reference [7] gave proof of why it was unnecessary to consider configurations of strictly convex bodies that were not in contact with the fluid interface. In this appendix, we will prove a result similar in character to that of Finn; our result will prove that a convex polygonal body in any stable configuration will have less energy than the configurations totally above or totally below the fluid interface. However before we get to the main result of this appendix, we will first prove a lemma for later use.

Lemma C.1. *Any configuration for which there exists a small perturbation to the "totally above" configuration will possess an energy less than or equal to the energy of the "totally above" configuration. Similarly, any configuration for which there exists a small perturbation to the "totally below" configuration will possess an energy less than or equal to the energy of the "totally below" configuration.*

Proof. Any configuration for which there exists a small perturbation to the "totally above" configuration will be contained primarily in the σ_1 medium, touching the fluid interface either at one point or where one flat side is incident with the interface as shown in Figure C.1. The energy of the body touching the fluid interface will be given by

$$E = l_1\sigma_1 + l_2\sigma_2 - l_3\sigma$$

where l_1, l_2 are the lengths touching the σ_1 and σ_2 media respectively and l_3 is the length removed from the fluid interface by the body. Clearly, $l_1 + l_2$ is the perimeter of the body. The energy of the "totally above" configuration is then given by

$$E_a = (l_1 + l_2)\sigma_1$$

Appendix C is reprinted with permission from reference [14].

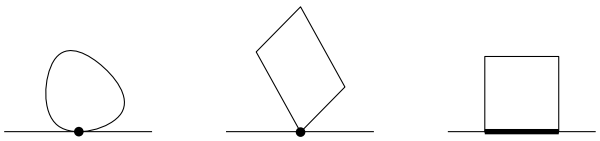

Figure C.1: *The figure shows that when there exists a small perturbation to the "totally above" configuration, the body is contained mostly in the σ_1 fluid with either one point or a straight side touching the fluid interface.*

and so we see that

$$\begin{aligned} E - E_a &= l_1\sigma_1 + l_2\sigma_2 - l_3\sigma - (l_1 + l_2)\sigma_1 \\ &= l_2(\sigma_2 - \sigma_1) - l_3\sigma. \end{aligned}$$

In the case where the body touches the fluid interface in only one point, we have that $l_2 = l_3 = 0$ implying that $E = E_a$. In the case where the body touches the fluid interface along a flat side of the body, we have that $l_2 = l_3 \neq 0$ and so

$$\begin{aligned} E - E_a &= l_2(\sigma_2 - \sigma_1 - \sigma) \\ &= -\sigma l_2(\cos\gamma + 1) \\ &< 0 \end{aligned}$$

since $\gamma \neq 0, \pi$, and thus through both cases we see that $E \leq E_a$ which proves the first half of the result. The case for configurations near "totally below" can be proved similarly. □

We now make use of the prior lemma to prove the main result of this appendix.

Lemma C.2. *A convex polygonal body in any stable configuration will have less energy than the configurations totally above or totally below the fluid interface.*

Proof. Since the polygonal body is in a stable configuration, we know that there must be two corners on the fluid interface (from Theorem 5.1) and the stability condition for polygonal cross-sections must hold. That is, we must have

$$\pi - \min(\gamma_1^+, \gamma_2^+) < \gamma < \min(\gamma_1^-, \gamma_2^-)$$

where the four angles γ_1^+, γ_2^+, γ_1^- and γ_2^- are as defined earlier in the stability condition for polygonal cross-sections (Theorem 5.2).

We will consider vertical variations of the body only, in terms of a single parameter h. We will define $h = 0$ to be the stable configuration while $h > 0$ corresponds to the body being pulled upward and $h < 0$ corresponds to the body being pulled downward. We

also define four angles Ψ_1^+, Ψ_2^+, Ψ_1^- and Ψ_2^- all of which are functions of h and are shown in Figure C.2. We note that the energy function will be continuous while the body is in contact with the fluid interface; there *may* be jumps in energy as the body is raised or lowered beyond contact with the fluid interface.

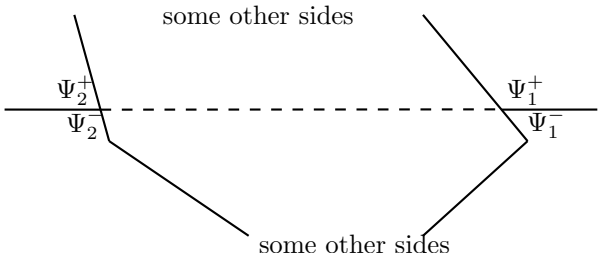

Figure C.2: *The four angles Ψ_1^+, Ψ_2^+, Ψ_1^- and Ψ_2^- (which are functions of h).*

Due to convexity, both $\Psi_1^-(h)$ and $\Psi_2^-(h)$ are non-decreasing as h increases, and both $\Psi_1^+(h)$ and $\Psi_2^+(h)$ are non-increasing as h increases. (Due to the non-smooth nature of the body, these angles may not change continuously.)

We first define the function

$$f(h) = \min\{\Psi_1^-(h), \Psi_2^-(h)\}$$

and we note that

$$f(0) = \min\{\Psi_1^-(0), \Psi_2^-(0)\} = \min\{\gamma_1^-, \gamma_2^-\}.$$

Since $\Psi_1^-(h)$ and $\Psi_2^-(h)$ are non-decreasing, $f(h)$ is also non-decreasing and thus we have for all $h > 0$ that

$$\begin{aligned}
& f(0) \leq f(h) \\
\implies \quad & \min\{\gamma_1^-, \gamma_2^-\} \leq \min\{\Psi_1^-(h), \Psi_2^-(h)\} \\
\implies \quad & \gamma < \min\{\Psi_1^-(h), \Psi_2^-(h)\} \\
\implies \quad & \gamma < \Psi_1^-(h), \Psi_2^-(h).
\end{aligned}$$

Then, since $h > 0$, this corresponds to pulling the body upward and we note that

$$\begin{aligned}
& \frac{\partial E}{\partial t_1}\Big|_{(t_1^*, t_2^*)} < 0 \\
\iff \quad & (\sigma_1 - \sigma_2)(-\|\vec{r'}(t_1^*)\|) + \sigma \left(\frac{\vec{r'}(t_1^*) \cdot [\vec{r}(t_2^*) - \vec{r}(t_1^*)]}{\|\vec{r}(t_2^*) - \vec{r}(t_1^*)\|} \right) < 0 \\
\iff \quad & \frac{\vec{r'}(t_1^*)}{\|\vec{r'}(t_1^*)\|} \cdot \frac{\vec{r}(t_2^*) - \vec{r}(t_1^*)}{\|\vec{r}(t_2^*) - \vec{r}(t_1^*)\|} < \frac{\sigma_1 - \sigma_2}{\sigma} \\
\iff \quad & \cos \Psi_1^-(h) < \cos \gamma \\
\iff \quad & \gamma < \Psi_1^-(h)
\end{aligned}$$

and that

$$\begin{aligned}
& & \frac{\partial E}{\partial t_2}\Big|_{(t_1^*,t_2^*)} > 0 \\
\iff & (\sigma_1-\sigma_2)(\|\vec{r'}(t_2^*)\|) - \sigma\left(\frac{\vec{r'}(t_2^*)\cdot[\vec{r}(t_2^*)-\vec{r}(t_1^*)]}{\|\vec{r}(t_2^*)-\vec{r}(t_1^*)\|}\right) > 0 \\
\iff & \frac{\vec{r'}(t_2^*)}{\|\vec{r'}(t_2^*)\|}\cdot\frac{\vec{r}(t_2^*)-\vec{r}(t_1^*)}{\|\vec{r}(t_2^*)-\vec{r}(t_1^*)\|} < \frac{\sigma_1-\sigma_2}{\sigma} \\
\iff & \cos\Psi_2^-(h) < \cos\gamma \\
\iff & \gamma < \Psi_2^-(h)
\end{aligned}$$

and so since $\gamma < \Psi_1^-(h)$ and $\gamma < \Psi_2^-(h)$ for $h > 0$ we then have that when $h > 0$ (which corresponds to pulling the body up) $\frac{\partial E}{\partial t_1}\big|_{(t_1^*,t_2^*)} < 0$ and $\frac{\partial E}{\partial t_2}\big|_{(t_1^*,t_2^*)} > 0$. Then since pulling the body vertically up decreases t_1^* and increases t_2^*, this leads to increasing energy for $h > 0$.

Next we define the function

$$g(h) = \pi - \min\{\Psi_1^+(h), \Psi_2^+(h)\}$$

and we note that

$$g(0) = \pi - \min\{\Psi_1^+(0), \Psi_2^+(0)\} = \pi - \min\{\gamma_1^+, \gamma_2^+\}.$$

Since $\Psi_1^+(h)$ and $\Psi_2^+(h)$ are non-increasing, $g(h)$ is non-decreasing and thus we have for all $h < 0$ that

$$\begin{aligned}
& g(h) \le g(0) \\
\implies & \pi - \min\{\Psi_1^+(h), \Psi_2^+(h)\} \le \pi - \min\{\gamma_1^+, \gamma_2^+\} \\
\implies & \pi - \min\{\Psi_1^+(h), \Psi_2^+(h)\} < \gamma \\
\implies & \max\{\pi - \Psi_1^+(h), \pi - \Psi_2^+(h)\} < \gamma \\
\implies & \pi - \Psi_1^+(h), \pi - \Psi_2^+(h) < \gamma.
\end{aligned}$$

Then, since $h < 0$, this corresponds to pulling the body downward and we note that

$$\begin{aligned}
& \frac{\partial E}{\partial t_1}\Big|_{(t_1^*,t_2^*)} > 0 \\
\iff & \frac{\vec{r'}(t_1^*)}{\|\vec{r'}(t_1^*)\|}\cdot\frac{\vec{r}(t_2^*)-\vec{r}(t_1^*)}{\|\vec{r}(t_2^*)-\vec{r}(t_1^*)\|} > \frac{\sigma_1-\sigma_2}{\sigma} \\
\iff & \cos(\pi-\Psi_1^+(h)) > \cos\gamma \\
\iff & \pi - \Psi_1^+(h) < \gamma
\end{aligned}$$

and that

$$\begin{aligned} & \frac{\partial E}{\partial t_2}\Big|_{(t_1^*,t_2^*)} < 0 \\ \iff \quad & \frac{\vec{r'}(t_2^*)}{\|\vec{r'}(t_2^*)\|} \cdot \frac{\vec{r}(t_2^*) - \vec{r}(t_1^*)}{\|\vec{r}(t_2^*) - \vec{r}(t_1^*)\|} > \frac{\sigma_1 - \sigma_2}{\sigma} \\ \iff \quad & \cos(\pi - \Psi_2^-(h)) > \cos\gamma \\ \iff \quad & \pi - \Psi_2^-(h) < \gamma \end{aligned}$$

and so since $\gamma > \pi - \Psi_1^+(h)$ and $\gamma > \pi - \Psi_2^+(h)$ for $h < 0$ we then have that when $h < 0$ (which corresponds to pulling the body down) $\frac{\partial E}{\partial t_1}\big|_{(t_1^*,t_2^*)} > 0$ and $\frac{\partial E}{\partial t_2}\big|_{(t_1^*,t_2^*)} < 0$. Then since pulling the body vertically down increases t_1^* and decreases t_2^*, this leads to decreasing energy for $h < 0$.

Thus, we have concluded that for $h < 0$ the energy is decreasing and for $h > 0$ the energy is increasing. However, this will only be true for h such that the body remains in contact with the fluid interface. In addition, we note that the energy derivatives will exist everywhere except at a finite number of h values corresponding to configurations where the fluid interface intersects a corner of the body. Using the prior lemma, we can now give a qualitative sketch of the energy as a function of h from which it is clear that the claim is true. (See Figure C.3.) □

This lemma tells us that when we are searching for floating configurations of a polygonal body, any stable configuration will always have less energy than configurations not in contact with the fluid interface. This is the reason that we proceed to study configurations touching the fluid interface while disregarding the configurations not in contact.

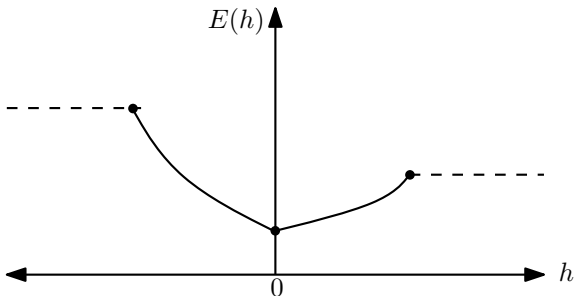

Figure C.3: *A qualitative sketch of the energy as a function of h. Note that the dotted sections of the graph indicate that the energy will be constant at a value greater than or equal to the value indicated.*

Appendix D

Intersection of an Ellipse and a Line in Equal Contact Angles

Lemma D.1. *If a line intersects an ellipse at two distinct points with equal contact angles different from* 0 *and* π*, then the line must be parallel to one of the axes of the ellipse.*

Proof. Consider a counter-clockwise parametrization of an ellipse

$$\vec{r}(t) = (g\cos t, h\sin t)$$

for $t \in [0, 2\pi]$ with $g \neq h$. Consider any line intersecting the ellipse in two points. Let t_1 and t_2 be the parameter values in $[0, 2\pi]$ with $t_1 < t_2$ such that $\vec{r}(t_1)$ and $\vec{r}(t_2)$ are the two points of intersection between the line and the ellipse. Consider the two tangent lines to the ellipse at the two points of intersection. For now, we will assume that the tangent lines are not parallel and will therefore intersect at one point P. We consider the triangle formed between the point P and the two points of intersection. Since the line meets the ellipse in equal contact angles, the triangle must be isosceles. We let the length of the two equal sides be λ. (See Figure D.1.) We can then express the point P in two different ways,

$$\begin{aligned} P &= \vec{r}(t_1) + \lambda \cdot \frac{\vec{r'}(t_1)}{\|\vec{r'}(t_1)\|} \\ &= (g\cos t_1, h\sin t_1) + \lambda \cdot \frac{(-g\sin t_1, h\cos t_1)}{\sqrt{g^2\sin^2 t_1 + h^2\cos^2 t_1}} \end{aligned}$$

Appendix D is reprinted with permission from reference [14].

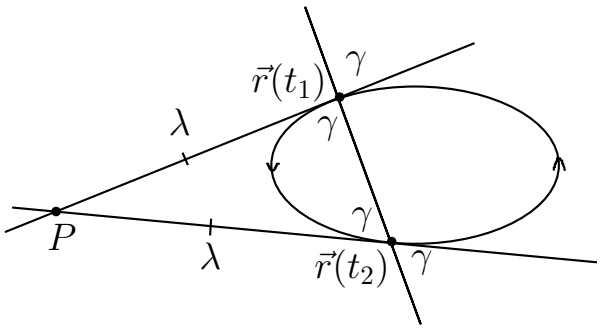

Figure D.1: *The ellipse-line intersection in consideration showing the intersection of the tangents at point P.*

and

$$\begin{aligned} P &= \vec{r}(t_2) - \lambda \cdot \frac{\vec{r'}(t_2)}{\|\vec{r'}(t_2)\|} \\ &= (g\cos t_2, h\sin t_2) - \lambda \cdot \frac{(-g\sin t_2, h\cos t_2)}{\sqrt{g^2\sin^2 t_2 + h^2\cos^2 t_2}}. \end{aligned}$$

Together these give

$$(g\cos t_1, h\sin t_1) + \frac{\lambda(-g\sin t_1, h\cos t_1)}{\sqrt{g^2\sin^2 t_1 + h^2\cos^2 t_1}} = (g\cos t_2, h\sin t_2) - \frac{\lambda(-g\sin t_2, h\cos t_2)}{\sqrt{g^2\sin^2 t_2 + h^2\cos^2 t_2}}. \tag{D.1}$$

Then taking the scalar product of equation (D.1) with the vector $(h\cos t_1, g\sin t_1)$ gives

$$\begin{aligned} gh + \lambda\cdot(0) &= gh(\cos t_1\cos t_2 + \sin t_1\sin t_2) + \lambda gh\frac{(\cos t_1\sin t_2 - \cos t_2\sin t_1)}{\sqrt{g^2\sin^2 t_2 + h^2\cos^2 t_2}} \\ 1 &= \cos(t_1 - t_2) + \frac{\lambda\sin(t_2 - t_1)}{\sqrt{g^2\sin^2 t_2 + h^2\cos^2 t_2}}. \end{aligned} \tag{D.2}$$

Now, taking the scalar product of equation (D.1) with the vector $(h\cos t_2, g\sin t_2)$ gives

$$\begin{aligned} gh(\cos t_1\cos t_2 + \sin t_1\sin t_2) + \lambda gh\frac{(\cos t_1\sin t_2 - \cos t_2\sin t_1)}{\sqrt{g^2\sin^2 t_1 + h^2\cos^2 t_1}} &= gh + \lambda\cdot(0) \\ \cos(t_1 - t_2) + \frac{\lambda\sin(t_2 - t_1)}{\sqrt{g^2\sin^2 t_1 + h^2\cos^2 t_1}} &= 1. \end{aligned} \tag{D.3}$$

Then subtracting (D.2) and (D.3) gives that

$$\begin{aligned} \frac{\sin(t_2 - t_1)}{\sqrt{g^2\sin^2 t_2 + h^2\cos^2 t_2}} - \frac{\sin(t_2 - t_1)}{\sqrt{g^2\sin^2 t_1 + h^2\cos^2 t_1}} &= 0 \\ \sin(t_2 - t_1)\cdot\left[\frac{1}{\sqrt{g^2\sin^2 t_2 + h^2\cos^2 t_2}} - \frac{1}{\sqrt{g^2\sin^2 t_1 + h^2\cos^2 t_1}}\right] &= 0. \end{aligned}$$

This implies that either $\sin(t_2 - t_1) = 0$ or $g^2 \sin^2 t_1 + h^2 \cos^2 t_1 = g^2 \sin^2 t_2 + h^2 \cos^2 t_2$. If $\sin(t_2 - t_1) = 0$, then $t_2 = t_1 + \pi$. Substituting $t_2 = t_1 + \pi$ into equation (D.1) we have

$$\begin{aligned}(g\cos t_1, h\sin t_1) &= (-g\cos t_1, -h\sin t_1)\\ (g\cos t_1, h\sin t_1) &= \vec{0}\end{aligned}$$

which is a contradiction. Hence it must be that

$$\begin{aligned}g^2 \sin^2 t_1 + h^2 \cos^2 t_1 &= g^2 \sin^2 t_2 + h^2 \cos^2 t_2\\ (g^2 - h^2)\sin^2 t_2 &= (g^2 - h^2)\sin^2 t_1\\ \sin t_1 &= \pm \sin t_2.\end{aligned}$$

If $\sin t_1 = \sin t_2$ then the y-components of the two points of intersection are the same and so the intersecting line must be horizontal. If $\sin t_1 = -\sin t_2$ then the y-components of the two points of intersection are negatives of each other. The corresponding x-components must also be the same; if not, then $t_2 = t_1 + \pi$ which would give the same contradiction as before. Thus in this case the intersecting line is vertical.

Thus the intersecting line is either vertical or horizontal and so it will be parallel to one of the axes of the ellipse.

In the case where the tangents are parallel, the angle of contact must be $\frac{\pi}{2}$. The line will consequently be incident to either the major or minor axis of the ellipse and hence the result remains true in this special case. □

Appendix E

Miscellaneous Detailed Calculations from Section 5.3

In this appendix we will show in detail the various calculations used in Section 5.3 which are not shown in that section for the sake of continuity and clarity.

E.1 The Triangle

In Subsection 5.3.1, Tables 5.1, 5.2, and 5.3 were given comparing the energies of the six different configurations for the triangular cross-section for each value of $\gamma \in (0, \pi)$, one table for each of the three different cases. In this section, we give a detailed account of how these tables came to be. We first recall that the energies of the six configurations were given by

$$\begin{aligned} E_{1a} &= (a+b)\sigma_1 + c\sigma_2 - c\sigma \\ E_{1b} &= c\sigma_1 + (a+b)\sigma_2 - c\sigma \\ E_{2a} &= (a+c)\sigma_1 + b\sigma_2 - b\sigma \\ E_{2b} &= b\sigma_1 + (a+c)\sigma_2 - b\sigma \\ E_{3a} &= (b+c)\sigma_1 + a\sigma_2 - a\sigma \\ E_{3b} &= a\sigma_1 + (b+c)\sigma_2 - a\sigma \end{aligned}$$

and we start by directly comparing each pair of energies.[1]

[1]Recall that the lengths of the sides of the triangles are a, b and c and they satisfy the relationship $0 \leq a \leq b \leq c$. In addition, due to the triangle inequality, we have that $a + b > c$, $a + c > b$, and $b + c > a$.

$$\begin{aligned} E_{1a} - E_{1b} &= (a+b)\sigma_1 + c\sigma_2 - c\sigma - c\sigma_1 - (a+b)\sigma_2 + c\sigma \\ &= (a+b-c)\sigma_1 - (a+b-c)\sigma_2 \\ &= \sigma(a+b-c)\cos\gamma \end{aligned}$$

- When $0 < \gamma < \frac{\pi}{2}$ we have that $E_{1a} > E_{1b}$.
- When $\gamma = \frac{\pi}{2}$ we have that $E_{1a} = E_{1b}$.
- When $\frac{\pi}{2} < \gamma < \pi$ we have that $E_{1a} < E_{1b}$.

$$\begin{aligned} E_{1a} - E_{2a} &= (a+b)\sigma_1 + c\sigma_2 - c\sigma - (a+c)\sigma_1 - b\sigma_2 + b\sigma \\ &= (b-c)\sigma_1 + (c-b)\sigma_2 + (b-c)\sigma \\ &= (b-c)(\sigma_1 - \sigma_2 - \sigma) \\ &= -(c-b)\sigma\left[\cos\gamma + 1\right] \\ &\leq 0 \end{aligned}$$

- Equality is only possible when $b = c$ but we will ignore this case because when $b = c$ configurations 1a and 2a are the same. Hence we have that $E_{1a} < E_{2a}$ for all γ in $(0, \pi)$.

$$\begin{aligned} E_{1a} - E_{2b} &= (a+b)\sigma_1 + c\sigma_2 - c\sigma - b\sigma_1 - (a+c)\sigma_2 + b\sigma \\ &= a\sigma_1 - c\sigma - a\sigma_2 + b\sigma \\ &= a(\sigma_1 - \sigma_2) + (b-c)\sigma \\ &= a\sigma\left[\cos\gamma + \frac{b-c}{a}\right] \end{aligned}$$

- When $0 < \gamma < \arccos\left(\frac{c-b}{a}\right)$ we have that $E_{1a} > E_{2b}$.
- When $\gamma = \arccos\left(\frac{c-b}{a}\right)$ we have that $E_{1a} = E_{2b}$.
- When $\arccos\left(\frac{c-b}{a}\right) < \gamma < \pi$ we have that $E_{1a} < E_{2b}$.

$$\begin{aligned} E_{1a} - E_{3a} &= (a+b)\sigma_1 + c\sigma_2 - c\sigma - (b+c)\sigma_1 - a\sigma_2 + a\sigma \\ &= (a-c)\sigma_1 + (c-a)\sigma_2 + (a-c)\sigma \\ &= (a-c)\left[\sigma_1 - \sigma_2 + \sigma\right] \\ &= -\sigma(c-a)\left[\cos\gamma + 1\right] \\ &\leq 0 \end{aligned}$$

- Equality is only possible when $a = c$ but we will ignore this case because when $a = c$ the triangle becomes equilateral and so 1a and 3a are the same. Hence we have that $E_{1a} < E_{3a}$ for all γ in $(0, \pi)$.

$$\begin{aligned} E_{1a} - E_{3b} &= (a+b)\sigma_1 + c\sigma_2 - c\sigma - \sigma_1 - (b+c)\sigma_2 + a\sigma \\ &= b(\sigma_1 - \sigma_2) + (a-c)\sigma \\ &= b\sigma\left[\cos\gamma + \frac{a-c}{b}\right] \end{aligned}$$

- When $0 < \gamma < \arccos\left(\frac{c-a}{b}\right)$ we have that $E_{1a} > E_{3b}$.
- When $\gamma = \arccos\left(\frac{c-a}{b}\right)$ we have that $E_{1a} = E_{3b}$.
- When $\arccos\left(\frac{c-a}{b}\right) < \gamma < \pi$ we have that $E_{1a} < E_{3b}$.

$$\begin{aligned} E_{1b} - E_{2a} &= c\sigma_1 + (a+b)\sigma_2 - c\sigma - (a+c)\sigma_1 - b\sigma_2 + b\sigma \\ &= a(\sigma_2 - \sigma_1) + (b-c)\sigma \\ &= a\sigma\left[-\cos\gamma + \frac{b-c}{a}\right] \end{aligned}$$

- When $0 < \gamma < \arccos\left(\frac{b-c}{a}\right)$ we have that $E_{1b} < E_{2a}$.
- When $\gamma = \arccos\left(\frac{b-c}{a}\right)$ we have that $E_{1b} = E_{2a}$.
- When $\arccos\left(\frac{b-c}{a}\right) < \gamma < \pi$ we have that $E_{1b} > E_{2a}$.

$$\begin{aligned} E_{1b} - E_{2b} &= c\sigma_1 + (a+b)\sigma_2 - c\sigma - b\sigma_1 - (a+c)\sigma_2 + b\sigma \\ &= (c-b)\sigma_1 + (b-c)\sigma_2 + (b-c)\sigma \\ &= \sigma(c-b)\left[\cos\gamma - 1\right] \\ &\leq 0 \end{aligned}$$

- Equality is only possible when $b = c$ but we will ignore this case because when $b = c$ configurations 1b and 2b are the same. Hence we have that $E_{1b} < E_{2b}$ for all γ in $(0, \pi)$.

$$\begin{aligned} E_{1b} - E_{3a} &= c\sigma_1 + (a+b)\sigma_2 - c\sigma - (b+c)\sigma_1 - a\sigma_2 + a\sigma \\ &= b\sigma_2 - b\sigma_1 + (a-c)\sigma \\ &= b\sigma\left[-\cos\gamma + \frac{a-c}{b}\right] \end{aligned}$$

- When $0 < \gamma < \arccos\left(\frac{a-c}{b}\right)$ we have that $E_{1b} < E_{3a}$.

- When $\gamma = \arccos\left(\frac{a-c}{b}\right)$ we have that $E_{1b} = E_{3a}$.
- When $\arccos\left(\frac{a-c}{b}\right) < \gamma < \pi$ we have that $E_{1b} > E_{3a}$.

$$\begin{aligned} E_{1b} - E_{3b} &= c\sigma_1 + (a+b)\sigma_2 - c\sigma - a\sigma_1 - (b+c)\sigma_2 + a\sigma \\ &= (c-a)\sigma_1 - (c-a)\sigma_2 - (c-a)\sigma \\ &= \sigma(c-a)\left[\cos\gamma - 1\right] \\ &\leq 0 \end{aligned}$$

- Equality is only possible when $a = c$ but we will ignore this case because when $a = c$ the triangle becomes equilateral so configurations 1b and 3b are the same. Hence we have that $E_{1b} < E_{3b}$ for all γ in $(0, \pi)$.

$$\begin{aligned} E_{2a} - E_{2b} &= (a+c)\sigma_1 + b\sigma_2 - b\sigma - b\sigma_1 - (a+c)\sigma_2 + b\sigma \\ &= (a+c-b)\sigma_1 + (b-a-c)\sigma_2 \\ &= (a+c-b)(\sigma_1 - \sigma_2) \\ &= \sigma(a-b+c)\cos\gamma \end{aligned}$$

- When $0 < \gamma < \frac{\pi}{2}$ we have that $E_{2a} > E_{2b}$.
- When $\gamma = \frac{\pi}{2}$ we have that $E_{2a} = E_{2b}$.
- When $\frac{\pi}{2} < \gamma < \pi$ we have that $E_{2a} < E_{2b}$.

$$\begin{aligned} E_{2a} - E_{3a} &= (a+c)\sigma_1 + b\sigma_2 - b\sigma - (b+c)\sigma_1 - a\sigma_2 + a\sigma \\ &= (a-b)\sigma_1 + (b-a)\sigma_2 + (a-b)\sigma \\ &= -\sigma(b-a)\left[\cos\gamma + 1\right] \\ &\leq 0 \end{aligned}$$

- Equality is only possible when $a = b$ but we will ignore this case because when $a = b$ configurations 2a and 3a are the same. Hence, $E_{2a} < E_{3a}$ for all γ in $(0, \pi)$.

$$\begin{aligned} E_{2a} - E_{3b} &= (a+c)\sigma_1 + b\sigma_2 - b\sigma - a\sigma_1 - (b+c)\sigma_2 + a\sigma \\ &= c\sigma_1 - c\sigma_2 + (a-b)\sigma \\ &= c\sigma\left[\cos\gamma + \frac{a-b}{c}\right] \end{aligned}$$

- When $0 < \gamma < \arccos\left(\frac{b-a}{c}\right)$ we have that $E_{2a} > E_{3b}$.
- When $\gamma = \arccos\left(\frac{b-a}{c}\right)$ we have that $E_{2a} = E_{3b}$.

- When $\arccos\left(\frac{b-a}{c}\right) < \gamma < \pi$ we have that $E_{2a} < E_{3b}$.

$$\begin{aligned} E_{2b} - E_{3a} &= b\sigma_1 + (a+c)\sigma_2 - b\sigma - (b+c)\sigma_1 - a\sigma_2 + a\sigma \\ &= c(\sigma_2 - \sigma_1) + (a-b)\sigma \\ &= c\sigma\left[-\cos\gamma + \frac{a-b}{c}\right] \end{aligned}$$

- When $0 < \gamma < \arccos\left(\frac{a-b}{c}\right)$ we have that $E_{2b} > E_{3a}$.
- When $\gamma = \arccos\left(\frac{a-b}{c}\right)$ we have that $E_{2b} = E_{3a}$.
- When $\arccos\left(\frac{a-b}{c}\right) < \gamma < \pi$ we have that $E_{2b} < E_{3a}$.

$$\begin{aligned} E_{2b} - E_{3b} &= b\sigma_1 + (a+c)\sigma_2 - b\sigma - a\sigma_1 - (b+c)\sigma_2 + a\sigma \\ &= (b-a)\left[\sigma_1 - \sigma_2 - \sigma\right] \\ &= \sigma(b-a)\left[\cos\gamma - 1\right] \\ &\leq 0 \end{aligned}$$

- Equality is only possible when $a = b$ but we will ignore this case because when $a = b$ configurations 2b and 3b are the same. Hence, $E_{2b} < E_{3b}$ for all γ in $(0, \pi)$.

$$\begin{aligned} E_{3a} - E_{3b} &= (b+c)\sigma_1 + a\sigma_2 - a\sigma - a\sigma_1 - (b+c)\sigma_2 + a\sigma \\ &= (b+c-a)(\sigma_1 - \sigma_2) \\ &= \sigma(b+c-a)\cos\gamma \end{aligned}$$

- When $0 < \gamma < \frac{\pi}{2}$ we have that $E_{3a} > E_{3b}$.
- When $\gamma = \frac{\pi}{2}$ we have that $E_{3a} = E_{3b}$.
- When $\frac{\pi}{2} < \gamma < \pi$ we have that $E_{3a} < E_{3b}$.

Having now compared each of the energies directly it is apparent that there are six "special" values of γ at which the relationships between various energies change. We need to deduce the relationships between these special values as well as their relationships to 0, $\frac{\pi}{2}$, and to π. These special values are

$$\begin{aligned} &\arccos\left(\frac{c-b}{a}\right) && \arccos\left(\frac{b-c}{a}\right) = \pi - \arccos\left(\frac{c-b}{a}\right) \\ &\arccos\left(\frac{c-a}{b}\right) && \arccos\left(\frac{a-c}{b}\right) = \pi - \arccos\left(\frac{c-a}{b}\right) \\ &\arccos\left(\frac{b-a}{c}\right) && \arccos\left(\frac{a-b}{c}\right) = \pi - \arccos\left(\frac{b-a}{c}\right). \end{aligned}$$

We see that

$$\begin{aligned}
\frac{c-b}{a}-\frac{c-a}{b} &= \frac{bc-b^2}{ab}-\frac{ac-a^2}{ab} \\
&= \frac{1}{ab}\left[-b^2+bc-ac+a^2\right] \\
&= \frac{1}{ab}\left[(a+b)(a-b)-c(a-b)\right] \\
&= \frac{a-b}{ab}\left[a+b-c\right] \\
&= \frac{b-a}{ab}\left[c-(a+b)\right] \\
&\leq 0
\end{aligned}$$

since $b \geq a$ and $a+b>c$. Thus we have that

$$\frac{c-b}{a} \leq \frac{c-a}{b}.$$

We also see that

$$\begin{aligned}
\frac{c-a}{b}-\frac{b-a}{c} &= \frac{c^2-ac}{bc}-\frac{b^2-ab}{bc} \\
&= \frac{1}{bc}\left[(c-b)(c+b)+a(b-c)\right] \\
&= \frac{c-b}{bc}\left[c+b-a\right] \\
&\geq 0
\end{aligned}$$

and so we have that

$$\frac{c-a}{b} \geq \frac{b-a}{c}.$$

However, comparing $\frac{c-b}{a}$ and $\frac{b-a}{c}$ will not be as direct. We start by noting that

$$\begin{aligned}
\frac{c-b}{a}-\frac{b-a}{c} &= \frac{c^2-bc}{ac}-\frac{ab-a^2}{ac} \\
&= \frac{1}{ac}\left[c^2-bc-ab+a^2\right] \\
&= \frac{1}{ac}\left[a^2-b(a+c)+c^2\right]
\end{aligned}$$

and so there will be three different cases:

$$\begin{aligned}
b < \frac{a^2+c^2}{a+c} &\implies \frac{c-b}{a} > \frac{b-a}{c} \\
b = \frac{a^2+c^2}{a+c} &\implies \frac{c-b}{a} = \frac{b-a}{c} \\
b > \frac{a^2+c^2}{a+c} &\implies \frac{c-b}{a} < \frac{b-a}{c}
\end{aligned}$$

which implies that

$$\begin{aligned} b < \frac{a^2+c^2}{a+c} \quad &\Longrightarrow \quad \frac{b-a}{c} < \frac{c-b}{a} \leq \frac{c-a}{b} \\ b = \frac{a^2+c^2}{a+c} \quad &\Longrightarrow \quad \frac{b-a}{c} = \frac{c-b}{a} \leq \frac{c-a}{b} \\ b > \frac{a^2+c^2}{a+c} \quad &\Longrightarrow \quad \frac{c-b}{a} < \frac{b-a}{c} \leq \frac{c-a}{b} \end{aligned}$$

and so finally we have that

$$\begin{aligned} b < \frac{a^2+c^2}{a+c} \quad &\Longrightarrow \quad \arccos\left(\frac{c-a}{b}\right) \leq \arccos\left(\frac{c-b}{a}\right) < \arccos\left(\frac{b-a}{c}\right) \\ b = \frac{a^2+c^2}{a+c} \quad &\Longrightarrow \quad \arccos\left(\frac{c-a}{b}\right) \leq \arccos\left(\frac{c-b}{a}\right) < \arccos\left(\frac{b-a}{c}\right) \\ b > \frac{a^2+c^2}{a+c} \quad &\Longrightarrow \quad \arccos\left(\frac{c-a}{b}\right) \leq \arccos\left(\frac{b-a}{c}\right) < \arccos\left(\frac{c-b}{a}\right) \end{aligned}$$

and so we can now determine the relationships between the energies of the six configurations for each of the three cases (which are dependant on the value of b) and for each value of γ. There are of course three cases, $b < \frac{a^2+c^2}{a+c}$, $b = \frac{a^2+c^2}{a+c}$ and $b > \frac{a^2+c^2}{a+c}$. The relationships between the various energies as determined in this section can now be summarized in Tables 5.1, 5.2, and 5.3 shown earlier in Subsection 5.3.1.

E.2 The Square

In Subsection 5.3.2, Table 5.4 was given comparing the energies of the three different configurations for the square cross-section for each value of $\gamma \in (0, \pi)$. In this section, we give a detailed account of how this table was determined. We first recall that the energies of the three configurations were given by

$$\begin{aligned} E_1 &= 3\sigma_1 + \sigma_2 - \sigma \\ E_2 &= 2\sigma_1 + 2\sigma_2 - \sqrt{2}\sigma \\ E_3 &= \sigma_1 + 3\sigma_2 - \sigma \end{aligned}$$

and we start by directly comparing each pair of energies.

$$\begin{aligned} E_1 - E_2 &= 3\sigma_1 + \sigma_2 - \sigma - 2\sigma_1 - 2\sigma_2 + \sqrt{2}\sigma \\ &= \sigma_1 - \sigma_2 + (\sqrt{2}-1)\sigma \\ &= \sigma[\cos\gamma + \sqrt{2} - 1] \end{aligned}$$

Calculations from Section E.2 are reprinted with permission from reference [14].

- When $\gamma < \arccos(1-\sqrt{2})$ we have that $E_1 > E_2$.
- When $\gamma = \arccos(1-\sqrt{2})$ we have that $E_1 = E_2$.
- When $\gamma > \arccos(1-\sqrt{2})$ we have that $E_1 < E_2$.

$$\begin{aligned} E_1 - E_3 &= 3\sigma_1 + \sigma_2 - \sigma - \sigma_1 - 3\sigma_2 + \sigma \\ &= 2\sigma_1 - 2\sigma_2 \\ &= 2\sigma\cos\gamma \end{aligned}$$

- When $\gamma < \frac{\pi}{2}$ we have that $E_1 > E_3$.
- When $\gamma = \frac{\pi}{2}$ we have that $E_1 = E_3$.
- When $\gamma < \frac{\pi}{2}$ we have that $E_1 < E_3$.

$$\begin{aligned} E_2 - E_3 &= 2\sigma_1 + 2\sigma_2 - \sqrt{2}\sigma - \sigma_1 - 3\sigma_2 + \sigma \\ &= \sigma_1 - \sigma_2 + (1-\sqrt{2})\sigma \\ &= \sigma[\cos\gamma + 1 - \sqrt{2}] \end{aligned}$$

- When $\gamma < \arccos(\sqrt{2}-1)$ we have that $E_2 > E_3$.
- When $\gamma = \arccos(\sqrt{2}-1)$ we have that $E_2 = E_3$.
- When $\gamma > \arccos(\sqrt{2}-1)$ we have that $E_2 < E_3$.

The relationships between the three energies change depending on the value of γ. The relationships between the three energies for each value of $\gamma \in (0, \pi)$ are summarized in Table 5.4 shown in Subsection 5.3.2.

E.3 The Rectangle

In Subsection 5.3.3, Tables 5.6, 5.7, and 5.8 were given comparing the energies of the five different configurations for the rectangular cross-section for each value of $\gamma \in (0, \pi)$ for three different cases. In this section, we give a detailed account of how these tables came to be. We first recall that the energies of the five configurations were given by[2]

$$\begin{aligned} E_1 &= (b+2)\sigma_1 + b\sigma_2 - b\sigma \\ E_2 &= b\sigma_1 + (b+2)\sigma_2 - b\sigma \\ E_3 &= (2b+1)\sigma_1 + \sigma_2 - \sigma \\ E_4 &= \sigma_1 + (2b+1)\sigma_2 - \sigma \\ E_5 &= (b+1)(\sigma_1 + \sigma_2) - \sqrt{1+b^2}\sigma \end{aligned}$$

[2]Recall that the rectangle had side lengths 1 and $b > 1$.

and now they can directly compared.

$$\begin{aligned} E_1 - E_2 &= (2+b)\sigma_1 + b\sigma_2 - b\sigma - b\sigma_1 - (2+b)\sigma_2 + b\sigma \\ &= 2\sigma_1 - 2\sigma_2 \\ &= 2\sigma\cos\gamma \end{aligned}$$

- When $0 < \gamma < \frac{\pi}{2}$ we have that $E_1 > E_2$.
- When $\gamma = \frac{\pi}{2}$ we have that $E_1 = E_2$.
- When $\frac{\pi}{2} < \gamma < \pi$ we have that $E_1 < E_2$.

$$\begin{aligned} E_1 - E_3 &= (2+b)\sigma_1 + b\sigma_2 - b\sigma - \sigma_1 - (2b+1)\sigma_1 - \sigma_2 + \sigma \\ &= (1-b)\sigma_1 + (b-1)\sigma_2 + (1-b)\sigma \\ &= \sigma(b-1)[\frac{\sigma_2 - \sigma_1}{\sigma} - 1] \\ &= \sigma(b-1)[-\cos\gamma - 1] \\ &< 0 \end{aligned}$$

- So $E_1 < E_3$ for all values of γ in $(0, \pi)$.

$$\begin{aligned} E_1 - E_4 &= (2+b)\sigma_1 + b\sigma_2 - b\sigma - \sigma_1 - (2b+1)\sigma_2 + \sigma \\ &= (b+1)(\sigma_1 - \sigma_2) + (1-b)\sigma \\ &= \sigma(b+1)[\cos\gamma + \frac{1-b}{b+1}] \end{aligned}$$

- When $0 < \gamma < \arccos\left(\frac{b-1}{b+1}\right)$ we have that $E_1 > E_4$.
- When $\gamma = \arccos\left(\frac{b-1}{b+1}\right)$ we have that $E_1 = E_4$.
- When $\arccos\left(\frac{b-1}{b+1}\right) < \gamma < \pi$ we have that $E_1 < E_4$.

$$\begin{aligned} E_1 - E_5 &= (2+b)\sigma_1 + b\sigma_2 - b\sigma - (b+1)\sigma_1 - (b+1)\sigma_2 + \sqrt{1+b^2}\sigma \\ &= \sigma_1 - \sigma_2 + (\sqrt{1+b^2} - b)\sigma_1 \\ &= \sigma[\cos\gamma + \sqrt{1+b^2} - b] \end{aligned}$$

- When $0 < \gamma < \arccos\left(b - \sqrt{1+b^2}\right)$ we have that $E_1 > E_5$.
- When $\gamma = \arccos\left(b - \sqrt{1+b^2}\right)$ we have that $E_1 = E_5$.
- When $\arccos\left(b - \sqrt{1+b^2}\right) < \gamma < \pi$ we have that $E_1 < E_5$.

$$\begin{aligned} E_2 - E_3 &= b\sigma_1 + (2+b)\sigma_2 - b\sigma - (2b+1)\sigma_1 - \sigma_2 + \sigma \\ &= (-b-1)\sigma_1 + (1+b)\sigma_2 + (1-b)\sigma \\ &= (b+1)\sigma\left[\frac{\sigma_2 - \sigma_1}{\sigma} + \frac{1-b}{1+b}\right] \\ &= (b+1)\sigma\left[-\cos\gamma + \frac{1-b}{b+1}\right] \end{aligned}$$

- When $0 < \gamma < \arccos\left(\frac{1-b}{b+1}\right)$ we have that $E_2 < E_3$.
- When $\gamma = \arccos\left(b - \sqrt{1+b^2}\right)$ we have that $E_2 = E_3$.
- When $\arccos\left(b - \sqrt{1+b^2}\right) < \gamma < \pi$ we have that $E_2 > E_3$.

$$\begin{aligned} E_2 - E_4 &= b\sigma_1 + (2+b)\sigma_2 - b\sigma - \sigma_1 - (2b+1)\sigma_2 + \sigma \\ &= (b-1)\sigma_1 + (1-b)\sigma_2 + (1-b)\sigma \\ &= (b-1)[\sigma_1 - \sigma_2 - \sigma] \\ &= (b-1)\sigma[\cos\gamma - 1] \\ &< 0 \end{aligned}$$

- So $E_2 < E_4$ for all values of γ in $(0, \pi)$.

$$\begin{aligned} E_2 - E_5 &= b\sigma_1 + (2+b)\sigma_2 - b\sigma - (b+1)\sigma_1 - (b+1)\sigma_2 + \sqrt{1+b^2}\sigma \\ &= -\sigma_1 + \sigma_2 + (\sqrt{1+b^2} - b)\sigma \\ &= \sigma[-\cos\gamma + \sqrt{1+b^2} - b] \end{aligned}$$

- When $0 < \gamma < \arccos(\sqrt{1+b^2} - b)$ we have that $E_2 < E_5$.
- When $\gamma = \arccos(\sqrt{1+b^2} - b)$ we have that $E_2 = E_5$.
- When $\arccos(\sqrt{1+b^2} - b) < \gamma < \pi$ we have that $E_2 > E_5$.

$$\begin{aligned} E_3 - E_4 &= (2b+1)\sigma_1 + \sigma_2 - \sigma - \sigma_1 - (2b+1)\sigma_2 + \sigma \\ &= (2b+1)(\sigma_1 - \sigma_2) + (\sigma_2 - \sigma_1) \\ &= (\sigma_1 - \sigma_2)[2b + 1 - 1] \\ &= 2b\sigma\cos\gamma \end{aligned}$$

- When $0 < \gamma < \frac{\pi}{2}$ we have that $E_3 > E_4$.

- When $\gamma = \frac{\pi}{2}$ we have that $E_3 = E_4$.
- When $\frac{\pi}{2} < \gamma < \pi$ we have that $E_3 < E_4$.

$$\begin{aligned} E_3 - E_5 &= (2b+1)\sigma_1 + \sigma_2 - \sigma + (b+1)(\sigma_1 + \sigma_2) + \sqrt{1+b^2}\sigma \\ &= b\sigma_1 - b\sigma_2 + (\sqrt{1+b^2} - 1)\sigma \\ &= b\sigma \left[\cos\gamma + \frac{\sqrt{1+b^2} - 1}{b} \right] \end{aligned}$$

- When $0 < \gamma < \arccos\left(\frac{1-\sqrt{1+b^2}}{b}\right)$ we have that $E_3 > E_5$.
- When $\gamma = \arccos\left(\frac{1-\sqrt{1+b^2}}{b}\right)$ we have that $E_3 = E_5$.
- When $\arccos\left(\frac{1-\sqrt{1+b^2}}{b}\right) < \gamma < \pi$ we have that $E_3 < E_5$.

$$\begin{aligned} E_4 - E_5 &= \sigma_1 + (2b+1)\sigma_2 - \sigma - (b+1)(\sigma_1 + \sigma_2) + \sqrt{1+b^2}\sigma \\ &= b(\sigma_2 - \sigma_1) + (\sqrt{1+b^2} - 1)\sigma \\ &= \sigma b \left[-\cos\gamma + \frac{\sqrt{1+b^2} - 1}{b} \right] \end{aligned}$$

- When $0 < \gamma < \arccos\left(\frac{\sqrt{1+b^2}-1}{b}\right)$ we have that $E_4 < E_5$.
- When $\gamma = \arccos\left(\frac{\sqrt{1+b^2}-1}{b}\right)$ we have that $E_4 = E_5$.
- When $\arccos\left(\frac{\sqrt{1+b^2}-1}{b}\right) < \gamma < \pi$ we have that $E_4 > E_5$.

After having compared the energies of the five configurations directly it is clear that the relationships between the various energies change depending on the value of γ. To determine these relationships, it will be necessary to know the relationships between the following nine values:

$$0, \quad -1, \quad \frac{b-1}{b+1}, \quad b - \sqrt{b^2+1}, \quad \frac{1-b}{b+1}, \quad 1, \quad \sqrt{b^2+1} - b, \quad \frac{1-\sqrt{b^2+1}}{b}, \quad \text{and} \quad \frac{\sqrt{1+b^2}-1}{b}.$$

Then we will need to compare the inverse cosine of these values to determine the order of the angles at which the relationships between the energies change.

We have that $\sqrt{b^2+1}-b$, $\frac{b-1}{b+1}$, and $\frac{\sqrt{1+b^2}-1}{b}$ are all positive and less than 1. We first see that

$$\begin{aligned}\sqrt{1+b^2}-b-\frac{\sqrt{1+b^2}-1}{b} &= \frac{b\sqrt{1+b^2}-b^2-\sqrt{1+b^2}+1}{b}\\ &= \frac{(b-1)\sqrt{1+b^2}+(1-b^2)}{b}\\ &= \frac{(b-1)}{b}\left[\sqrt{1+b^2}-(b+1)\right]\\ &< 0\end{aligned}$$

and that

$$\begin{aligned}\frac{\sqrt{1+b^2}-1}{b}-\frac{b-1}{b+1} &= \frac{1}{(b+1)b}\left[(\sqrt{1+b^2}-1)(b+1)-(b-1)b\right]\\ &= \frac{1}{(b+1)b}\left[b\sqrt{1+b^2}+\sqrt{1+b^2}-b-1-b^2+b\right]\\ &= \frac{1}{(b+1)b}\left[\sqrt{1+b^2}(b+1)-(b^2+1)\right]\\ &= \frac{\sqrt{1+b^2}}{(b+1)b}\left[b+1-\sqrt{b^2+1}\right]\\ &> 0\end{aligned}$$

so we have that $\sqrt{1+b^2}-b<\frac{\sqrt{1+b^2}-1}{b}$ and $\frac{\sqrt{1+b^2}-1}{b}>\frac{b-1}{b+1}$. However, setting $\sqrt{1+b^2}-b=\frac{b-1}{b+1}$ we see that we do in fact get a solution:

$$\begin{aligned}\sqrt{1+b^2}-b &= \frac{b-1}{b+1}\\ (\sqrt{1+b^2}-b)(b+1) &= b-1\\ b\sqrt{1+b^2}+\sqrt{1+b^2}-b^2-b &= b-1\\ \sqrt{1+b^2}(b+1) &= b^2+2b-1\\ (1+b^2)(b+1)^2 &= (b^2+2b-1)^2\\ 2b^2+2b &= 2b^3+2b^2-4b\\ 2b^3 &= 6b\\ b^2 &= 3 && \text{since } b\neq 0\\ b &= \sqrt{3} && \text{since } b>1.\end{aligned}$$

We can then show that

- when $1<b<\sqrt{3}$ we have that $\sqrt{1+b^2}-b>\frac{b-1}{b+1}$,
- when $b=\sqrt{3}$ we have that $\sqrt{1+b^2}-b=\frac{b-1}{b+1}$, and

- when $b > \sqrt{3}$ we have that $\sqrt{1+b^2} - b < \frac{b-1}{b+1}$.

So, we have that

$$\begin{array}{rcccccc} 1 < b < \sqrt{3} & \Rightarrow & \dfrac{b-1}{b+1} & < & \sqrt{1+b^2} - b & < & \dfrac{\sqrt{1+b^2}-1}{b} \\ b = \sqrt{3} & \Rightarrow & \dfrac{b-1}{b+1} & = & \sqrt{1+b^2} - b & < & \dfrac{\sqrt{1+b^2}-1}{b} \\ b > \sqrt{3} & \Rightarrow & \sqrt{1+b^2} - b & < & \dfrac{b-1}{b+1} & < & \dfrac{\sqrt{1+b^2}-1}{b}. \end{array}$$

Given these relations, we can now write out the relationships between the energies of the five configurations for each value of γ and each of the three cases for the value of b in Tables 5.6, 5.7 and 5.8, shown in Subsection 5.3.3.

E.4 The Regular Pentagon

In Subsection 5.3.4, Table 5.10 was given comparing the energies of the four different configurations for the pentagonal cross-section for each value of $\gamma \in (0, \pi)$. In this section, we give a detailed account of how this table was determined. We first recall that the energies of the four configurations were given by

$$\begin{aligned} E_1 &= 4\sigma_1 + \sigma_2 - \sigma \\ E_2 &= 3\sigma_1 + 2\sigma_2 - \varphi\sigma \\ E_3 &= 2\sigma_1 + 3\sigma_2 - \varphi\sigma \\ E_4 &= \sigma_1 + 4\sigma_2 - \sigma \end{aligned}$$

and we start by directly comparing each pair of energies.

$$\begin{aligned} E_1 - E_2 &= 4\sigma_1 + \sigma_2 - \sigma - 3\sigma_1 - 2\sigma_2 + \varphi\sigma \\ &= \sigma_1 - \sigma_2 + (\varphi - 1)\sigma \\ &= \sigma\left[\cos\gamma + \frac{1}{\varphi}\right] \end{aligned}$$

- When $0 < \gamma < \pi - \arccos\left(\frac{1}{\varphi}\right)$ we have that $E_1 > E_2$.
- When $\gamma = \pi - \arccos\left(\frac{1}{\varphi}\right)$ we have that $E_1 = E_2$.
- When $\pi - \arccos\left(\frac{1}{\varphi}\right) < \gamma < \pi$ we have that $E_1 < E_2$.

$$\begin{aligned} E_1 - E_3 &= 4\sigma_1 + \sigma_2 - \sigma - 2\sigma_1 - 3\sigma_2 + \varphi\sigma \\ &= 2\sigma_1 - 2\sigma_2 + (\varphi - 1)\sigma \\ &= 2\sigma \left[\cos\gamma + \frac{\varphi - 1}{2} \right] \end{aligned}$$

- When $0 < \gamma < \frac{3\pi}{5}$ we have that $E_1 > E_3$.
- When $\gamma = \frac{3\pi}{5}$ we have that $E_1 = E_3$.
- When $\frac{3\pi}{5} < \gamma < \pi$ we have that $E_1 < E_3$.

$$\begin{aligned} E_1 - E_4 &= 4\sigma_1 + \sigma_2 - \sigma - \sigma_1 - 4\sigma_2 + \sigma \\ &= 3(\sigma_1 - \sigma_2) \\ &= 3\sigma\cos\gamma \end{aligned}$$

- When $0 < \gamma < \frac{\pi}{2}$ we have that $E_1 > E_4$.
- When $\gamma = \frac{\pi}{2}$ we have that $E_1 = E_4$.
- When $\frac{\pi}{2} < \gamma < \pi$ we have that $E_1 < E_4$.

$$\begin{aligned} E_2 - E_3 &= 3\sigma_1 + 2\sigma_2 - \varphi\sigma - 2\sigma_1 - 3\sigma_2 + \varphi\sigma \\ &= \sigma_1 - \sigma_2 \\ &= \sigma\cos\gamma \end{aligned}$$

- When $0 < \gamma < \frac{\pi}{2}$ we have that $E_2 > E_3$.
- When $\gamma = \frac{\pi}{2}$ we have that $E_2 = E_3$.
- When $\frac{\pi}{2} < \gamma < \pi$ we have that $E_2 < E_3$.

$$\begin{aligned} E_2 - E_4 &= 3\sigma_1 + 2\sigma_2 - \varphi\sigma - \sigma_1 - 4\sigma_2 + \sigma \\ &= 2\sigma_1 - 2\sigma_2 + (1 - \varphi)\sigma \\ &= 2\sigma \left[\cos\gamma - \frac{\varphi - 1}{2} \right] \end{aligned}$$

- When $0 < \gamma < \frac{2\pi}{5}$ we have that $E_2 > E_4$.
- When $\gamma = \frac{2\pi}{5}$ we have that $E_2 = E_4$.
- When $\frac{2\pi}{5} < \gamma < \pi$ we have that $E_2 < E_4$.

$$\begin{aligned} E_3 - E_4 &= 2\sigma_1 + 3\sigma_2 - \varphi\sigma - \sigma_1 - 4\sigma_2 + \sigma \\ &= \sigma_1 - \sigma_2 + (1-\varphi)\sigma \\ &= \sigma_1 - \sigma_2 - \frac{1}{\varphi}\sigma \\ &= \sigma\left[\cos\gamma - \frac{1}{\varphi}\right] \end{aligned}$$

- When $0 < \gamma < \arccos\left(\frac{1}{\varphi}\right)$ we have that $E_3 > E_4$.
- When $\gamma = \arccos\left(\frac{1}{\varphi}\right)$ we have that $E_3 = E_4$.
- When $\arccos\left(\frac{1}{\varphi}\right) < \gamma = \pi$ we have that $E_3 < E_4$.

The relationships between the four energies change depending on the value of γ. The relationships between the four energies can now be summarized in Table 5.10, shown in Subsection 5.3.4.

E.5 The Regular Hexagon

In Subsection 5.3.5, Table 5.12 was given comparing the energies of the five different configurations for the hexagonal cross-section for each value of $\gamma \in (0, \pi)$. In this section, we give a detailed account of how this table was determined. We first recall that the energies of the five configurations were given by

$$\begin{aligned} E_1 &= 5\sigma_1 + \sigma_2 - \sigma \\ E_2 &= 4\sigma_1 + 2\sigma_2 - \sqrt{3}\sigma \\ E_3 &= 3\sigma_1 + 3\sigma_2 - 2\sigma \\ E_4 &= 2\sigma_1 + 4\sigma_2 - \sqrt{3}\sigma \\ E_5 &= \sigma + 5\sigma_2 - \sigma \end{aligned}$$

and we start by directly comparing each pair of energies.

$$\begin{aligned} E_1 - E_2 &= 5\sigma_1 + \sigma_2 - \sigma - 4\sigma_1 - 2\sigma_2 + \sqrt{3}\sigma \\ &= \sigma_1 - \sigma_2 + (\sqrt{3} - 1)\sigma \\ &= \sigma\left[\cos\gamma + \sqrt{3} - 1\right] \end{aligned}$$

- When $0 < \gamma < \arccos\left(1 - \sqrt{3}\right)$ we have that $E_1 > E_2$.
- When $\gamma = \arccos\left(1 - \sqrt{3}\right)$ we have that $E_1 = E_2$.

- When $\arccos\left(1-\sqrt{3}\right) < \gamma < \pi$ we have that $E_1 < E_2$.

$$\begin{aligned} E_1 - E_3 &= 5\sigma_1 + \sigma_2 - \sigma - 3\sigma_1 - 3\sigma_2 + 2\sigma \\ &= 2\sigma_1 - 2\sigma_2 + \sigma \\ &= 2\sigma\left[\cos\gamma + \frac{1}{2}\right] \end{aligned}$$

- When $0 < \gamma < \frac{2\pi}{3}$ we have that $E_1 > E_3$.
- When $\gamma = \frac{2\pi}{3}$ we have that $E_1 = E_3$.
- When $\frac{2\pi}{3} < \gamma < \pi$ we have that $E_1 < E_3$.

$$\begin{aligned} E_1 - E_4 &= 5\sigma_1 + \sigma_2 - \sigma - 2\sigma_1 - 4\sigma_2 + \sqrt{3}\sigma \\ &= 3\sigma_1 - 3\sigma_2 + (\sqrt{3}-1)\sigma \\ &= 3\sigma\left[\cos\gamma + \frac{\sqrt{3}-1}{3}\right] \end{aligned}$$

- When $0 < \gamma < \arccos\left(\frac{1-\sqrt{3}}{3}\right)$ we have that $E_1 > E_4$.
- When $\gamma = \arccos\left(\frac{1-\sqrt{3}}{3}\right)$ we have that $E_1 = E_4$.
- When $\arccos\left(\frac{1-\sqrt{3}}{3}\right) < \gamma < \pi$ we have that $E_1 < E_4$.

$$\begin{aligned} E_1 - E_5 &= 5\sigma_1 + \sigma_2 - \sigma - \sigma_1 - 5\sigma_2 + \sigma \\ &= 4(\sigma_1 - \sigma_2) \\ &= 4\sigma\cos\gamma \end{aligned}$$

- When $0 < \gamma < \frac{\pi}{2}$ we have that $E_1 > E_5$.
- When $\gamma = \frac{\pi}{2}$ we have that $E_1 = E_5$.
- When $\frac{\pi}{2} < \gamma < \pi$ we have that $E_1 < E_5$.

$$\begin{aligned} E_2 - E_3 &= 4\sigma_1 + 2\sigma_2 - \sqrt{3}\sigma - 3\sigma_1 - 3\sigma_2 + 2\sigma \\ &= \sigma_1 - \sigma_2 + (2-\sqrt{3})\sigma \\ &= \sigma\left[\cos\gamma + 2 - \sqrt{3}\right] \end{aligned}$$

- When $0 < \gamma < \arccos\left(\sqrt{3}-2\right)$ we have that $E_2 > E_3$.

- When $\gamma = \arccos\left(\sqrt{3}-2\right)$ we have that $E_2 = E_3$.
- When $\arccos\left(\sqrt{3}-2\right) < \gamma < \pi$ we have that $E_2 < E_3$.

$$\begin{aligned} E_2 - E_4 &= 4\sigma_1 + 2\sigma_2 - \sqrt{3}\sigma - 2\sigma_1 - 4\sigma_2 + \sqrt{3}\sigma \\ &= 2(\sigma_1 - \sigma_2) \\ &= 2\sigma\cos\gamma \end{aligned}$$

- When $0 < \gamma < \frac{\pi}{2}$ we have that $E_2 > E_4$.
- When $\gamma = \frac{\pi}{2}$ we have that $E_2 = E_4$.
- When $\frac{\pi}{2} < \gamma < \pi$ we have that $E_2 < E_4$.

$$\begin{aligned} E_2 - E_5 &= 4\sigma_1 + 2\sigma_2 - \sqrt{3}\sigma - \sigma_1 - 5\sigma_2 + \sigma \\ &= 3\sigma_1 - 3\sigma_2 + (1-\sqrt{3})\sigma \\ &= 3\sigma\left[\cos\gamma + \frac{1-\sqrt{3}}{3}\right] \end{aligned}$$

- When $0 < \gamma < \arccos\left(\frac{\sqrt{3}-1}{3}\right)$ we have that $E_2 > E_5$.
- When $\gamma = \arccos\left(\frac{\sqrt{3}-1}{3}\right)$ we have that $E_2 = E_5$.
- When $\arccos\left(\frac{\sqrt{3}-1}{3}\right) < \gamma < \pi$ we have that $E_2 < E_5$.

$$\begin{aligned} E_3 - E_4 &= 3\sigma_1 + 3\sigma_2 - 2\sigma - 2\sigma_1 - 4\sigma_2 + \sqrt{3}\sigma \\ &= \sigma_1 - \sigma_2 + (\sqrt{3}-2)\sigma \\ &= \sigma\left[\cos\gamma + \sqrt{3} - 2\right] \end{aligned}$$

- When $0 < \gamma < \arccos\left(2-\sqrt{3}\right)$ we have that $E_3 > E_4$.
- When $\gamma = \arccos\left(2-\sqrt{3}\right)$ we have that $E_3 = E_4$.
- When $\arccos\left(2-\sqrt{3}\right) < \gamma < \pi$ we have that $E_3 < E_4$.

$$\begin{aligned} E_3 - E_5 &= 3\sigma_1 + 3\sigma_2 - 2\sigma - \sigma_1 - 5\sigma_2 + \sigma \\ &= 2\sigma_1 - 2\sigma_2 - \sigma \\ &= 2\sigma\left[\cos\gamma - \frac{1}{2}\right] \end{aligned}$$

- When $0 < \gamma < \frac{\pi}{3}$ we have that $E_3 > E_5$.
- When $\gamma = \frac{\pi}{3}$ we have that $E_3 = E_5$.
- When $\frac{\pi}{3} < \gamma < \pi$ we have that $E_3 < E_5$.

$$\begin{aligned} E_4 - E_5 &= 2\sigma_1 + 4\sigma_2 - \sqrt{3}\sigma - \sigma_1 - 5\sigma_2 + \sigma \\ &= \sigma_1 - \sigma_2 + (1 - \sqrt{3})\sigma \\ &= \sigma \left[\cos\gamma + 1 - \sqrt{3}\right] \end{aligned}$$

- When $0 < \gamma < \arccos\left(\sqrt{3} - 1\right)$ we have that $E_4 > E_5$.
- When $\gamma = \arccos\left(\sqrt{3} - 1\right)$ we have that $E_4 = E_5$.
- When $\arccos\left(\sqrt{3} - 1\right) < \gamma < \pi$ we have that $E_4 < E_5$.

Again, the relationships between the energies of the various configurations change depending on the value of γ. The relationships can now be summarized in Table 5.12 shown in Subsection 5.3.5.

Appendix F

Proof of Lemma F.1 used in Result 5.5

Consider an n-sided regular polygon. We let the number of vertices interior to fluid 1 be m. Clearly, to have floating configurations in contact with the fluid interface, we must have that $0 \leq m \leq n-2$. We wish to establish expressions for the four floating angles $\gamma_1^+, \gamma_2^+, \gamma_1^-$ and γ_2^- as functions of the vertex parameter m, which we will do in the proof of the following lemma.

Lemma F.1. *The floating angles for an n-sided regular polygon in a configuration with two corners on the fluid interface and m vertices above the fluid interface in fluid 1 will be*

$$\gamma_1^+ = \gamma_2^+ = \pi\left(1 - \frac{m}{n}\right) \qquad \textit{and} \qquad \gamma_1^- = \gamma_2^- = \frac{\pi}{n}(m+2)$$

for integer m, $0 \leq m \leq n-2$.

Proof. Due to the symmetry of the regular polygon, it is clear that we will have that $\gamma_1^+ = \gamma_2^+$ and $\gamma_1^- = \gamma_2^-$. The remainder of the proof will focus on γ_1^+ and γ_1^- and we will prove the claim by induction using two base cases and an inductive step.

Base Case: m=0

When there are no vertices in fluid 1, the configuration is as depicted in Figure F.1. We have that

$$\begin{aligned} \gamma_1^+ &= \pi & \qquad \gamma_1^- &= \frac{2\pi}{n} \\ &= \pi\left(1 - \frac{0}{n}\right) & &= (0+2)\frac{\pi}{n} \\ &= \pi\left(1 - \frac{m}{n}\right) & &= (m+2)\frac{\pi}{n} \end{aligned}$$

Appendix F is reprinted with permission from reference [14].

and so the result is true for the first base case.

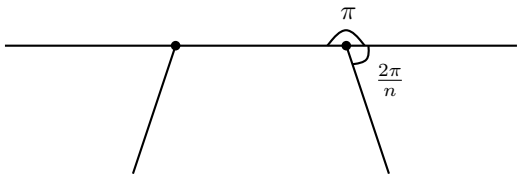

Figure F.1: *The upper floating angle is clearly π and the lower floating angle is found using the fact that the n exterior angles (which are all equal) must sum to 2π.*

Base Case: m=1

When there is only one vertex in fluid 1, the configuration is as depicted in Figure F.2. We then have that

$$\begin{aligned}\gamma_1^+ &= \pi - \alpha & \gamma_1^- &= \frac{2\pi}{n} + \alpha \\ &= \pi - \frac{\pi}{n} & &= \frac{2\pi}{n} + \frac{\pi}{n} \\ &= \pi\left(1 - \frac{1}{n}\right) & &= (1+2)\frac{\pi}{n} \\ &= \pi\left(1 - \frac{m}{n}\right) & &= (m+2)\frac{\pi}{n}\end{aligned}$$

and so the result is true for the second base case as well.

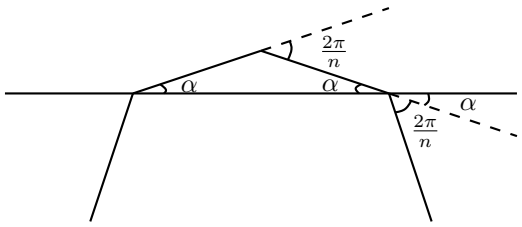

Figure F.2: *Since the polygon is regular, the portion above the fluid interface is an isosceles triangle, and consequently the two base angles are the same. We call this angle α, which we find to be equal to $\frac{\pi}{n}$. We can then use it to determine the floating angles γ_1^+ and γ_1^-.*

Inductive Step

We will assume that the result is true when there are m vertices in fluid 1, and we wish to show that it is true when there are $m+2$ vertices in fluid 1. Consider the configuration

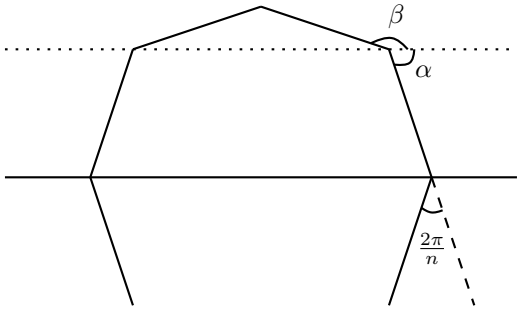

Figure F.3: *The depiction of a body floating with $m+2$ vertices in fluid 1. The dotted line represents the placement of the fluid interface when there were m vertices in fluid 1.*

with $m+2$ vertices in fluid 1, depicted in Figure F.3. By the induction hypothesis, we have that $\alpha = \gamma_1^-(m)$ and $\beta = \gamma_1^+(m)$ and thus

$$\alpha = (m+2)\frac{\pi}{n} \qquad\qquad \beta = \pi\left(1 - \frac{m}{n}\right).$$

Then since we have parallel horizontal lines, it is clear that

$$\begin{aligned}\gamma_1^- &= \frac{2\pi}{n} + \alpha \\ &= \frac{2\pi}{n} + (m+2)\frac{\pi}{n} \\ &= (m+2+2)\frac{\pi}{n}\end{aligned}$$

and that

$$\begin{aligned}\gamma_1^+ &= \alpha + \beta - \gamma_1^- \\ &= (m+2)\frac{\pi}{n} + \pi\left(1 - \frac{m}{n}\right) - (m+4)\frac{\pi}{n} \\ &= \pi\left(1 - \frac{m}{n} - \frac{2}{n}\right) \\ &= \pi\left(1 - \frac{m+2}{n}\right)\end{aligned}$$

and so the the result is true for $m+2$. By induction, this completes the proof. □